CELL-BASED UTROPHIN QUANTIFICATION PLATFORM FOR DRUG SCREENING IN DUCHENNE MUSCULAR DYSTROPHY

Patricia Soblechero Martín

PhD in Molecular Biology and Biomedicine

Department of Biochemistry and Molecular Biology

2024

Universidad del País Vasco Euskal Herriko Unibertsitatea

CELL-BASED UTROPHIN QUANTIFICATION PLATFORM FOR DRUG SCREENING IN DUCHENNE MUSCULAR DYSTROPHY

DOCTORAL THESIS

by

Patricia Soblechero Martín

Memory to achieve a PhD in Molecular Biology and Biomedicine

by

The University of the Basque Country

Department of Biochemistry and Molecular Biology

Bilbao, 2024

This thesis project has been developed at Biobizkaia Health Research Institute, under the supervision of Dr Virginia Arechavala Gomeza (Nucleic Acid Therapeutics for Rare Diseases (NAT-RD) group, Biobizkaia HRI) and Dr Ainara Vallejo Illarramendi, University of the Basque Country and Biogipuzkoa HRI.

Funding received for developing the current thesis.

Edición genética avanzada para el tratamiento de la Distrofia Muscular de Duchenne (ENiGMA: EdiciónN Genética MusculAr). Proyectos de Investigación en Salud. Instituto de Salud Carlos III-PI15/00333 (2016-2020).

Cuantificación de utrofina en distrofias musculares. Departamento de Salud, Gobierno Vasco-2016111029 (2017-2018).

CRISPR/Cas gene editing of animal model cultures for a faster transfer of DMD treatments to the clinic. Duchenne Parent Project Spain-05/2016 (2017-2019).

Validación de un método de selección de fármacos moduladores de la expresión de utrofina. Departamento de Salud, Gobierno Vasco- 2018222035 (2018).

Optimización de un protocolo de PCR digital para la cuantificación de la expresión de utrofina. Departamento de Salud, Gobierno Vasco- 2020333012 (2020).

Rio Hortega Fellowship Program. Instituto de Salud Carlos III- CM19/00104 (2020-2022).

Desarrollo preclínico de un compuesto modulador de la utrofina para el tratamiento de las distrofias de Duchenne y Becker. Departamento de Salud, Gobierno Vasco-2021333002 (2021).

AUTHORSHIP DECLARATION

This thesis contains work that has been published.

Title: **Utrophin modulator drugs as potential therapies for Duchenne and Becker muscular dystrophies.**

Authors: Soblechero-Martín P, López-Martínez A, de la Puente-Ovejero L, Vallejo-Illarramendi A, Arechavala-Gomeza V.

Published in: Neuropathol Appl Neurobiol. 2021;10.1111/nan.12735. doi:10.1111/nan.12735.

Location in the thesis: Introduction

Student contribution to work: First author paper. Manuscript preparation and revisions.

Title: **Duchenne muscular dystrophy cell culture models created by CRISPR/Cas9 gene editing and their application in drug screening.**

Authors: Soblechero-Martín P, Albiasu-Arteta E, Anton-Martinez A, de la Puente-Ovejero L, Garcia-Jimenez I, González-Iglesias G, Larrañaga-Aiestaran I, López-Martínez A, Poyatos-García J, Ruiz-Del-Yerro E, Gonzalez F, Arechavala-Gomeza V.

Published in: Sci Rep. 2021 Sep 14;11(1):18188. doi: 10.1038/s41598-021-97730-5. PMID: 34521928; PMCID: PMC8440673.

Location in the thesis: Results

Student contribution to work: First author paper. Performed experiments, statistical analyses, manuscript preparation and revisions.

Congress presentations related to the subject of the current thesis.

1. A novel platform to quantify utrophin expression in cell culture. Presented at the 18th International Congress of Neuromuscular Disorders 2021 (ICNMD 2021). Online.
   Soblechero-Martin P, Lopez-Martinez A, Arechavala-Gomeza V.

2. A novel platform to quantify utrophin expression in cell culture. Presented at the 14th UK Neuromuscular Translational Research Conference. Online (2021).
   Soblechero-Martin P, Lopez-Martinez A, Arechavala-Gomeza V.

3. A CRISPR/Cas9 edition protocol for human myoblasts to generate disease models. Presented at the European Society for Gene and Cell Therapy, abstract published in Human Gene Therapy, Barcelona, Spain (2019).
   Soblechero-Martin P, Albiasu-Arteta E, Anton-Martinez A, Garcia-Jimenez I, Gonzalez-Grassi F, Gonzalez-Iglesias G, Larranaga-Aiestaran I, Lopez-Martinez A, Poyatos-Garcia J, Ruiz-Del-Yerro E, Arechavala-Gomeza V.

4. Advanced therapies for neuromuscular diseases. Presented at the Inaugural Meeting: Delivery of Antisense RNA Therapies (DARTER) COST ACTION CA17103 (2019)
   Soblechero-Martin P, Gonzalez-Iglesias G, Albiasu-Arteta E, Anton-Martinez A, Lopez-Martinez A, Poyatos-Garcia J, Arechavala-Gomeza V.

5. P.291 Overcoming barriers to establish a CRISPR/Cas9 edition protocol for human myoblasts. Presented in the World Muscle Society Congress, Copenhagen, Denmark (2019).
   Soblechero-Martin P, Albiasu-Arteta E, Poyatos-García J, González-Iglesias G, Anton-Martínez A, López-Martínez A, Arechavala-Gomeza V.
   DOI: https://doi.org/10.1016/j.nmd.2019.06.405

6. CRISPR/Cas gene editing in Duchenne muscular dystrophy cultures to test new treatments for the disease. Presented in NEUROGUNE 2018. Vitoria, Spain (2018).
   Soblechero-Martin P, Garcia-Jimenez I, Ruiz-Del-Yerro E, Albiasu-Arteta E, Arechavala-Gomeza V.

7. Mytoblots for the evaluation of new treatments in neuromuscular disorders. Presented in NEUROGUNE 2018. Vitoria, Spain (2018).
   Ruíz-del-Yerro E, Soblechero-Martín P, Larranaga-Aiestaran I, Albiasu-Arteta E, Arechavala-Gomeza V.

8. Mytoblots for the evaluation of new treatments in neuromuscular disorders. Presented in 15th International Congress of Neuromuscular Disorders 2018 (ICNMD 2018). Vienna, Austria (2018). Soblechero-Martin P, Garcia-Jimenez I, Ruiz-Del-Yerro E, Albiasu-Arteta E, Arechavala-Gomeza V.

INDEX

FIGURE INDEX

TABLE INDEX

LIST OF ABBREVIATIONS

A		
	AChR	Acetylcholine receptors
	AhR	Aryl hydrocarbon receptor
	AICAR	5-aminoimidazole-4-carboxamide-1-β-D ribofuranoside
	AMPK	Adenosine monophosphate activated protein kinase
	AONs	Antisense oligonucleotides
	AREs	AU-rich elements
	AVV	Adeno-associated virus
B		
	BMD	Becker muscular dystrophy
	BSA	Bovine serum albumin
C		
	CNS	Central nervous system
	COX	Cyclo-oxygenase
	CRISPR	Clustered regularly interspaced short palindromic repeats
	CRISPRa	CRISPR transcriptional activators
	CRISPRi	CRISPR transcriptional repressors
	CTD	C-terminal domain
D		
	DGC	Dystrophin glycoprotein complex
	dko	Double knock out
	DM	Differentiation medium
	DMD	Duchenne muscular dystrophy
	DSB	Double stranded break
E		
	EMA	European Medicines Agency
F		
	FACS	Fluorescence activated cell sorting
	FBS	Foetal bovine serum
	FDA	Food and drug administration
G		
	GABPα/β	GA-binding protein alpha/beta
	GHSPMD	German shorthaired pointer deletional-null canine model
	GRMD	golden retriever muscular dystrophy
H		
	HDR	Homology-directed repair
	HEK 293	Human embryonic kidney 293 cells
	hiPSCs	Human induced pluripotent stem cells
	HTS	High throughput screening
I		
	IRES	internal ribosome entry site
	ITAFs	IRES trans-acting factors
	IMTR	inhibitory miRNA target region

K		
	KSRP	K-homology splicing regulator protein
M		
	µDys	Micro-dystrophin
	µUtrn	Micro-utrophin
	MAPK	Mitogen-activated protein kinase
N		
	NFAT	Calcineurin-nuclear factor of activated T-cells
	NF-κB	Nuclear factor kappa B
	NHEJ	Non-homologous end joining
	nNOS	Neuronal nitric oxide synthase
	NMJs	Neuromuscular junctions
	NTD	N-terminal actin-binding domain
	NSAID	Nonsteroidal anti-inflammatory drug
O		
	ORF	Open reading frame
P		
	PAM	Protospacer-adjacent motif
	PGC-1α	Peroxisome proliferator-activated receptor gamma coactivator 1α
	PPAR-β/δ	Peroxisome-proliferator-activated receptor beta/delta
	PTCs	Premature stop codons
R		
	ROS	Reactive Oxygen Species
S		
	SBOs	Site-blocking oligonucleotides
	sgRNA	Single guide RNAs
	SIRT	Sirtuin
	SMCM	Skeletal muscle complete medium
U		
	UGC	Utrophin glycoprotein complex
	UTRs	Untranslated regions
Z		
	ZF-ATFs	Zinc finger transcription factors

RESUMEN

La distrofia muscular de Duchenne (DMD) es una enfermedad genética causada por mutaciones en el gen *DMD* que provocan la ausencia de distrofina, una proteína esencial en el mantenimiento de la integridad muscular. Es una enfermedad recesiva, ligada al cromosoma X que afecta a aproximadamente 1 de cada 5000 varones nacidos vivos. Se caracteriza por una degeneración muscular progresiva y, por tanto, los pacientes con DMD suelen experimentar debilidad progresiva y finalmente pérdida de la capacidad de deambulación alrededor de la pubertad, junto con otros síntomas como cardiomiopatía y debilidad diafragmática. En última instancia, la muerte prematura en pacientes con DMD a menudo ocurre debido a complicaciones cardíacas o respiratorias, aunque los avances en cuidados paliativos han contribuido a mejoras en la esperanza de vida.

Las mutaciones en el gen de la distrofina también pueden provocar distrofia muscular de Becker (BMD), una forma menos grave caracterizada por mutaciones que respetan el marco de lectura del gen *DMD*. Esto resulta en la producción de una proteína más corta y parcialmente funcional.

A pesar de los avances significativos en la comprensión de la base molecular de la enfermedad, hasta la fecha, no existe cura para la DMD y los corticosteroides son el tratamiento de elección. Sin embargo, en los últimos años han surgido diversas estrategias terapéuticas, principalmente centradas en restablecer la expresión de distrofina. Actualmente, existen hasta cuatro oligonucleótidos antisentido (AONs) para conseguir restaurar el marco de lectura del gen *DMD* (terapia de salto del exón) que han recibido la aprobación condicional de la FDA. Sin embargo, estas terapias son específicas de cada mutación, limitando su aplicabilidad a un conjunto pequeño de pacientes. Por otro lado, la FDA otorgó recientemente la aprobación acelerada para la primera terapia génica recombinante basada en la administración de un gen capaz de producir micro-distrofina, ofreciendo esperanza a todos los pacientes con DMD independientemente de su mutación.

Un enfoque alternativo potencialmente aplicable a todos los pacientes, independientemente de su mutación genética, consiste en la regulación al alza de la utrofina, una proteína que comparte una homología significativa en secuencia y características estructurales con la distrofina. En el músculo adulto sano, la utrofina se

localiza mayoritariamente en las uniones neuromusculares y miotendinosas, sin embargo, en los pacientes con DMD la ausencia de distrofina conduce a la sobreexpresión de utrofina en el sarcolema de las fibras musculares como mecanismo compensatorio, aunque resulta insuficiente para compensar completamente las funciones de esta proteína. Diversos estudios preclínicos indican que elevar los niveles de utrofina al menos 2 veces por encima de los niveles basales podrían proporcionar beneficios funcionales, por eso la regulación positiva de la utrofina se está explorando como potencial tratamiento de la DMD.

Se han propuesto diversos enfoques para mejorar la expresión de utrofina, como la administración sistémica de micro-utrofinas recombinantes o también la terapia génica con micro-utrofinas. Por otro lado, aunque avances en tecnologías de edición génica, como CRISPR-Cas9 ofrecen la posibilidad de manipular los niveles de expresión de la utrofina, uno de los enfoques más frecuentes de los últimos años ha sido la búsqueda de pequeñas moléculas que actúen bien como reguladores de su transcripción directamente o a nivel postranscripcional. En estudios preclínicos, numerosos compuestos han demostrado activar eficazmente la expresión de utrofina y algunos incluso han avanzado a ensayos clínicos. Sin embargo, entender las diversas vías involucradas en la regulación de la utrofina sigue siendo un desafío que requiere seguir investigando para identificar posibles terapias. Además, las dificultades en la reproducibilidad de resultados entre diferentes laboratorios obstaculizan la transición a la clínica de estas terapias y, por lo tanto, optimizar los métodos de cuantificación de utrofina es crucial para evaluar la eficacia de terapias basadas en su expresión.

Los principales objetivos de este proyecto han sido; en primer lugar, establecer una plataforma de cuantificación de utrofina en cultivos celulares para ser utilizada en la evaluación de posibles terapias; segundo, crear un modelo celular mediante edición génica que sobre exprese endógenamente utrofina y; por último, encontrar nuevas dianas terapéuticas basadas en el incremento de utrofina aplicables a la DMD.

Inicialmente, hemos optimizado dos métodos, el In Cell Western en miotubos o myoblot y la PCR digital (ddPCR) para la cuantificación de utrofina en cultivos celulares. Para optimizar los myoblots de utrofina, hubo que identificar las placas de cultivos más

adecuadas, para evitar interferencias. Además, tras realizar un ensayo de linealidad celular, seleccionamos el número óptimo de células para la siembra tanto de mioblastos control como DMD. Finalmente, seleccionamos el anticuerpo y la concentración que ofrecía la mejor relación señal/ruido para la cuantificación.

Por otro lado, los pasos de optimización de la ddPCR incluyeron, entre otros, la selección de la cantidad de cDNA molde y la temperatura adecuada para establecer el umbral que permitiesen diferenciar correctamente las gotas negativas de las positivas. Dadas las ventajas que ofrece la combinación de ambas técnicas, proponemos su uso como una plataforma de semi-alto rendimiento para la cuantificación de utrofina en el cribado de fármacos.

Además, utilizando herramientas de edición génica CRISPR/Cas9 creamos un modelo celular denominado DMD-UTRN-Model. La edición se llevó a cabo generando varios cortes en la región 3'UTR del gen *UTRN* para aumentar la expresión de utrofina mediante la interrupción de sitios de unión de microARN inhibitorios. Posteriormente, tras confirmar la escisión y la ausencia de cortes indeseados fuera del objetivo, el modelo celular fue evaluado utilizando una batería de pruebas de caracterización que incluyeron la cuantificación de la expresión de utrofina mediante métodos tradicionales y los desarrollados como parte de nuestra plataforma, la evaluación la diferenciación a miotubos y el estudio de posibles cambios en otras proteínas que constituyen el complejo distrofina/utrofina-glicoproteína (DGC/UGC). En esta evaluación hemos demostrado que la expresión de utrofina en el modelo DMD-UTRN-Model está significativamente incrementada con respecto a los cultivos sin editar. Por otro lado, comprobamos que la expresión de algunos factores de diferenciación miogénica, están significativamente disminuidos en el modelo DMD-UTRN, efecto que atribuimos al propio proceso de edición y la posterior selección celular. Finalmente, aunque observamos que la expresión de α-sarcoglicano y β-distroglicano aumentan ligeramente en los cultivos del modelo DMD-UTRN, lo que podría indicar restauración del complejo distrofina/utrofina-glicoproteína, no se encontraron diferencias significativas en comparación con los miotubos de DMD, posiblemente porque la expresión de ambas proteínas se incrementa con la diferenciación a miotubos, que está reducida en el modelo DMD-UTRN. En base a estos resultados, concluimos que el modelo DMD-UTRN

podría ser de utilidad como un control positivo en la evaluación de fármacos que sobre expresan utrofina, y también como prueba de concepto de una posible opción terapéutica para aumentar la expresión de utrofina.

Tanto la optimización de la plataforma de cuantificación de utrofina como la creación del modelo DMD-UTRN nos han facilitado la realización de un amplio cribado de medicamentos en colaboración con la empresa SOM Biotech utilizando un panel de 60 compuestos de reposicionamiento farmacéutico, así como la exploración de nuevas dianas para la sobre expresión de la utrofina.

En el primer estudio se analizaron, utilizando el ensayo de myoblot, 60 pequeñas moléculas junto con ezutromid y halofuginona como controles positivos en una concentración genérica de 5 µM durante 24 horas, y 44 de ellas mostraron un aumento en la expresión de utrofina en miotubos de DMD en comparación con células no tratadas. Posteriormente, se analizaron seis de esos compuestos (C03, C13, C32, C42, ezutromid y halofuginona), y se trataron los mioblastos con 0.01, 0.1, 1 y 10 µM de los fármacos seleccionados durante 24 o 48 horas. Tras este tratamiento, el análisis por ddPCR mostró una regulación al alza de la expresión a nivel de RNA tras los tratamientos con los controles y los compuestos C03 y C13, aunque no se pudieron replicar en estas condiciones nivel de proteína, con la excepción del tratamiento con halofuginona.

En esta búsqueda de nuevas dianas, y tras revisar la bibliografía existente, nos pareció interesante estudiar la relación entre los inhibidores de histona deacetilasas (HDACi) y la expresión de utrofina en cultivos DMD. La acetilación de histonas es uno de los mecanismos epigenéticos que controla la expresión génica y actualmente se conocen hasta 18 tipos de histonas deacetilasas (HDACs) en humanos. La desregulación de HDACs a menudo se asocia con varias patologías, entre ellas las distrofias musculares, donde, por ejemplo, se ha demostrado la sobreexpresión de algunas HDACs en los músculos esqueléticos, lo que sugiere a los HDACi como potenciales terapias. De hecho, este mismo año la FDA ha aprobado el medicamento oral Duvyzat (givinostat) comercializado por Italfarmaco, para la distrofia muscular de Duchenne tras demostrar en ensayos clínicos su eficacia para retrasar la progresión de la enfermedad.

Hay muchos tipos de HDACs y las de clase III se conocen como sirtuinas. En humanos, la familia de las sirtuinas consta de siete miembros (Sirt1 - Sirt7) que regulan la actividad de diferentes proteínas nucleares y citoplasmáticas, participando en funciones clave en la regulación del metabolismo, el estrés celular y la longevidad. Diferentes sirtuinas han demostrado estar desreguladas en varias enfermedades, incluida la DMD, despertando un interés considerable como posibles objetivos terapéuticos en los últimos años. Algunas de ellas, como la sirtuina 1 y la sirtuina 6, se han relacionado directamente con cambios en la expresión de utrofina en la DMD. Varios estudios han demostrado que algunos agentes exógenos pueden aumentar la expresión/actividad de la sirtuina 1, aumentando así la expresión de utrofina y mejorando la patología de la DMD. Más recientemente, un estudio demostró que la sirtuina 6 estaba significativamente aumentada en los cultivos de células del modelo de ratón *mdx* y que suprimía la expresión de utrofina en músculos distróficos. La inactivación de la sirtuina 6 aumentó la expresión de utrofina y eliminó varios marcadores patológicos característicos de los ratones *mdx*.

En base a estos hallazgos, en este trabajo estudiamos la relación entre la sirtuina 2 y la expresión de utrofina en miotubos humanos control y DMD. Cuantificando tanto la expresión de *SIRT2* mediante ddPCR como la proteína sirtuina 2 mediante myoblot, comprobamos que están significativamente aumentadas en los miotubos DMD en comparación con los controles. Posteriormente, planteamos como hipótesis que inhibir la expresión de la sirtuina 2 podría aumentar los niveles de utrofina en cultivos de células DMD y para seleccionamos un inhibidor selectivo de la sirtuina 2, el compuesto AGK2, para estudiarlo. Los miotubos DMD se trataron con concentraciones crecientes de AGK2 que en todos los casos provocaron un aumento significativo en la expresión de utrofina, superando la expresión del modelo DMD-UTRN que utilizamos como control positivo. Tras ello, decidimos realizar un pequeño ensayo *in vivo* y estudiar la expresión de utrofina en ratones *mdx* tratados con AGK2. El ensayo de inmunohistoquímica verificó que el tratamiento con AGK2 aumentaba la expresión de utrofina en las fibras musculares de los ratones, tanto control como *mdx*. No hemos encontrados referencias anteriores que atestigüen la relación entre la sirtuina 2 y la utrofina en cultivos de músculo humano y, aunque se necesitan más estudios, proponemos la sirtuina 2 como

un objeto de estudio potencial en la DMD y su inhibición como posible nuevo enfoque para la regulación al alza de la utrofina.

SUMMARY

Duchenne muscular dystrophy (DMD) is a genetic disease caused by mutations in the *DMD* gene, resulting in the absence of dystrophin, an essential protein for maintaining muscle integrity. DMD is a recessive, X-linked disease that affects approximately 1 in 5000 live male births. It is characterised by progressive muscle degeneration, and as the disease progresses, DMD patients typically experience progressive weakness and eventual loss of ambulation around puberty, along with other symptoms such as cardiomyopathy and diaphragmatic weakness. Ultimately, premature death in DMD patients often occurs due to cardiac or respiratory complications, although advances in palliative care have contributed to improvements in their life expectancy.

Mutations in the dystrophin gene can also cause Becker muscular dystrophy (BMD), a milder disease characterised by mutations that preserve the open reading frame of the *DMD* gene. This results in the production of a shorter, partially functional, protein.

Despite significant advances in understanding the molecular basis of the disease, to date there is no cure for DMD, and corticosteroids are the current treatment of choice. However, in recent years various therapeutic strategies have emerged, mainly focused on restoring dystrophin expression. Currently, there are four antisense oligonucleotides (AONs) designed to restore the reading frame of the *DMD* gene (exon skipping therapy) that have received conditional FDA approval. However, these therapies are mutation-specific, limiting their applicability to a subset of patients. On the other hand, the FDA recently granted accelerated approval for the first gene therapy based on the administration of a gene capable of producing micro-dystrophin, offering hope to all DMD patients regardless of their mutation.

An alternative approach potentially applicable to all patients regardless of their genetic mutation is the upregulation of utrophin, a protein that shares significant sequence homology and structural characteristics with dystrophin. In healthy adult muscle, utrophin is predominantly located at neuromuscular and myotendinous junctions. However, in DMD patients, the absence of dystrophin leads to the compensatory upregulation of utrophin on the sarcolemma of muscle fibers, although it is insufficient to fully compensate for the functions of this protein. Various preclinical studies indicate that raising utrophin levels at least 2 times above baseline could provide functional

benefits, so positive regulation of utrophin is being explored for the potential treatment of DMD.

Various approaches have been proposed to enhance utrophin expression, such as systemic administration of recombinant micro-utrophins or gene therapy with micro-utrophins. Furthermore, advances in gene editing technologies, such as CRISPR/Cas9, offer the possibility of manipulating utrophin expression levels. However, one of the most common approaches in recent years has been the search for small molecules that act either as transcriptional regulators or at the post-transcriptional level of utrophin expression. In preclinical studies, numerous compounds have been shown to effectively activate utrophin expression, and some have even advanced to clinical trials. However, understanding the various pathways involved in utrophin regulation remains a challenge that requires further research to identify potential new therapies. Additionally, difficulties in reproducibility of results across different laboratories hinder the transition to clinical use of these therapies, and thus, optimizing utrophin quantification methods is crucial for evaluating the efficacy of novel therapies.

The main objectives of this project have been, firstly, to establish a utrophin quantification platform in cell cultures for use in the evaluation of potential therapies; secondly, to create a cellular model through gene editing that overexpresses endogenous utrophin; and lastly, to find new therapeutic targets based on utrophin upregulation applicable to DMD.

Initially, we optimized two methods, the In Cell Western of myotubes or “myoblot” and digital PCR (ddPCR) for utrophin quantification in cell cultures. To carry out the myoblot assay, we selected a specific type of culture plates, selected the appropriate number of cells for seeding both control myoblasts and DMD cultures and the antibody and concentration that offered the best signal-to-noise ratio.

On the other hand, optimization steps for ddPCR included, among others, selecting the optimal amount of cDNA template, the appropriate temperature and to establish the threshold that allowed for correct differentiation of negative and positive droplets. Given the advantages offered by combining both techniques, we propose their use as a semi-high-throughput platform for utrophin quantification in drug screening.

Subsequently, using a CRISPR/Cas9-mediated strategy, we created a cellular model that we called DMD-UTRN-Model. The gene editing was carried out by generating several cuts in the 3'UTR region of the UTRN gene and disrupting binding sites of inhibitory microRNAs to increase utrophin expression. Subsequently, after confirming the excision and absence of undesired off-target cuts, the cellular model was evaluated using a battery of characterization tests that included quantification of utrophin expression using both traditional and our recently developed methods, as well as the evaluation of differentiation of cultures into myotubes, and the study of possible changes in other proteins of the dystrophin/utrophin associated complex. In this evaluation, we demonstrated that utrophin expression in the DMD-UTRN-Model is significantly increased compared to original unedited DMD myotubes. On the other hand, we showed the expression of some myogenic differentiation factors, was significantly decreased in the DMD-UTRN model which could be attributed to the aggressive gene editing process and the single cell sorting process. We also observed that the expression of α-sarcoglycan and β-dystroglycan was slightly increased in the cultures of the DMD-UTRN model, which could indicate a functional restoration of the utrophin associated complex, but which was not statistically, maybe because expression of this both proteins is related with myotube formation, reduced in the DMD-UTRN-Model. significant. Based on these results, we conclude that the DMD-UTRN model could be useful as a positive control in the evaluation of drugs that aim to overexpress utrophin, and as a proof of concept for a potential therapeutic option to increase utrophin expression.

Both the optimization of the utrophin quantification platform and the creation of the DMD-UTRN model have facilitated the completion of a broad drug screening in collaboration with a biotech company (SOM Biotech) testing a panel of repurposing compounds. In this study, 60 small molecules were analysed at a concentration of 5 µM for 24 hours along with ezutromid and halofuginone as positive controls using the myoblot assay. Treatment with 44 of them showed an increase in utrophin expression in DMD myotubes compared to untreated cells and six of these compounds showing a bigger response (C03, C13, C32, C42, ezutromid, and halofuginone) were analysed further: myoblasts were treated with 0.01, 0.1, 1, and 10 µM concentrations for 24 or 48 hours with the selected drugs and ddPCR analyses showed upregulation of utrophin

at RNA levels after treatment with the positive controls halofuginone and ezutromid and compounds C03 and C13 . At protein level, only halofuginone showed an increase of utrophin expression in these conditions.

In the search for new targets, after reviewing the existing literature, we became interested in the relationship between histone deacetylase inhibitors (HDACi) and utrophin expression in DMD cultures. Histone acetylation is one of the epigenetic mechanisms that control gene expression and up to 18 types of histone deacetylases (HDACs) are currently known in humans. HDAC dysregulation is often associated with various pathologies, including muscular dystrophies, where overexpression of some HDACs in skeletal muscle has been described, suggesting HDACis as potential therapies. In fact, this year the FDA has approved the oral drug Duvyzat (givinostat) marketed by Italfarmaco for the treatment of Duchenne muscular dystrophy after demonstrating in clinical trials its efficacy in delaying disease progression.

There are several types of HDACs, and class III are known as sirtuins. In humans, the sirtuin family consists of seven members (Sirt1 - Sirt7) that regulate the activity of different nuclear and cytoplasmic proteins, participating in key functions in the regulation of metabolism, cellular stress, and longevity. Different sirtuins have been shown to be dysregulated in various diseases, including DMD, sparking considerable interest as potential therapeutic targets in recent years. Some of them, such as sirtuin 1 and sirtuin 6, have been directly related to changes in utrophin expression in DMD. Several studies have shown that some exogenous agents can increase sirtuin 1 expression/activity, thereby increasing utrophin expression and improving DMD pathology. More recently, a study demonstrated that sirtuin 6 was significantly increased in cell cultures of the *mdx* mouse model and suppressed utrophin expression in dystrophic muscles. Inactivation of sirtuin 6 increased utrophin expression and eliminated several pathological markers characteristic of *mdx* mice.

Based on these findings, in this work we studied the relationship between sirtuin 2 and utrophin expression in control and DMD human myotubes. We studied the expression of *SIRT2* by ddPCR and quantified sirtuin 2 protein by myoblot, showing a significantly increase in DMD myotubes compared to controls. Subsequently, we hypothesized that

inhibiting sirtuin 2 expression could increase utrophin levels in DMD cell cultures and, for that purpose, we chose a selective sirtuin 2 inhibitor: the compound AGK2. We treated DMD myotubes with increasing concentrations of AGK2 and found a significant increase in utrophin expression at all tested concentrations, surpassing the expression of the DMD-UTRN model used as a positive control. Then, we decided to conduct a small *in vivo* trial and study utrophin expression in *mdx* mice treated with AGK2. The immunohistochemistry assay verified that treatment with AGK2 increased utrophin expression in muscle fibres in both control and *mdx* mice groups. As far as we know, the relationship between sirtuin 2 and utrophin in human muscle cultures has never been reported before and, although further studies are needed, we propose sirtuin 2 as a potential target in DMD research and the inhibition of sirtuin 2 as a novel approach for upregulating utrophin.

INTRODUCTION

Duchenne muscular dystrophy

Duchenne muscular dystrophy (DMD) is a fatal neuromuscular disease caused by a variety of mutations in the *DMD* gene, located on Xp21, which encodes dystrophin (1), a large structural protein essential for maintaining muscle integrity. Characterised by severe and progressive muscle wasting and weakness, DMD is the most common inherited muscle disease, affecting approximately 1 in 5000 live male births worldwide because of its X-linked recessive inheritance, although female carriers can occasionally develop symptoms (2, 3).

The *DMD* gene is the largest gene identified to date. It contains many independent, tissue-specific promoters and produces several dystrophin isoforms in addition to the full-length muscle isoform (Dp427m), such as the full-length dystrophins Dp427c and Dp427p dystrophins, which are expressed in cortical neurons and cerebellar Purkinje cells respectively; and shorter isoforms including Dp260, Dp140, Dp116, and Dp71, which have been identified in the central nervous system, retina, and kidney (4) (Figure 1).

The full-length muscle dystrophin isoform has four main domains: an N-terminal actin-binding domain (NTD), a central spectrin-like repeat region, a cysteine-rich domain (CR) and a C-terminal domain (CTD) (Figure 1). In the adult skeletal muscle, dystrophin provides a link between the extracellular matrix and the actin cytoskeleton by assembling into the dystrophin-glycoprotein complex (DGC) (5)(Figure 2).

During contractile activity in DMD patients, dystrophin absence leads to sarcolemmal fragility and fibre damage. In adult muscle, satellite cells can generate new fibres to replace the damaged ones, but eventually, after many cycles of degeneration and regeneration muscle tissue is replaced by adipose and connective tissue and clusters of inflammatory cells. In addition, a complex set of pathophysiological mechanisms underlies the pathogenesis of DMD, including aberrant ion homeostasis such as abnormal calcium influx, dysregulation of energy metabolism, increased oxidative stress and reactive oxygen species (ROS) and chronic inflammation phenotype in dystrophic fibres (6).

DMD patients are typically diagnosed in early childhood when they manifest their first signs of muscle weakness, motor delay and walking difficulties. With disease progression, patients experience loss of ambulation becoming wheelchair dependent around puberty as well as other symptoms such as cardiomyopathy and diaphragmatic weakness. In addition to skeletal muscle pathology, some DMD patients suffer from cognitive and behavioural problems that have been associated with distal mutations in the dystrophin gene due to loss of central nervous system (CNS) isoforms. Finally, DMD patients die prematurely due to cardiac or respiratory complications, although thanks to improvements in palliative care, have increased life expectancy and quality of life, and many patients may survive beyond the age of 30 (3).

Dystrophin mutations can also cause Becker muscular dystrophy (BMD), a milder form of dystrophy caused by in-frame mutations in the *DMD* gene, leading to the expression of a shorter and partially functional dystrophin protein. Individuals with BMD share signs and symptoms with patients with DMD, but they present a much later disease onset, a milder muscle involvement and a near average life expectancy (7).

Utrophin protein and its role in Duchenne muscular dystrophy

Utrophin, originally known as “dystrophin-related protein”, is a 395 kDa autosomal paraloge of dystrophin that is naturally overexpressed at the sarcolemma of regenerating fibres in Duchenne and Becker patients as well as in the *mdx* Duchenne mouse model. Utrophin has therefore been proposed as a surrogate protein that may compensate for the lack of dystrophin.

Utrophin is encoded by the *UTRN* gene, located in the human chromosome 6q24 (8). To date, two full-length utrophin isoforms have been identified, utrophin A and B. These isoforms are transcribed from two different promoters, A and B. The two mRNAs differ at their 5’ ends, resulting in two identical functional proteins with slightly different N-terminal domains and different expression patterns. While utrophin A is expressed in a variety of structures, including neuromuscular junctions, choroid plexus, pia mater, and renal glomerulus (9), utrophin B remains restricted to the endothelial cells (10).

Interestingly, five novel 5' utrophin isoforms (A', B', C, D, and F) have recently been identified in human adult and embryonic tissues, but they remain to be fully characterised (11). Like in the *DMD* gene, the *UTRN* gene transcripts also have internal promoters producing shorter transcripts such as Up71, Up140, and G-utrophin, which are expressed in many tissues with functions not yet fully understood (12) (Figure 1).

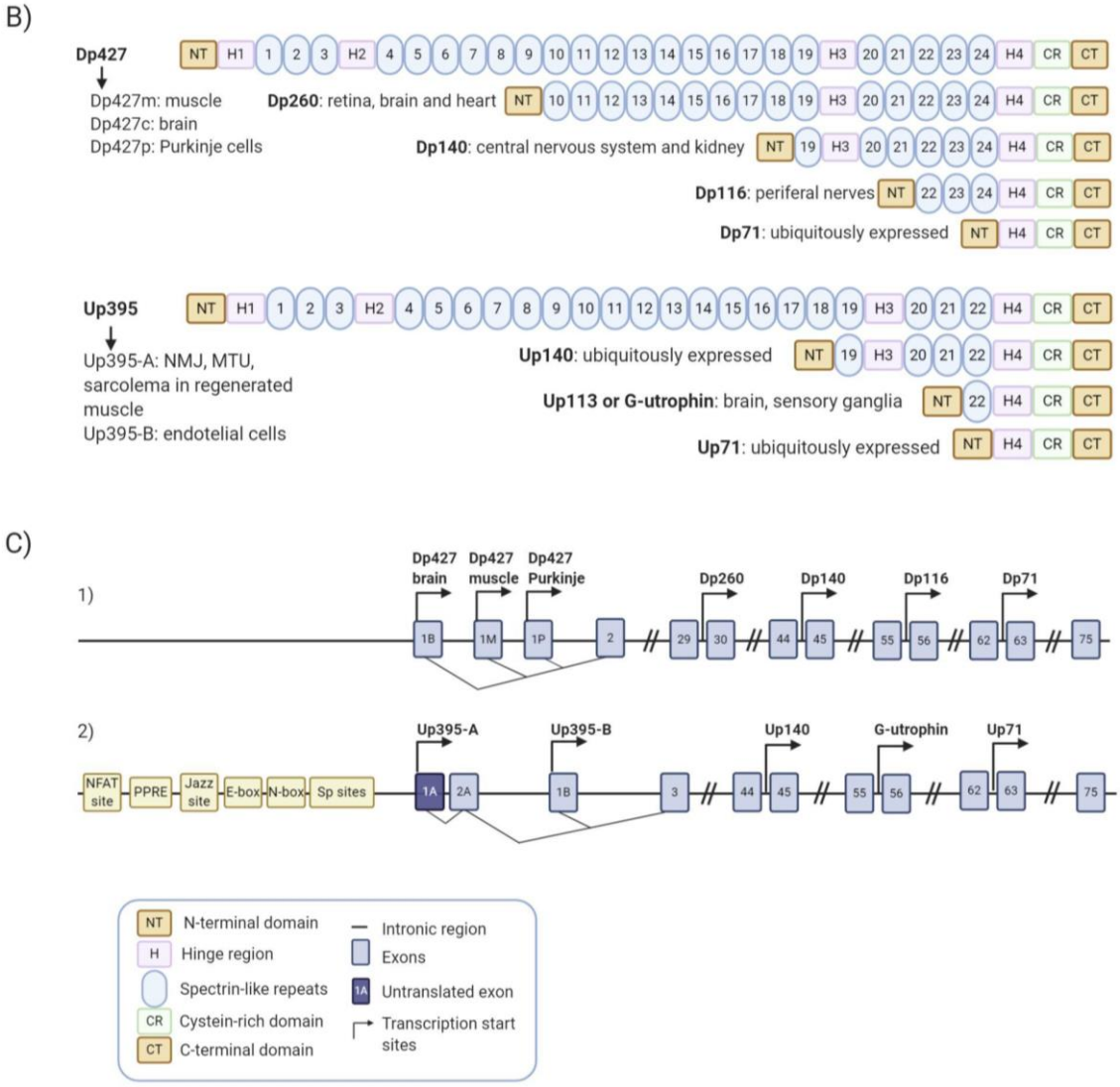

Figure 1. Dystrophin and utrophin isoforms.

Schematic representation of the full length and truncated dystrophin (A) and utrophin (B) protein isoforms including their most representative expression in tissues. (C1 and C2) Blue boxes show the specific exons, the black line represents the intronic regions and the transcription start sites of the different promoters are indicated by arrows within the dystrophin (C1) and the utrophin (C2) gene. (C1) Full-length dystrophin expression is driven by three promoters Dp427 brain, muscle and Purkinje and the smaller isoforms are produced from four internal promoters, Dp260, Dp140, Dp116 and Dp71. (C2) Full-length utrophin expression is driven by two promoters Up395-A and Up395-B and the smaller isoforms are produced from three internal promoters Up140, G-utrophin and Up71. Different elements of the utrophin A promoter are also specified in the panel. Adapted from Soblechero-Martin P, *et al*(13). Created with BioRender.com.

Utrophin protein binds to the cell membrane through the utrophin glycoprotein complex and shares the four main domains with dystrophin, but with some structural and mechanical differences (Figure 2). Utrophin differs from dystrophin in its interactions with actin (5) and contains fewer spectrin-like repeats, sharing only a 35% homology in the central domain with dystrophin. Moreover, a significant difference in the mechanical behaviour between spectrin repeats has recently been demonstrated (14). Crucially, they also differ in their ability to recruit neuronal nitric oxide synthase (nNOS), which cannot be recruited by utrophin(15). nNOS, a signalling protein associated with the DGC that produces nitric oxide (NO), is considerably reduced in dystrophic muscle fibres, leading to functional ischaemia due to decreased contraction-induced vasodilation.

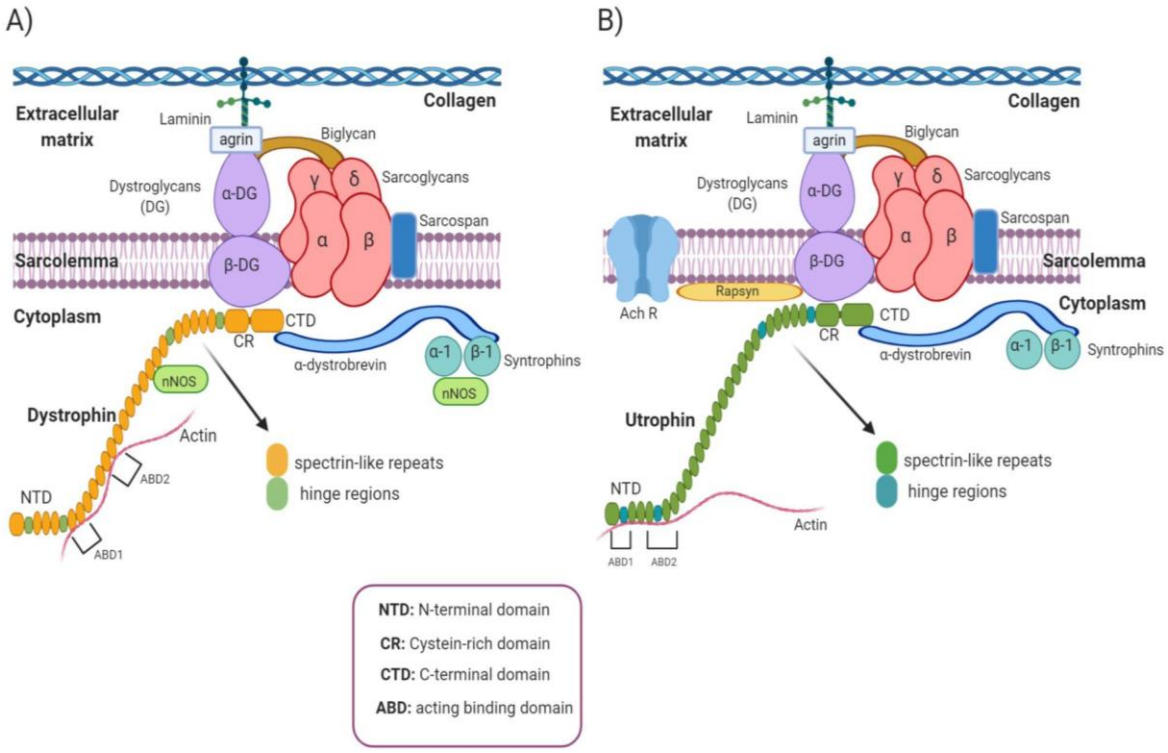

Figure 2. Schematic representation of dystrophin and utrophin glycoprotein complexes (DGC/UGC).

A) Dystrophin glycoprotein complex (DGC) and (B) utrophin glycoprotein complex (UGC) consist of dystrophin (or utrophin), syntrophins, dystrobrevins, sarcoglycans, sarcospan, and dystroglycans distributed in cytoplasmic, transmembrane, and extracellular protein complex. The cytoplasmic part includes α1 and β1 syntrophin isoforms and α-dystrobrevin; transmembrane part includes the sarcoglycan (α, β, γ, δ) and sarcospan complex. Dystroglycan complex consists in the extracellular component, α-dystroglycan (α-DG) which binds to agrin and laminin in the extracellular matrix and the transmembrane isoform β -dystroglycan (β-DG). Biglycan is another extracellular matrix component of the DGC/UGC that

binds to α-dystroglycan and α- and γ-sarcoglycan. Finally, β-DG binds to dystrophin or utrophin, completing the link between the actin-based cytoskeleton and the extracellular matrix. Furthermore, utrophin is associated with large acetylcholine receptors (AChR) clusters at the crests of post-junctional folds in neuromuscular junctions (NMJs). Notice that the main differences between dystrophin and utrophin are their lateral interactions with actin and the impossibility of the UGC to recruit nNOS. Adapted from Soblechero-Martin P, *et al* (13). Created with BioRender.com

While dystrophin is predominantly expressed in muscle and to a lesser extent in the brain, utrophin is widely expressed in several non-skeletal muscle tissues such as lung, kidney, and liver (16). During foetal muscle development and at early gestational stages, utrophin is present at the sarcolemma of muscle fibres. After birth, utrophin is progressively silenced by the Ets-2 repressor factor and replaced by dystrophin in adult muscle fibers. Thereafter, utrophin disappears from the membrane, and its expression is confined to the neuromuscular and myotendinous junctions, where it participates in postsynaptic membrane maintenance and acetylcholine receptor clustering (17, 18). However, there is an increase in utrophin expression and redistribution of this protein to the sarcolemma in the dystrophic muscle, in mature dystrophin-deficient fibres, regenerating fibres, and dystrophin-competent revertant fibres found in both DMD and BMD patients, as well as in *mdx* mice, compared to healthy individuals (19, 20).

Utrophin overexpression in DMD

The natural increase of utrophin in DMD is a repair process that has been proposed as a compensatory mechanism to mitigate the lack of dystrophin (20-22). In addition, preclinical studies indicate an inverse correlation between utrophin expression and disease severity in DMD, suggesting that utrophin may play a role as a dystrophin surrogate. However, while some human studies report a positive effect of this utrophin expression on disease severity by delaying disease progression (23), others find no correlation (24).

The most widely used animal model for DMD research is the *mdx* mouse, which carries a nonsense point mutation (C to T transition) in exon 23 of the *Dmd* gene that completely abolishes dystrophin expression. Despite being dystrophin deficient, *mdx* mice have

mild clinical symptoms and a long lifespan, in contrast to DMD patients (25). Utrophin levels are increased at the sarcolemma of regenerating myofibres in the adult *mdx* skeletal muscle (26, 27), but this increase may also occur independently of regeneration (28). Moreover, experimental data suggest that upregulation of utrophin may compensate for dystrophin deficiency. The potential compensatory role of utrophin was investigated by generating double knockout mice for both dystrophin and utrophin genes (*dko*). These mice display a much more severe pathology compared to *mdx* mutants, as well as multiple systemic degenerative changes, in addition to earlier muscle degeneration (29). On the other hand, the *Fiona* mouse, a dystrophin-deficient *mdx* transgenic mouse that overexpresses utrophin, shows a correction of the dystrophic phenotype (27-30).

Over the years, preclinical studies have demonstrated that transgenic overexpression and pharmacological modulation of utrophin prevents skeletal muscle pathology in *mdx* mice. These studies reveal that a 2-fold increase in sarcolemmal utrophin completely rescues the mechanical function and effectively normalises classic markers of DMD-related muscle damage (31, 32). However, even a 1.5-fold increase may be beneficial in *mdx* mice, given that utrophin localises at the sarcolemma of dystrophic fibres (27). Utrophin levels also influence mitochondrial pathology, which contributes to oxidative stress and propagates muscle damage in DMD. While utrophin deficiency exacerbates the pathology, utrophin overexpression in the dystrophic muscle supports mitochondrial function in mouse models (33). Interestingly, another study focusing on the role of utrophin as a substitute for dystrophin in the male reproductive system discovered that full-length dystrophin deficiency disturbs the balance between germ cell proliferation and apoptosis during spermatogenesis. In this case, utrophin is also upregulated and translocated as a compensatory response to dystrophin deficiency (34). Taken together, data from animal models suggest that utrophin can functionally compensate for the lack of dystrophin.

Therapeutic strategies for Duchenne muscular dystrophy

To date, there is still no cure for DMD. Corticosteroids, such as prednisone or deflazacort, are the current standard of care and the only pharmacological intervention proven to delay the disease progression (35) despite the known adverse effects such as obesity and immunosuppression (36). Recently, a new dissociative corticosteroid called vamorolone has been developed as an alternative to classical corticosteroids, showing an improved efficacy profile and fewer side effects Vamorolone (AGAMREE®), developed by ReveraGen BioPharma and Santhera Pharmaceuticals, received approval from the European Medicines Agency (EMA) and the Food and Drug Administration (FDA)in October 2023, making it the first drug approved both in EU and USA for the treatment of patients with muscular dystrophy (37).

Additionally, DMD disease requires a multidisciplinary approach to care, which is essential for optimum management of the primary manifestations and secondary complications including rehabilitation, respiratory support, cardiac monitoring, and endocrine and nutritional management (38-40) among others.

Current therapeutic strategies for DMD could be divided into three lines: the first line focuses on targeting the primary defect aiming to restore dystrophin expression and/or function, the second line is based on utrophin upregulation to act as a dystrophin surrogate and the third line tries to mitigate the secondary pathology caused by the dystrophin deficiency, including muscle atrophy, inflammation, and fibrosis.

Dystrophin-targeted therapies

DMD-causing mutations include large and short deletions (65%), duplications (5–10%) and point mutations (10–15%), which are mainly frameshift mutations. In addition, its large size makes it susceptible to a high rate of sporadic mutations and over 7,000 different mutations have been reported. This makes the development of gene correction therapies suitable for patients with different dystrophin mutations

considerably challenging and most of these therapies are only applicable to a small group of patients sharing the specific mutations (41).

1. Read-through compounds

Readthrough strategies would be applicable in DMD patients carrying nonsense mutations, point mutations that promote the conversion of sense codons to nonsense codons (UAA, UAG, or UGA), called premature stop codons (PTCs), leading to translation termination and abolish dystrophin expression.

Readthrough compounds can recognise a mutated premature stop signal and encourage the cell machinery to ignore it, allowing protein translation to continue and producing a functional dystrophin protein.

The aminoglycoside antibiotic gentamicin was the first readthrough compound investigated to reach clinical trials for the treatment of DMD (42). However, the need for regular intravenous administration, and toxicity experienced after long term administration discouraged its use in the clinic.

Using luciferase-based high-throughput screening assays, PTC Therapeutics identified a compound called PTC124 or ataluren, which showed efficient read-through in the *mdx* mouse model (43). Ataluren is an orally bioavailable small readthrough molecule and was evaluated in two randomised, double-blind, placebo-controlled trials that did not meet the primary endpoints but showed a favourable benefit–risk profile and efficacy compared to placebo on several functional endpoints (44). Ataluren was never approved by the FDA, but the EMA considered the data and granted conditional approval in 2014, after which it was commercialised as Translarna®. The conditional approval was subject to annual renewal based on the results of additional studies required of the marketing authorisation holder. After several studies carried out in the recent years and a re-evaluation of the data obtained, the EMA's human medicines committee (CHMP) recommended in January 2024 that the marketing authorisation for Translarna® in the EU should not be renewed, concluding that its benefit-risk balance was negative and its efficacy in DMD patients with nonsense mutations had not been confirmed. Once this

recommendation is confirmed by the European Commission, the medicine will no longer be authorised in the EU.

2. Exon skipping

Exon skipping therapies are applicable to DMD patients carrying frameshift mutations, mutations that cause a shift in the translational open reading frame (ORF) of the amino acid chain, resulting in the absence of dystrophin.

The restoration of the reading frame is achieved with antisense oligonucleotides (AONs): small single-stranded nucleic acid oligomers capable of specifically binding to a target sequence in the pre-mRNA and modulating splicing. This binding prevents the inclusion of the target exon in the mature RNA, thereby removing one or more exons and generating an in-frame sequence.

To date, four different mutation-specific RNA treatments for DMD have been conditionally approved by the FDA: eteplirsen (45), golodirsen (46), viltolarsen (47) and casimersen (48) (Table1) while other six candidates are in varying stages of Phase II trials: ATL1102 (Antisense Therapeutics), SCAAV9.U7.ACCA (Astellas Pharma), SRP-5051 (Sarepta), NS-089/NCNP-02 (NS Pharma), WVE-N531 (Wave Life Sciences), and DS-5141B (Daiichi Sankyo) (49).

Table 1. Exon skipping therapies approved by the FDA.

Drug name	Commercial name	Skipped exon	% of patient application	Manufacture	Approval year
Eteplirsen	Exondys 51®	51	13	Sarepta Therapeutics	2017
Golodirsen	Vyondys 53®	53	13		2019
Vitolarsen	Viltepso®	53	13	NS Pharma	2020
Casimersen	Amondys 45®	45	8	Sarepta Therapeutics	2021

These therapies aim to restore the ORF to produce a truncated but partially functional protein, as in BMD. However, they are only applicable to a small percentage of DMD

patients, and their approval is controversial due to the low efficacy in dystrophin restoration and the limited clinical efficacy demonstrated to date (50). Moreover, their delivery and uptake into the muscle tissue is challenging (51) and in addition they have a transient effect and need to be administered repeatedly with the high associated costs this involves.

3. Gene therapy

One of the main challenges in the development of gene therapy for DMD is that the whole dystrophin gene is too large to be packaged in adeno-associated viruses (AAV), which are currently the most used delivery vectors (52). For this reason, miniature versions of the dystrophin gene that lack unnecessary domains (called “mini” or “micro” dystrophins) have been engineered. Micro-dystrophins can be packaged into adeno-associated viruses and encode a shorter, but functional, version of the dystrophin protein, mimicking dystrophin expression in BMD patients. AVV-micro-dystrophin gene therapy can be delivered to target cells, by intravenous or intramuscular injection, and AAV vectors are translocated to the cell nucleus where transgenes are released.

In 2023, the FDA granted accelerated approval for delandistrogene moxeparvovec, a gene therapy for the treatment of ambulatory paediatric patients with DMD aged 4-5 years. This new drug is developed by Sarepta Therapeutics and marketed under the name Elevidys, is the first gene therapy approved for the treatment of DMD (53).

4. CRISPR-Cas9 gene editing

Alternative mutation-specific strategies, like gene editing, have been under intense investigation in several laboratories worldwide. Gene editing using the clustered regularly interspaced short palindromic repeats (CRISPR) system is a promising therapeutic approach for DMD because it can permanently correct DMD mutations and restoring the reading frame and allowing the production of functional dystrophin.

CRISPR was originally discovered as an adaptive immune system in bacteria and archaea to defend against viruses and plasmids. Briefly, when prokaryotes are invaded by foreign

elements, they can integrate short fragments of the foreign sequence (protospacers) into their chromosome at the CRISPR site. The spacer sequences in CRISPR arrays are transcribed to generate CRISPR RNAs (crRNAS) which direct the Cas protein with endonuclease activity to cleave complementary nucleic acids of foreign DNA in a second invasion, thereby protecting the host (54, 55). Years later, it was discovered that the CRISPR/Cas system could be used as a DNA editing tool by designing guide RNAs to target specific regions in the genome, resulting in the silencing or activating of genes (56) (Figure 3).

The CRISPR/Cas9 editing system consists of two main components: the Cas endonuclease and the single guide RNA (sgRNA), that directs Cas to a specific complementary sequence target site in the genome that is immediately preceded by a specific protospacer adjacent motif (PAM) sequence. There are multiple Cas endonucleases that originate from different bacterial species. SpCas9C is the most studied and commonly used type of endonuclease for gene editing. Cas9 is derived from *Streptococcus pyogenes* and recognises and catalyses a double-stranded break (DSB) in the DNA at the position 3 base pairs upstream of its protospacer adjacent motif (PAM) sequence 5'-NGG-3' or 5'-NAG-3' (57).

Induction of targeted DSBs stimulates the two main endogenous cellular DNA repair mechanisms: non-homologous end joining (NHEJ) or homology-directed repair (HDR). In the NHEJ pathway. broken DNA ends are rejoined without templates, but often generate random insertions and deletions (indels) at the site of repair. It is often the pathway of choice when using CRISPR/Cas9 to generate genetic knockouts. The HDR pathway cells use homologous DNA as a repair template to precisely repair DNA by delivering a homologous donor DNA along with editing reagents, allowing precise modification of the genome (58).

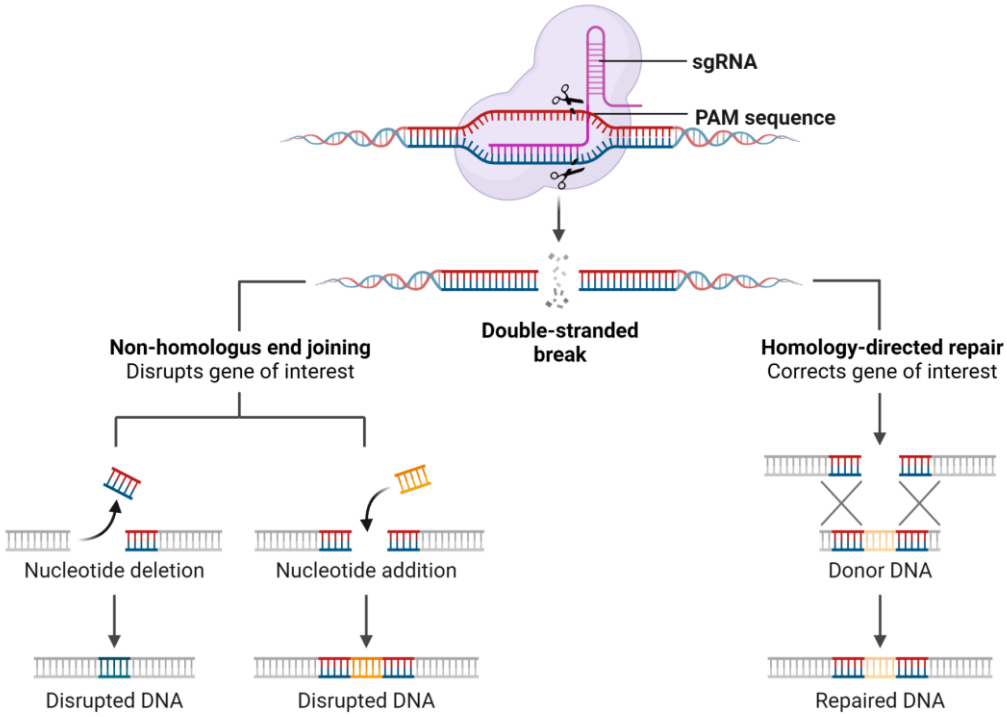

Figure 3. Schematic representation of CRISPR/Cas9 system.

CRISPR/Cas 9 components applied for gene editing and cellular DNA repair mechanisms after DSBs. Adapted from Dragt, E. (2020), BioRender.

CRISPR editing has been widely employed not only to permanently correct various *DMD* mutations in human myoblasts, induced pluripotent stem cells (iPSCs) and animal models but also to generate new cell and animal models of the disease (59-61) that closely mimic the wide variety of mutations observed in DMD patients. These models provide a tool for testing CRISPR therapy as well as other therapies (Figure 4).

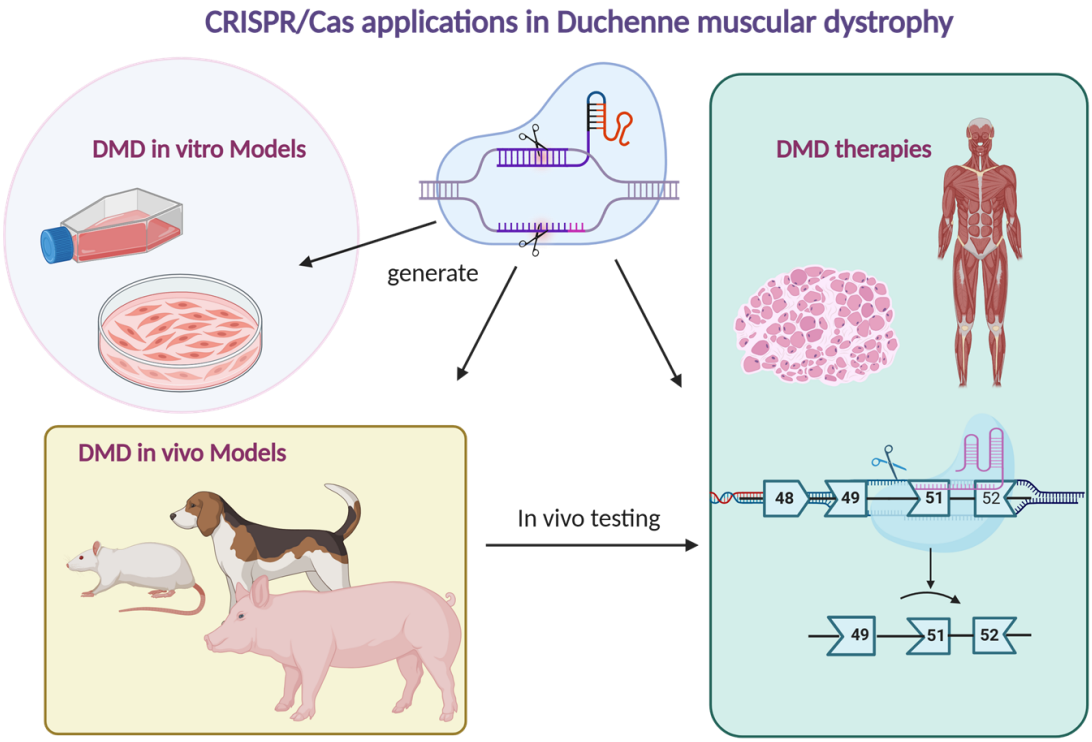

Figure 4. CRISPR/Cas9 applications in DMD.

CRISPR/Cas9 gene editing technology enables the rapid generation of cell cultures and animal models for Duchenne muscular dystrophy research and could serve as a therapy for the permanent correction of different mutations in the *DMD* gene. Adapted from Chey YCJ *et al.* From animal models to potential therapies. WIREs Mech Dis. 2023 Jan;15(1): e1580. doi: 10.1002/wsbm.1580. Epub 2022 Jul 31. PMID: 35909075; PMCID: PMC10078488.

The different CRISPR-Cas system approaches used by the DMD scientific community could be divided into traditional CRISPR methods that induce targeted DSBs in the DMD sequence (Figure 5A) and novel strategies that do not require DSBs, like base editing and prime editing (Figure 5B) (61).

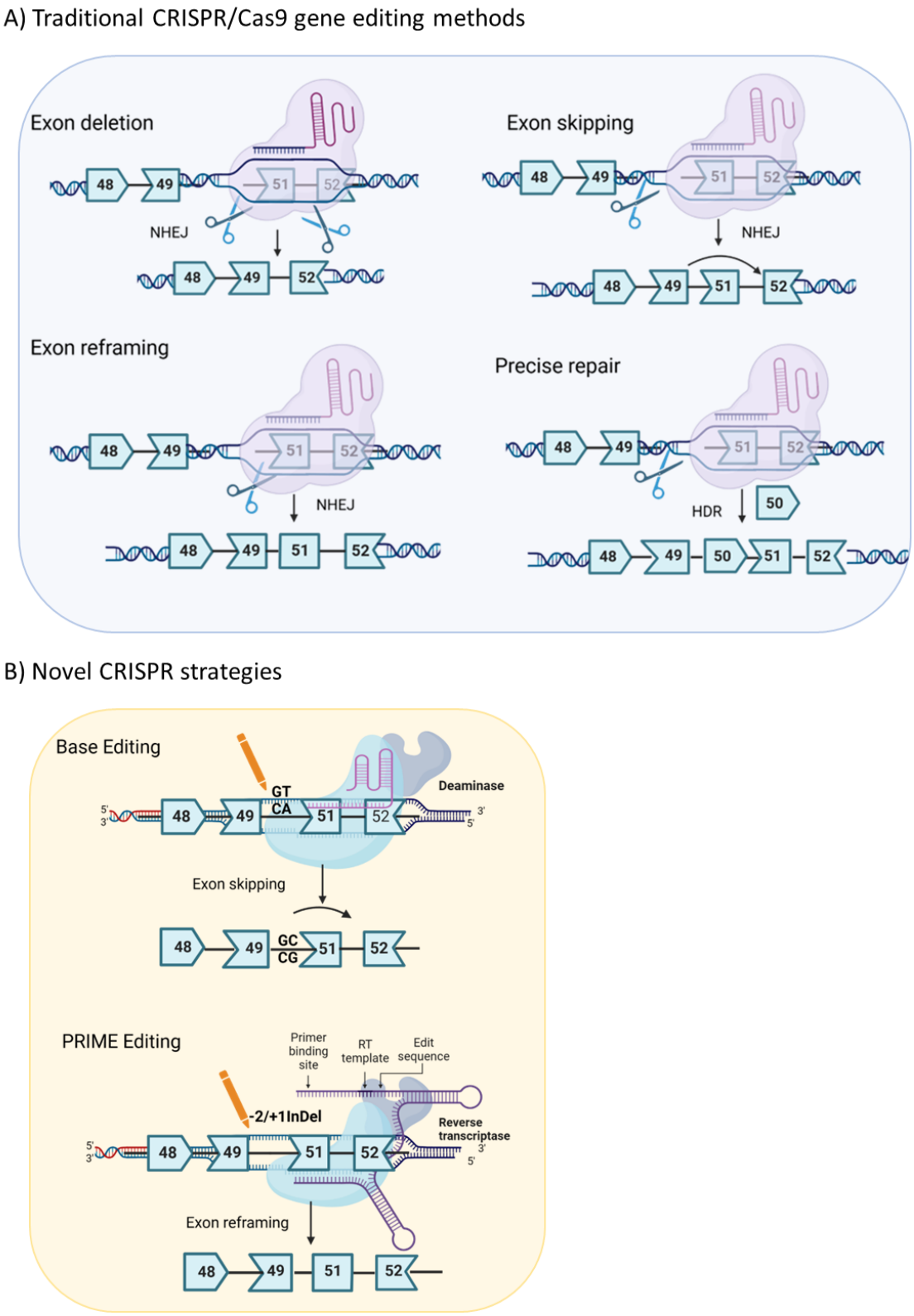

Figure 5. Therapeutic strategies for CRISPR-based genome editing.

Schematic illustration CRISPR strategies for DMD correction of reading frame-disruption in a hypothetical DMD patient carrying an exon 50 deletion. Reading frames are shown by exon shapes. A) Traditional CRISPR/Cas9 gene editing methods. Exon deletion, ORF restoration using two sgRNAs targeting intronic regions flanking the mutated exon in the *DMD* gene. Exon skipping, targeting one sgRNA to 5' or 3' splice sites disrupting a splice acceptor site leading to ORF restoration. Exon reframing, targeting a site upstream

of a premature stop codon and after the small indels generated by NHEJ repair restoring the ORF. Precise repair, using sgRNAs targeting to sites flanking the mutated *DMD* exon and a donor template with the correct sequence. B) Novel CRISPR strategies. Base editing uses a sgRNA and a Cas9 nickase fused with a cytosine or an adenine deaminase. Consists of editing of a single base (C:G > T:A or A:T > G:C) in the targeted site without the generation of DNA DSBs to repair a nonsense mutation or to induce exon skipping by altering a splicing site. In Prime editing the Cas9 nickase is fused with a modified reverse transcriptase and the prime editing guide RNA (pegRNA) includes a reverse transcriptase template (RT template), and a primer binding site. Prime editors can perform targeted small insertions, deletions, and base changing in a precise way. No DSBs are generated and the pegRNA acts as a donor template for precise gene repair not limited to the base pair type as it could potentially correct a variety of DMD-causing mutations. Created with BioRender.com.

In addition, new therapeutic approaches have aimed to engineer CRISPR systems to act as transcriptional activators (CRISPRa) or repressors (CRISPRi) to modulate different genes involved in DMD pathogenesis. An example could be the epigenetic upregulation of utrophin by targeting CRISPR/Cas9 to activate the utrophin promoter (62) or to remove some inhibitory microRNA target regions (63, 64).

Despite the potential of CRISPR/Cas9 technology in the treatment of DMD, several limitations need to be addressed, including the delivery strategy, immunogenicity, potential off-target activity, durability, and the extent of dystrophin restoration (65). To date, there are no CRISPR/Cas9 clinical trials for the treatment of DMD, but this is a reality for other hereditary diseases that are already undergoing phase I/II clinical trials.

In November 2023, the UK Medicines and Healthcare products Regulatory Agency (MHRA) became the first authority to approve Casgevy™ (exagamglogene autotemcel), a non-viral, *ex vivo* CRISPR/Cas9 gene-edited cell therapy for the treatment of transfusion-dependent β-thalassemia (TDT) and sickle cell disease (SCD), in which a patient's own haematopoietic stem and progenitor cells are edited through a precise double-strand break at the erythroid-specific enhancer region of the *BCL11A* gene. The FDA followed with an initial approval for SCD in December 2023, and a TDT approval in January 2024; while the EMA granted a conditional marketing authorisation reported in December 2023, valid for one year and renewable annually as further clinical data gets reported.

Other therapies for various diseases are already undergoing phase I/II or even phase III of clinical trials. One example would be the *in vivo* CRISPR therapy NTLA-2001, indicated

for the treatment of transthyretin amyloidosis, is currently in a phase III clinical trial to assess the safety and efficacy of a single dose of NTLA-2001 compared to placebo in more than 700 patients.

Strategies for utrophin upregulation in Duchenne muscular dystrophy

Overexpression of utrophin in Duchenne and Becker patients is a promising therapeutic strategy because it would be applicable regardless of their genetic mutation.

Thousands of candidates from drug libraries have been tested by high throughput screening (HTS) assays to find small molecules that increase utrophin A expression. Small molecules offer several advantages, including improved delivery and bioavailability compared to gene therapy or protein replacement and the ability to test compounds already approved for clinical use. Indeed, repurposing drugs for other indications may accelerate their transfer to the clinic and improve their chances of success. In various studies, both repurposed and newly synthesised compounds have shown promising results at the preclinical level and some of them, like ezutromid, metformin/citrulin have already reached clinical trials (66, 67).

Recent studies have identified several approaches to modulate utrophin levels (Figure 6) including direct mechanisms, such as protein or gene replacement, or indirect mechanisms, such as protein/mRNA stabilisation, transcriptional upregulation of the utrophin promoter and post-transcriptional regulation (see Table 2). However, utrophin expression is subject to regulation at multiple steps along its synthesis and degradation pathways, which need to be studied to improve pharmacological interventions. Interestingly, compounds that have been shown to have beneficial effects in dystrophic muscles are sometimes correlated with utrophin expression, providing new insights into the regulation of utrophin synthesis. An example of this is halofuginone (HT-100), an orally administered small molecule developed by Akashi Therapeutics, which entered clinical trials (NCT01847573) after it was shown to reduce fibrosis and inflammation in DMD patients and, interestingly, to increase utrophin levels in preclinical assays (68). Unfortunately, the trial was halted following the death of a DMD patient treated with the highest dose.

Table 2. Mechanisms of action of potential drugs that could modulate utrophin expression.

Adapted from Soblechero-Martin P, *et al* (13).

Direct mechanisms	1. *Protein replacement*	TAT-µUtrn (69, 70)
	2. *Gene therapy*	µUtro (71)
Indirect mechanisms	1. *UGC stabilisation*	Biglycan (72, 73) GalNAc2 (74, 75) rhLAM111 (76, 77) Sarcospan (78, 79)
	2. *Transcriptional upregulation*	Artificial zinc finger transcription factors (ZF-ATFs): Jazz (80) , Bagly (81), Utroup(82), JZif1(83) . Aryl hydrocarbon receptors (AhR) antagonists (84): Ezutromid or SMTC1100 (66, 85) and SMT022357(86, 87) Other small molecules: Nabumetone (88), Heregulin (89, 90), Okadaic acid (91), Adiponectin (92-94).
	3. *Post-trancriptional upregulation*	eEF1A2/IRES mediated translation: Betaxolol, Pravastatin and 6α-methylprednisolone 21 sodium succinate (PDN) (95). via microRNA targeting: Let-7c, miR-150, miR-196b, miR-296-5p, miR-133b, AntimiR 206 (96, 97). via p38 MAPK/KSRP: Heparin, Heparin/AICAR, Heparin/GALGT2 (98-100) Celecoxib (101) Anisomycin (102) Trichostatin A (103)
	4. *Oxidative phenotype promoters*	Via peroxisome proliferator-activated receptor (PPAR) agonists: GW501516 (104) Via AMPK/SIRT1 activators: AICAR (105) Resveratrol (106) Metformin (107) Adiponectin (94) Obestatin (108) Quercetin (109)

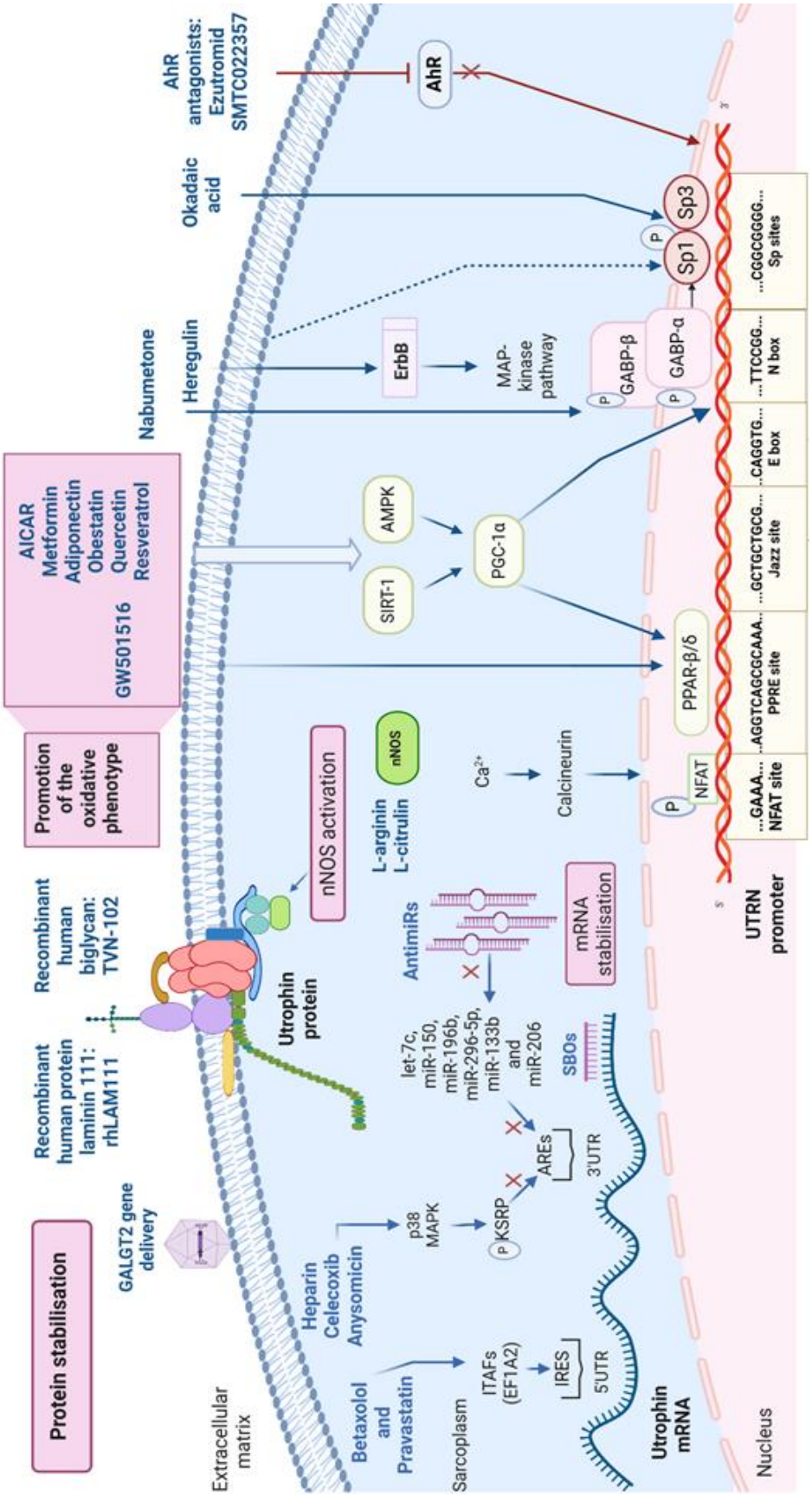

Figure 6. Therapeutic strategies for utrophin upregulation.

On the right, representation of the utrophin A promoter regulatory binding sites, their transcriptional upregulation mechanisms and the compounds involved in utrophin upregulation through these signalling pathways (in blue). The compounds that act through promotion of the slow and oxidative phenotype are included in the purple box. On the left, representation of the post-transcriptional pathways to enhance utrophin expression: mRNA stabilisation, nNOS activation and protein stabilisation and the compounds acting through these mechanisms (in blue). Adapted from Soblechero-Martin P, *et al* (13). Created with BioRender.com.

Direct mechanisms

1. *Protein replacement*

Direct protein replacement with recombinant full-length or truncated utrophin is an attractive potential method to directly increase utrophin levels *in vivo*.

Systemic administration of a recombinant ‘‘micro-utrophin” (µUtrn) protein combined with the cell-penetrating TAT protein (**TAT-µUtrn**), the transduction domain of the HIV-1, can functionally form a µUtrophin-glycoprotein complex at the sarcolemma. This therapeutic strategy can ameliorate the dystrophic phenotype both in *mdx* mice (70) and in dystrophin/utrophin double knockout (*dko*) mice (69).

Limitations of this strategy are posology and administration, as it would require frequent high-dose injections that could eventually trigger a harmful immune response. Nevertheless, this approach might be combined with other therapies to increase utrophin expression.

2. *Gene therapy*

As with dystrophin gene therapy, several preclinical studies using "micro-utrophin" (µUtro) gene delivery have been reported in recent years; studies conducted using AAV-µUtro in *mdx* mice reported restoration of the DGC, prevention of myofibre degeneration, normalisation of serum CK levels, and improvement in muscle function (110). In addition, further studies in double knockout (*dko*) mice and canine X-linked muscular dystrophy dogs have shown that **µUtro** expression ameliorates their severe pathological dystrophic phenotype (111). Modulation of utrophin expression could potentially treat many disease manifestations as AAV-µUtro transgene delivery

functionally replaces dystrophin in the heart and improves the skeletal and cardiac muscle phenotype in the D2/*mdx* mouse model (112). In addition, the *ex vivo UTRN* gene correction of mouse dystrophic iPS cells by µUtro gene transfection and subsequent transplantation into dystrophic *dko* mice has also demonstrated DGC restoration and improvement of contractile force (113).

Apart from all these promising results, for both protein and gene therapy studies, the delivery of µUtro instead of µDys has a potential advantage: a lower risk of eliciting an immune response since utrophin is naturally expressed at low levels in DMD patients. A recent study performed in the German Shorthaired Pointer deletional-null dog model (GSHPMD), reported a strong systemic cell-mediated immune response to µDys but not to µUtro. This supports the use of a non-immunogenic utrophin-based gene therapy approach for DMD (114). Furthermore, overexpression of utrophin rather than dystrophin could avoid the use of expensive and potentially toxic adjuvant immunosuppressive drug therapies (110).

Indirect mechanisms

1. *Utrophin-glycoprotein complex stabilisation*

Utrophin complex stabilisation is an alternative mechanism that has gained momentum in recent years with promising results. An example of this approach is the extracellular matrix biglycan, a proteoglycan that plays an essential role in muscle development. Biglycan is a component of the DGC/UGC, where it regulates the expression of sarcoglycans, dystrobrevins, syntrophins, and nNOS, by recruiting utrophin to the plasma membrane. In humans and mice, biglycan is most highly expressed in immature and regenerating muscle (115). Several studies in *mdx* mice have shown that systemically administered recombinant human biglycan upregulates utrophin and other DGC components at the sarcolemma, while ameliorating muscle pathology and improving muscle structure and function with no apparent toxicity (72, 73).

In 2016, the FDA granted orphan drug status to a recombinant human **biglycan** that can be administered systemically called TVN-102, developed by Tivorsan Pharmaceuticals as a potential treatment for DMD and BMD.

Similarly, the recombinant human protein laminin-111 (**rhLAM111**), another extracellular matrix protein, has been shown to upregulate other proteins such as utrophin and α7β1 integrin, both of which are capable of restoring muscle cell adhesion and stimulating muscle regeneration in DMD patients. Research in *mdx* mice has shown that rhLAM111 can strengthen muscles and improve muscle function. The underlying mechanisms of action reported included increased levels of several compensatory proteins and a 1.3-fold increase in utrophin. However, it is not entirely clear whether this increase in utrophin is sufficient to induce a phenotypic improvement (77, 116). Indeed, some studies claim that higher utrophin concentrations (1.5/2-fold increase) are necessary to achieve a therapeutic effect (27). In any case, recent results show that laminin prevents muscle disease progression in the canine model of DMD, the Golden Retriever Muscular Dystrophy dog (GRMD), and may therefore be a novel protein therapy for DMD patients (76).

Overexpression of **CT-GalNAc 2** (cytotoxic T cell N -acetylgalactosamine transferase), or Galgt2 protein, has been shown to increase synapse-associated proteins, including utrophin, and enhances their trafficking to the sarcolemma (117). AAV-mediated *GALGT2* gene delivery has been shown to protect both wild-type and dystrophin-*mdx* skeletal myofibres from injury induced by eccentric contraction. It also prevents muscular dystrophy and ameliorates the phenotype in several animal models (74, 118). Following these studies, the first phase I/IIa gene transfer clinical trial using AAVrh74-mediated *GALGT2* gene delivery in DMD in a small cohort of only two patients aimed to assess the safety and good tolerability of rAAVrh74.MCK.GALGT2 delivered into both femoral arteries using an isolated limb infusion (ILI) approach (119).

2. Transcriptional upregulation

The utrophin A promoter contains several regulatory motifs that could activate utrophin overexpression (Figure 7). The E-box and N-box motifs are essential for myogenic

differentiation, and synaptic expression of utrophin A (120). The E-box motif is a binding site for myogenic factors such as MyoD, myogenin, Myf5, and MRF4. In contrast, the N-box motif is targeted by the ETS-related transcription factor complex GA-binding protein (GABP) α/β, which is activated by nerve-derived and transcription factors. In addition, Sp-binding sites targeted by Sp1 and Sp3 zinc finger transcription factors can establish a cooperative interaction with GABP to stimulate the utrophin promoter (121). Also, the utrophin A promoter has been recently shown to contain a PPRE site targeted by the peroxisome-proliferator-activated receptor beta/delta (PPAR-β/δ). This PPRE site can also be stimulated by the 5' adenosine monophosphate-activated protein kinase (AMPK) and sirtuin 1 (SIRT1) signalling pathways, which activate the peroxisome proliferator-activated receptor-gamma coactivator 1α (PGC-1α) which, in turn, activates either PPARβ/δ or GABPα/β.

The calcineurin-nuclear factor of activated T-cells (NFAT) calcium-dependent signalling cascade is another pathway that positively regulates utrophin expression in the skeletal muscle. In this pathway, calcineurin dephosphorylates NFAT, enabling its entry into the nucleus and subsequent activation of the utrophin A promoter (122).

Figure 7. Utrophin A promoter transcriptional activating elements.

Nucleotide sequence of the human *UTRN* gene promoter including the transcriptional regulatory sites: NFAT binding site, PPRE site, Jazz binding site, E-box site, N-box site and Sp binding sites. The arrow indicates the transcription starting site. Adapted from Soblechero-Martin P, *et al* (13). Created with BioRender.com.

Utrophin upregulation by stimulating the activity of the utrophin A promoter is a promising pharmacological approach that has been extensively investigated using various strategies.

Artificial zinc finger transcription factors (ZF-ATFs):

One laboratory proposed the engineered artificial zinc finger transcription factors (ZF-ATFs) called "Jazz", which can bind the utrophin A promoter in both humans and mice. Systemic delivery of **ZF-ATFs** with AAVs can induce a significant rescue of muscle function in dystrophic *mdx* mice through utrophin upregulation (123). Indeed, several “Jazz” factors have shown remarkable efficacy in ameliorating the pathological phenotype of *mdx* mice and improving the morphology and plasticity of neuromuscular junctions. Among these, "JZif1", the most recently improved version, was developed using the backbone of the well-characterised human transcription factor Zif268/EGR1 to minimise immunogenicity and facilitate its clinical application.

Aryl hydrocarbon receptors (AhR) antagonists:

Ezutromid (SMTC1100) was the first orally bioavailable utrophin regulator to show increased *UTRN* transcription. It was identified using an HTS strategy with a luciferase reporter linked assay in murine H2K cells. Later, *in vitro* assays in human myoblasts showed an increase in utrophin expression at both mRNA and protein levels following ezutromid treatment, and further *in vivo* assays showed that a once-daily dose of ezutromid in *mdx* mice increased utrophin levels, as well as muscle strength and exercise tolerance (85). After these results, ezutromid was developed by Summit Therapeutics as a potential treatment for DMD and BMD. A Phase 1 placebo-controlled randomised clinical trial in healthy male volunteers and a Phase 1b placebo-controlled, randomised, double-blind study in boys with DMD showed that it was safe and well-tolerated. However, a Phase 2 clinical trial (NCT02858362) failed to meet both its primary (changes in leg muscle magnetic resonance parameters) and secondary endpoints (increased utrophin levels and decreased muscle damage). Based on these results, Summit Therapeutics abandoned the development program of ezutromid (66, 124). Recent studies have elucidated the mechanism of action of ezutromid as an aryl hydrocarbon

receptor (AhR) antagonist (84, 86). Similarly, other molecules that ameliorate *mdx* pathology like SMT022357 (31) or resveratrol (125) have also shown activity as AhR antagonists. Although the pathway between AhR antagonism and utrophin upregulation remains unknown, it appears to involve the stabilisation of active peroxisome proliferator-activated receptor gamma coactivator (PGC1α) (126). Indeed, moderately elevated levels of PGC1α ameliorate the dystrophic phenotype of *mdx* mice at the biochemical, histological, and functional levels (127). **SMT022357**, is a second-generation compound, is structurally related to ezutromid, sharing the same mechanism of action but with improved physicochemical properties and a more robust metabolic profile. SMT022357 administration has been associated with an increase in utrophin expression in skeletal, respiratory, and cardiac muscles and prevention of the dystrophic pathology in *mdx* mice (31).

Other small molecules:

Nabumetone is a long-acting non-steroidal anti-inflammatory drug, specifically a COX-1/COX-2 inhibitor, with a preference for COX-2 inhibition *in vitro*. It is used to treat pain and inflammation management in osteoarthritis and rheumatoid arthritis, and it is an example of pharmacological repurposing for DMD. HTS assays in C2C12 muscle cells showed that nabumetone could activate the utrophin A promoter and upregulate endogenous utrophin at the mRNA and protein levels (88).

Heregulin is a small nerve-derived growth factor capable of transactivating the utrophin A promoter via the N-box motif. Utrophin transcription induced by heregulin-mediated activation of GABPα/β occurs through the extracellular signal-related kinase (ERK) signalling pathway via the interaction of heregulin with the ErbB tyrosine kinase receptor (89, 128). Intraperitoneal injections of a small heregulin peptide in *mdx* mice resulted in upregulation of utrophin, together with a marked functional improvement in muscle pathology (129).

It has recently been shown that **okadaic acid**, a selective inhibitor of PP1 and PP2A phosphatases, can induce activation of utrophin A promoter during myogenesis through

Sp1 phosphorylation. There is evidence that okadaic acid increases utrophin A mRNA levels increased by approximately twofold in C2C12 myoblasts, but not in myotubes (91).

3. Post-transcriptional upregulation

While utrophin upregulation at the transcriptional level has been extensively studied over the years, an increasing number of recent studies support the importance of post-transcriptional and translational regulators of utrophin to identify new therapeutic targets.

eEF1A2/IRES mediated translation:

The full-length utrophin isoforms, A and B, have distinct 5'-untranslated regions (5'UTRs). The skeletal muscle isoform, utrophin A, has an internal ribosome entry site (IRES) in its 5'UTR that promotes expression through IRES-dependent translation mechanisms (130). IRES elements are thought to associate with the translational machinery, including some IRES trans-acting factors (ITAFs). EF1A2 has been reported as a suitable ITAF capable of modulating the activity of the utrophin A IRES.

A recent ELISA-based HTS assay has identified at least four FDA-approved drugs that target eEF1A2 and cause at least a 2-fold increase in utrophin in C2C12 muscle cells. Among them, **betaxolol and pravastatin**, appear to ameliorate the dystrophic phenotype of *mdx* mice via utrophin upregulation through IRES activation (95). Furthermore, in another study, utrophin protein levels are increased after 6α-methylprednisolone-21 sodium succinate (PDN) treatment of C2C12 myotubes, suggesting that the mechanism of action of glucocorticoids in muscle cells could be explained, at least in part, by the enhancement of utrophin translation due to IRES activation (131). These studies highlight the increasing interest in using repurposed drugs to activate this specific pathway, which upregulates endogenous utrophin levels in muscle by promoting protein synthesis from already synthesised transcripts.

Utrophin expression is also regulated at the 3' end of its UTR, where a few cis-elements, including conserved AU-rich elements (AREs), modulate the stability of utrophin mRNA transcripts. Several proteins can bind the AU-rich elements at the 3'UTR and regulate mRNA stability in a negative of positive manner. For example, 3'UTR repression has been

attributed to miRNAs and K-homology splicing regulator protein (KSRP) binding to these sites.

Via microRNA targeting:

Several miRNAs, including let-7c, miR-150, miR-196b, miR-296-5p, miR-133b, and miR-206 have been shown to repress utrophin expression (97, 132)and this has led to two therapeutic approaches: targeting the microRNAs directly by using **antimiRs** or blocking their binding site with site-blocking oligonucleotides (SBOs). Both mechanisms have been shown to upregulate utrophin expression and ameliorate the dystrophic phenotype *in vivo*. Intraperitoneal injections of specific SBOs designed to prevent let-7c miRNA binding to the utrophin 3'UTR resulted in higher utrophin protein expression in skeletal muscle and improvement of the dystrophic phenotype in *mdx* mice (133, 134). On the other hand, a three-month treatment with anti-MiR-206 increases utrophin in the muscles of *mdx* mouse compared to the untreated group (96).

Via p38 MAPK/KSRP:

Activation of p38 mitogen-activated protein kinase (MAPK) reduces the availability of KSRP to bind the 3'UTR AREs of utrophin, resulting in increased stability of existing mRNAs, increased utrophin protein production and reduced muscle damage (98). At least three approved drugs and activators of p38 MAPK, heparin, celecoxib and anisomycin, have demonstrated a significant utrophin upregulation efficacy in various preclinical studies.

Heparin, which is an anticoagulant commonly used in the clinic, significantly increases utrophin levels in both C2C12 (98) myoblasts and dystrophic fibres of *mdx* mice, leading to substantial morphological and functional improvements (99).

Celecoxib is a non-steroidal anti-inflammatory drug (NSAID) and a specific cyclo-oxygenase (COX)-2 inhibitor used for osteoarthritis and rheumatoid arthritis. This drug can activate the p38 MAPK pathway in skeletal muscle cells. Treated *mdx* mice showed a 1.5- to 2-fold increase in utrophin expression in the tibialis anterior, diaphragm, and heart muscles, and amelioration of the dystrophic phenotype, improving muscle strength (101).

Anisomycin is an antibiotic identified by HTS assays. It induces a 2.5-fold increase in utrophin levels in C2C12 muscle cells, *in vitro.* It has also been reported to significantly increase utrophin protein in the diaphragm of *mdx* mice treated daily with a low dose (102).

Another recent HTS screening study, targeting the 5' and 3' untranslated regions (UTRs), identified 27 hits capable of upregulating utrophin expression (103). In this study, the histone deacetylase inhibitor **trichostatin A** was identified as one of these hit compounds. Previous studies have shown that trichostatin A can activate the utrophin promoter (88). It also increases utrophin levels post-transcriptionally by interacting with the 5' and/or 3'UTR of the utrophin mRNA, resulting in a functional improvement of the *mdx* mouse. The remaining hits are yet to be further studied, but this is a good starting point for additional *in vitro* or *in vivo* assays.

4. Promotion of the oxidative phenotype

An alternative therapeutic strategy to increase utrophin expression in the skeletal muscle focuses on promoting the expression of the slow oxidative myogenic programme. The promotion of the slow oxidative phenotype has been achieved through various transcriptional and post-transcriptional pathways showing utrophin overexpression. This strategy has been shown to attenuate the dystrophic pathology in mdx animals (105).

Via peroxisome proliferator-activated receptor (PPAR) agonists:

One mechanism reported is PPAR-β/δ stimulation using the synthetic agonist **GW501516**. This molecule has also been found to stimulate the utrophin A promoter in C2C12 muscle cells and to improve sarcolemmal integrity in *mdx* mice, conferring protection against eccentric contraction-induced damage to muscle (104).

Chronic activation of AMPK also promotes the slow oxidative phenotype. Treatment of mdx mice with 5-aminoimidazole-4-carboxamide-1-β-D-ribofuranoside **(AICAR)** and other AMPK/PGC-1α activators significantly increased utrophin expression and was shown to be beneficial for the dystrophic phenotype and rescue of muscle function (105).

Via AMPK/SIRT1 activators:

One of the best-known pharmacological AMPK activators is metformin, a widely prescribed oral antidiabetic drug that has reached clinical trials for DMD in combination with the NOS modulators L-arginine and L-citrulline. **Metformin** has been shown to increase skeletal muscle utrophin content via AMPK activation and parallel or reciprocal increments in PGC-1α and PPAR-δ expression (107). Activation of skeletal muscle nNOS is also AMPK dependent (135). However, the partial response to metformin treatment in *mdx* muscles combined with the reduced quantity of NO in some studies supports the notion of combined therapy for DMD patients(107, 136). In the first proof-of-concept pilot study (NCT02516085) carried out in DMD patients, metformin in combination with **L-arginine** showed evident amelioration of muscular metabolism (137). Results from another study, a randomised, double-blind placebo-controlled clinical trial in 47 ambulatory DMD patients, combining **L-citrulline** (an L-arginine precursor) and metformin (NCT01995032), showed a clinically relevant but not statistically significant reduction in motor function decline in a specific subgroup of patients with no apparent side effects(67). Additional clinical trials are therefore needed to validate this approach. Interestingly, NOS-based therapy alone has also been shown to increase utrophin expression. In this context, L-arginine administration in *mdx* mice resulted in an almost 2-fold increase in utrophin in skeletal muscle, heart, and brain, accompanied by an improvement in the dystrophic phenotype (138). This study demonstrates that NOS expression has beneficial effects on skeletal muscle metabolism both *in vitro* and *in vivo*.

Activation of the AMPK-SIRT1-PGC-1α axis, leads to a cascade of biochemical events resulting in the downregulation of pro-inflammatory markers and the upregulation of utrophin. SIRT1 is a nuclear protein that belongs to the sirtuin family, a group of seven NAD-dependent histone deacetylase proteins. SIRT1 targets a variety of substrates involved in gene expression, cell survival, differentiation, and metabolism. Several experimental studies using natural SIRT1 activators like adiponectin, obestatin, quercetin or resveratrol have shown beneficial effects in *mdx* mice and on human cells too (139).

Treatment of myotubes from DMD patients with adiponectin results in downregulation of the nuclear factor kappa B (NF-κB) and inflammatory genes, and upregulation of

utrophin (92). Transgenic upregulation of **adiponectin** has shown significant beneficial properties in dystrophic *mdx* muscles (94). Recently, an orally administrable active adiponectin receptor agonist, called AdipoRon, has been identified. This small synthetic molecule has also been shown to attenuate the dystrophic phenotype in mdx mice offering a promising therapeutic prospect for DMD patients (93).

In the same line, **obestatin**, has shown activity in stabilising the sarcolemma of *mdx* skeletal muscle through the expression of utrophin, α-syntrophin, β-dystroglycan, and α7β1-integrin proteins, ameliorating the DMD phenotype (108).

Another molecule studied in preclinical assays that appears to upregulate utrophin through SIRT1 activation is **quercetin** (140). A diet enriched with this flavanol seems to rescue dystrophic muscle in *mdx* mice and provide physiological cardioprotection (109, 141)

Finally, administration of **resveratrol** to *mdx* mice has also been shown to stimulate the SIRT1-PGC-1α pathway, significantly upregulate utrophin expression, and activate the slow, oxidative myogenic program in *mdx* mouse muscle (142).

Moreover, a recent study analysed the expression of different sirtuins in *mdx* mice and detected decreased Sirt1 but increased Sirt6 expression both in quiescent muscle stem cells and in muscle fibres. They also found that in Sirt6 knockout mice muscles Utrn expression was substantially increased as well as UTRN protein levels compared to *mdx* muscles and moreover, inactivation of Sirt6 in *mdx* muscles resulted in improvement of the mdx phenotype (143). These findings lead the research to move further by using sirtuins as a molecular target in DMD and to explore the role of other members of the sirtuin family in DMD.

Taken all these discoveries together, utrophin upregulation appears to be a promising therapeutic approach, applicable to all DMD and BMD patients, which has been shown to functionally compensate for the lack of dystrophin, improving the pathological phenotype in several dystrophic models.

HYPOTHESIS AND OBJECTIVES

Utrophin upregulation is considered a promising therapeutic strategy applicable to treat all Duchenne and Becker patients regardless of their mutation and that could be used in combination with dystrophin restoration therapies.

In the evaluation of utrophin-based therapies in early stages of development, traditional methods such as luciferase high throughput screening assays, western blotting and quantitative PCR are commonly used, however a variety of non-standardised protocols and lack of good positive controls difficult the *in vitro* assessment of new drugs.

In this thesis project, we hypothesise that novel utrophin quantification methods like in-cell western assay (or myoblot) and digital droplet PCR, combined with a cell culture model generated by gene editing to serve as a positive control, could suppose a reliable platform to evaluate utrophin modulating potential therapies.

Aims

The main objective of this thesis project is providing the neuromuscular research community with improved methods for utrophin quantification and new cell culture models to be used in therapies evaluation. We propose to achieve the following aims:

1. To establish and optimise a platform for in vitro utrophin quantification in a cellular model of DMD.
2. To develop a cell culture model that endogenously overexpresses utrophin using gene edition to serve as a positive control in utrophin overexpression screening methods.
3. To screen novel therapeutic candidates to identify small molecules capable of increasing utrophin expression.

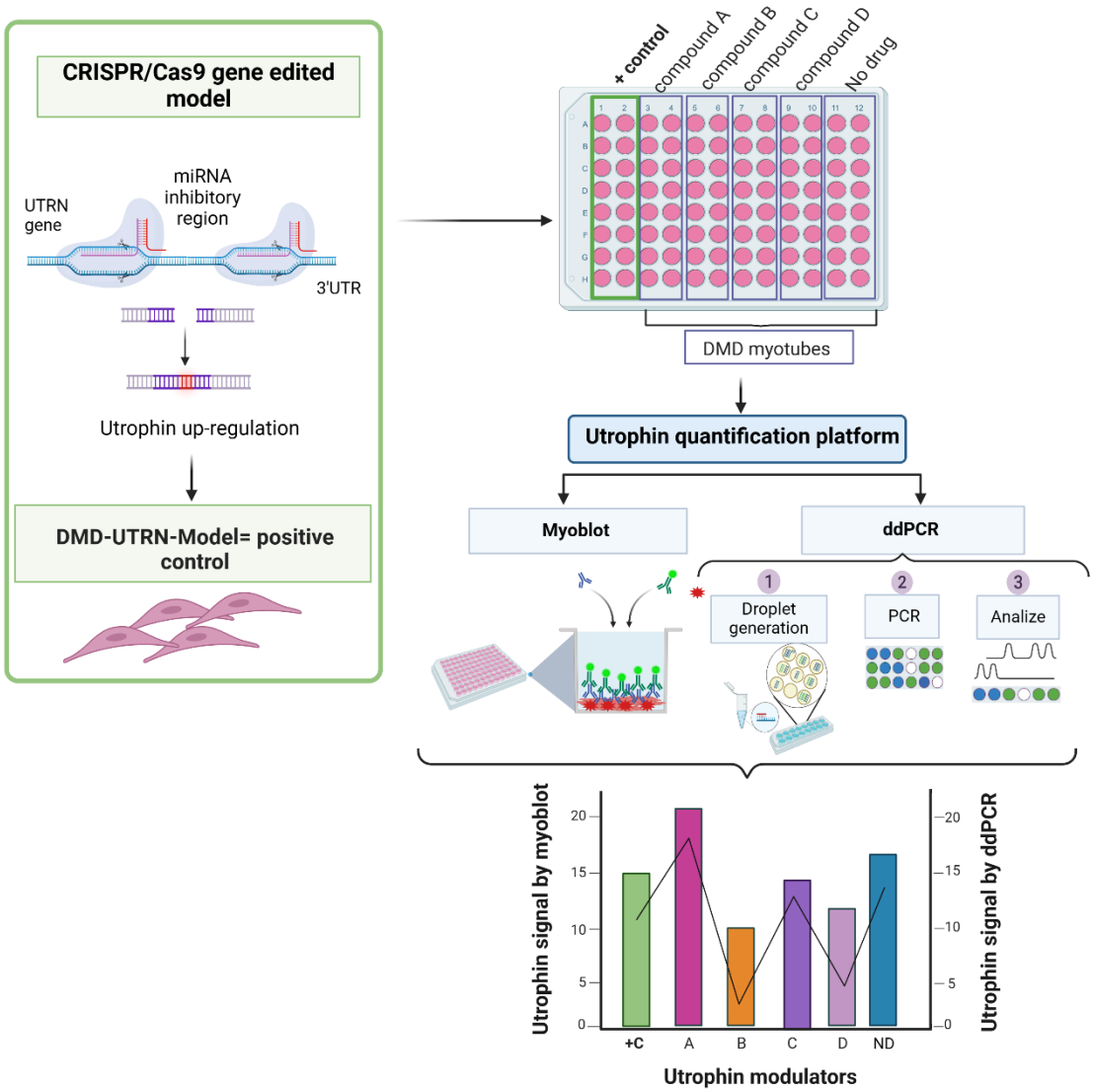

Figure 8. Schematic representation of aims and objectives.

The platform for in vitro utrophin quantification combines the new generated by CRISPR/Cas gene edited cell culture model (DMD-UTRN-Model) to serve as a positive control with myoblot and digital droplet PCR (ddPCR) assays. This platform will be used to evaluate novel utrophin modulators candidates in DMD myotubes.

MATERIALS AND METHODS

Cell cultures

Human embryonic kidney 293 cells (HEK 293) were purchased from the European Collection of Authenticated Cell cultures via Sigma-Aldrich, Spain, and maintained following the manufacturer's protocols in high glucose DMEM supplemented with 1% L-glutamine and 1% penicillin/streptomycin (Gibco™). HEK 293 cells were used in the preliminary selection of single guide RNAs (sgRNAs) combinations for gene editing experiments.

Control human immortalised myoblasts (C8220) were provided by the Institut de Myologie in Paris, France and DMD638a human myoblasts, derived from muscle biopsies from a DMD patient, were provided by the Centre for Neuromuscular Diseases Biobank, London, UK and immortalised by the Immortalisation of Human Cells platform at the Institut de Myologie in Paris, France.

For growing and maintenance, myoblasts were cultured using skeletal muscle cell growth medium (SMCM) (Pelo Biotech) supplemented with 10% foetal bovine serum (FBS) (Gibco™), 1% L-glutamine, 1% penicillin/streptomycin and 0,05% gentamicin.

For differentiation into myotubes, myoblasts were seeded in 1% Matrigel coated plates in SMCM and, after reaching 80% confluency, switched to Differentiation Medium (DM), consisting of high glucose DMEM plus 2% horse serum (Gibco™) and 1% penicillin/streptomycin 10.000U/mL (Gibco™). When myotube formation was evident (after approximately 7 days in culture but depending on the cell type) cells were harvested or fixed for quantification of utrophin and other proteins by different methods.

MyoD transduction

To facilitate myotube formation (144) in characterisation experiments following gene editing, myoblasts were transduced with MyoD adenoviral particles (Applied Biological Materials Inc). Myoblasts were seeded in SMCM and, after reaching 80% confluence,

treated with MyoD adenoviral particles diluted 1:20 in DM for 3 hours. The medium was then removed and replaced with fresh DM, and the cells were incubated until myotube formation.

CRISPR/Cas9 gene editing workflow

Selection of candidate regions to up-regulate utrophin by gene editing.

The target region was selected using Target Scan browser tracks of the UCSC Genome Browser (UCSC Genome Browser Home) bioinformatic resource. The target for gene editing was based on previous work reporting increased utrophin expression levels by miRNA-mediated inhibition methods targeting the 3'UTR region of the utrophin gene (133, 134).

Single guide RNA design.

Specifically, 20 nucleotide-long single RNA guides (sgRNAs) containing a 5'-NGG-3' protospacer adjacent motif (PAM) sequence were designed using the online bioinformatics tool http://crispr.mit.edu (2017). Ten different guides (five upstream and five downstream the target region) flanking the microRNA repressor binding site in the UTR 3' of the *UTRN* gene were selected according to their score number (Table 3).

Table 3. List of single guide RNAs.

Name	Score	Sequence	PAM
sgRNA21	71	AACTTTGGGTTCTCTTTAGC	TGG
sgRNA22	66	GGTTCTCTTTAGCTGGGATC	TGG
sgRNA23	63	TATTTTAGAATAGGTTGGGT	GGG
sgRNA24	62	ACTTTGGGTTCTCTTTAGCT	GGG
sgRNA25	62	TCTAACTTTAAGCCTCCTTC	TGG
sgRNA26	76	GTGCTTTCTTGGGTATGACA	TGG
sgRNA27	68	CAAAGTCTAGAGCTTTTATC	AGG

sgRNA28	66	CAACTTGGAGTTGAGAGCTC	AGG
sgRNA29	64	TCAACTCCAAGTTGTAGATT	TGG
sgRNA30	63	TCCATCTTCATCCATTGCAT	TGG

The ten sgRNAs were cloned using BbsI sites into a plasmid containing Cas9 from S. pyogenes with 2A-EGFP pSpCas9 (BB)-2A-GFP (PX458) (Addgene plasmid # 48138, deposited by Feng Zhang) according to the recommended protocol (56) as follows.

Designing and annealing of sgRNA oligos.

Two oligos containing the N1-N20 forward and reverse guide sequence plus the BbsI restriction enzyme overhangs necessary for ligation (highlighted in bold) were synthesised by Thermo Fisher Scientific™.

When using CRISPR/Cas9 target sites that do not begin with a "G", an additional "G" was added at the start of the sgRNA sequence (highlighted in red). This was done because the PX458 plasmid allows the expression of the sgRNA by the human U6-promoter and the human U6-promoter requires a "G" base at the transcription start site to express the sgRNAs (Table 4).

sgRNA-oligo F: 5' –**CACC**(G)N_1NNNNNNNNNNNNNNNNNN$_{20}$ –3'

sgRNA-oligo R: 5' –**AAAC**N_1NNNNNNNNNNNNNNNNNN$_{20}$(C) –3'

Table 4. Top and bottom oligos designed for each sgRNA.

BbsI overhangs are highlighted in bold and additional G/C added to the sgRNA sequence are highlighted in red.

Name	Sequence (5'—3')
sgRNA21-oligo F	**CACC**GAACTTTGGGTTCTCTTTAGC
sgRNA21-oligo R	**AAAC**GCTAAAGAGAACCCAAAGTTC
sgRNA22-oligo F	**CACC**GGTTCTCTTTAGCTGGGATC

sgRNA22-oligo R	**AAAC**GATCCCAGCTAAAGAGAACC
sgRNA23-oligo F	**CACC**GTATTTTAGAATAGGTTGGGT
sgRNA23-oligo R	**AAAC**ACCCAACCTATTCTAAAATAC
sgRNA24-oligo F	**CACC**GACTTTGGGTTCTCTTTAGCT
sgRNA24-oligo R	**AAAC**AGCTAAAGAGAACCCAAAGTC
sgRNA25-oligo F	**CACC**GTCTAACTTTAAGCCTCCTTC
sgRNA25-oligo R	**AAAC**GAAGGAGGCTTAAAGTTAGAC
sgRNA26-oligo F	**CACC**GTGCTTTCTTGGGTATGACA
sgRNA26-oligo R	**AAAC**TGTCATACCCAAGAAAGCAC
sgRNA27-oligo F	**CACC**GCAAAGTCTAGAGCTTTTATC
sgRNA27-oligo R	**AAAC**GATAAAAGCTCTAGACTTTGC
sgRNA28-oligo F	**CACC**GCAACTTGGAGTTGAGAGCTC
sgRNA28-oligo R	**AAAC**GAGCTCTCAACTCCAAGTTGC
sgRNA29-oligo F	**CACC**GTCAACTCCAAGTTGTAGATT
sgRNA29-oligo R	**AAAC**AATCTACAACTTGGAGTTGAC
sgRNA30-oligo F	**CACC**GTCCATCTTCATCCATTGCAT
sgRNA30-oligo R	**AAAC**ATGCAATGGATGAAGATGGAC

The oligos were resuspended to a final concentration of 100 µM. For annealing and phosphorylation of the sgRNA oligo pairs, 1 µl oligo F (100 µM) and 1 µl of oligo R (100 µM) with 1 µl of T4 PNK in 10× T4 ligation buffer and ddH2O were mixed. The mixture was incubated in a thermocycler using the following parameters: 37 °C for 30''; 95 °C for 5'; ramp down from 95°C to 25 °C (5 °C per minute). Phosphorylated and annealed oligo duplexes were diluted 1:200 in ddH2O and stored at -20ºC until use.

Digestion and dephosphorylation of the expression vector

Digestion of pSpCas9(BB) with BbsI enzyme allows the replacement of the restriction sites with direct insertion of annealed oligos upstream of the sgRNA scaffold (Figure 9).

The digestion reaction was performed by mixing 1 µg of plasmid with 5 U/µl of BbsI in the NEB buffer and ddH2O. The mixture was incubated at 37°C for 3 hours and then at 65 °C for 20 minutes to inactivate the restriction enzyme. A dephosphorylation reaction was carried out by mixing 5µg of BsbI digested plasmid with Antarctic phosphatase (AP) 5U/µl in the AP reaction buffer and ddH2O. The mixture was incubated at 37°C for 30 minutes and then at 70 °C for 20 minutes. The digested and dephosphorylated vector was loaded onto a 1% agarose gel and the linearised vector was extracted using the QIAquick™ Gel Extraction Kit (Qiagen). The digested, dephosphorylated, and purified vectors were stored at -20ºC until further use.

Ligation of sgRNA oligos with the vector.

For the ligation reactions, 1 ng of linearised vectors and 1.5 µl of the annealed oligos were mixed with 1 µl of T4 DNA ligase enzyme in ligase buffer and ddH2O, and then incubated overnight at 16 °C, followed by 10 minutes at 65 ºC.

The ligation reaction was treated with Plasmid-Safe™ ATP-Dependent DNAse (New England Biolabs) for 30 minutes at 37 °C to digest linear DNA and prevent unwanted recombination products and used directly to transform competent cells.

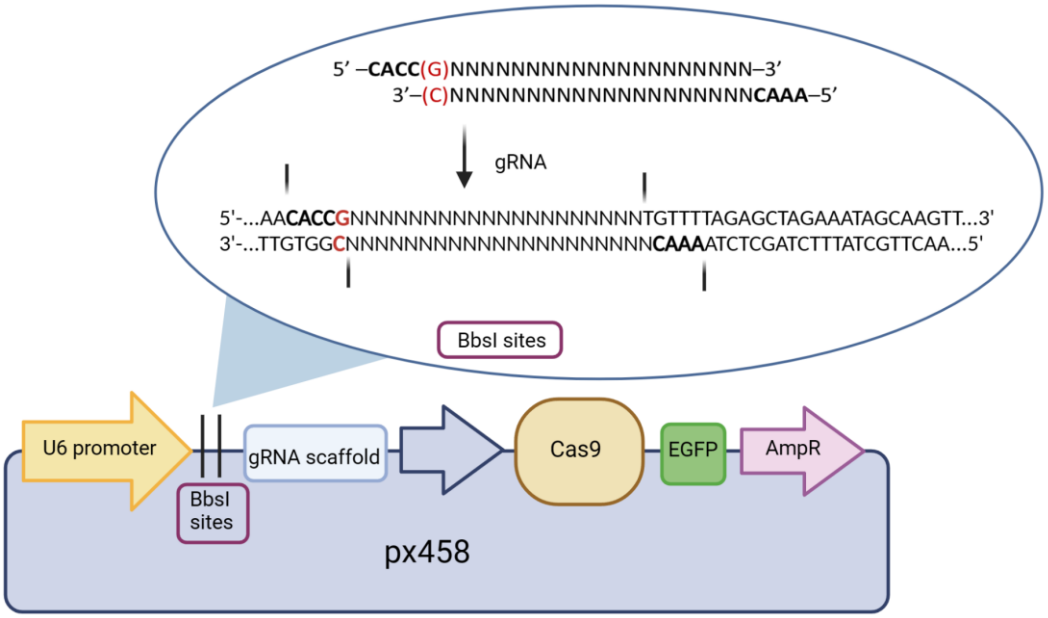

Figure 9. Scheme of the guide sequence oligos ligation using BbsI sites into plasmid containing the gRNA scaffold, Cas9, GFP and ampicillin resistance (pX458) during the cloning process.

Created with BioRender.com.

Propagation of recombinant plasmid into bacteria.

The "One Shot™ Stbl3™ Chemically Competent *E. coli*" (Invitrogen) protocol was followed for plasmid propagation into bacteria. Briefly, after slowly thawing chemically competent *E. coli* on ice, 50 µl of bacterial dilution was mixed with 5 µl of the ligation mix, incubated on ice for 30 minutes, and heat-shocked in a water bath at 42°C for 90 seconds. Then, they were incubated for 3 minutes on ice and 1 ml of LB medium was added. The final mixture was incubated again for 30 minutes at 37°C on a shaker at 200 rpm.

Finally, bacteria were seeded onto LB-Agar plates containing 50 µg/ml ampicillin and incubated overnight at 37°C. The next day, individual colonies were resuspended in 10 µl of ddH2O: 5 µl were inoculated into LB medium containing 50 µg/ml ampicillin for overnight incubation at 37 °C on a shaker at 200 rpm and purified the next day using the QIAprep® spin miniprep kit (Qiagen); the other 5 µl were used directly as a template for genomic PCR reaction and Sanger sequencing to verify that the sgRNA sequence was inserted into the plasmid. PCR amplification was performed using Taq DNA Polymerase (Recombinant, Invitrogen) and the 5' (TTTATGGCGAGGCGGCGG) and 3' (GTGGGCTTGTACTCGGTCAT) primers, under the following conditions: 94ºC for 3 minutes, followed by 25 cycles of 94ºC for 20 seconds, 63ºC for 20 seconds, 72ºC for 1 minute and a final extension step for 5 minutes at 72ºC. The PCR amplicons were analysed by Sanger sequencing at the sequencing platform of Biobizkaia Health Research Institute using the sequencing primer TTTATGGCGAGGCGGCGG (Figure 10).

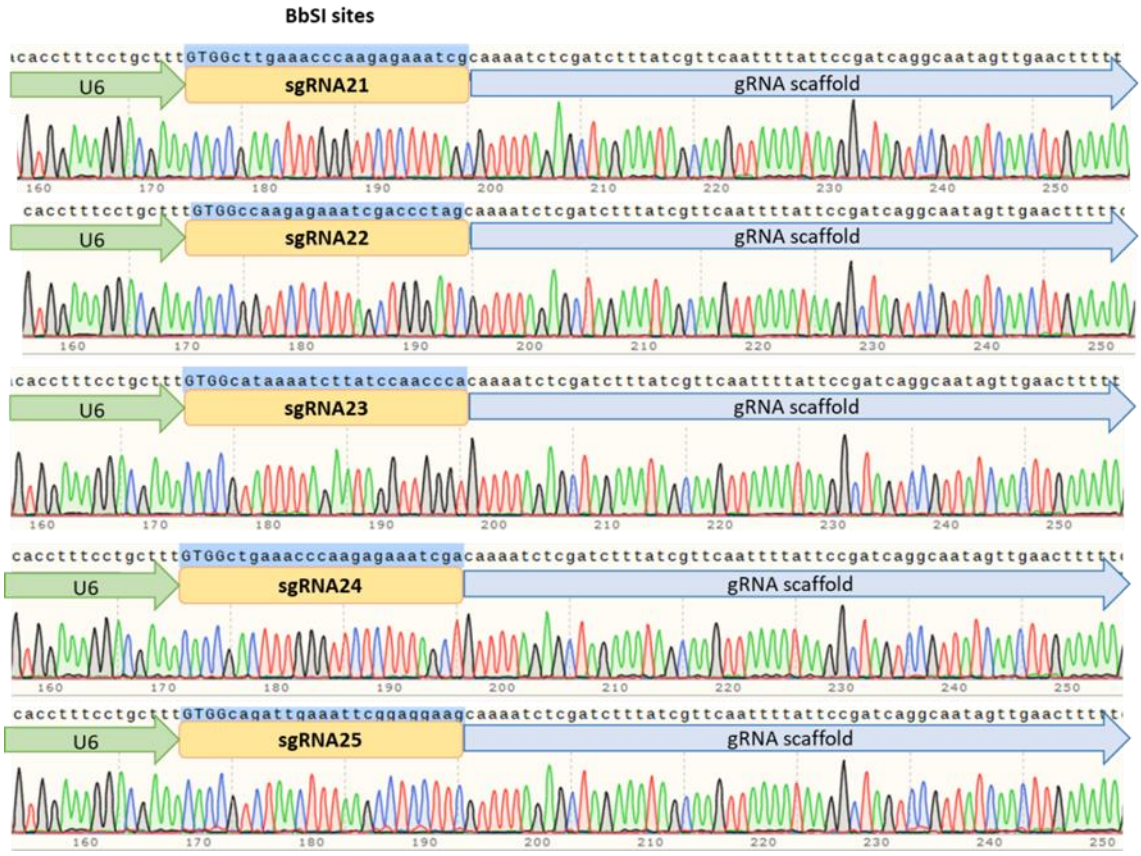
BbSI sites
U6
sgRNA21
gRNA scaffold
U6
sgRNA22
gRNA scaffold
U6
sgRNA23
gRNA scaffold
U6
sgRNA24
gRNA scaffold
U6
sgRNA25
gRNA scaffold

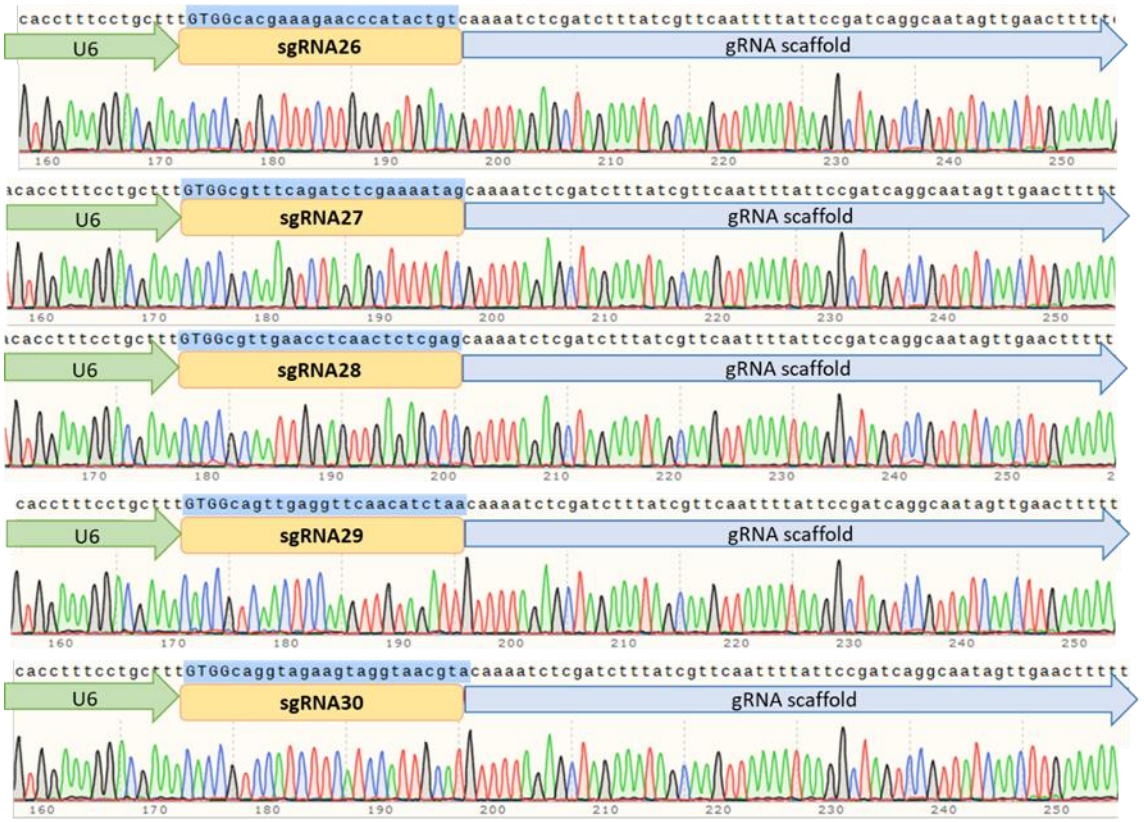

Figure 10. Sequencing results verifying the correct sgRNA insertion in the plasmid.

Chromatograms show sgRNAs are inserted in BbsI sites, downstream the U6 promoter (green arrow) and upstream the sgRNA scaffold (blue arrow), as expected. sgRNAs sequences (from 21 to 30) are highlighted in blue above the sequencing chromatogram obtained after Sanger sequencing. Sequences were analysed using SnapGene software.

Test plasmid integrity by PstI digestion.

To test plasmid integrity, a digestion reaction using PstI restriction enzymes was performed by mixing 1 µg of plasmid DNA with 1 µl of PstI enzyme in NEB buffer 3.1 and ddH2O and then incubating the mixture at 37 °C for 15 minutes followed by 20 minutes at 80ºC.

The reaction products were resolved on a 1.5% TAE-agarose gel and the resulting fragments were compared with the expected gel fragments obtained by a virtual simulation in SnapGene, confirming the integrity of the plasmid (Figure 11).

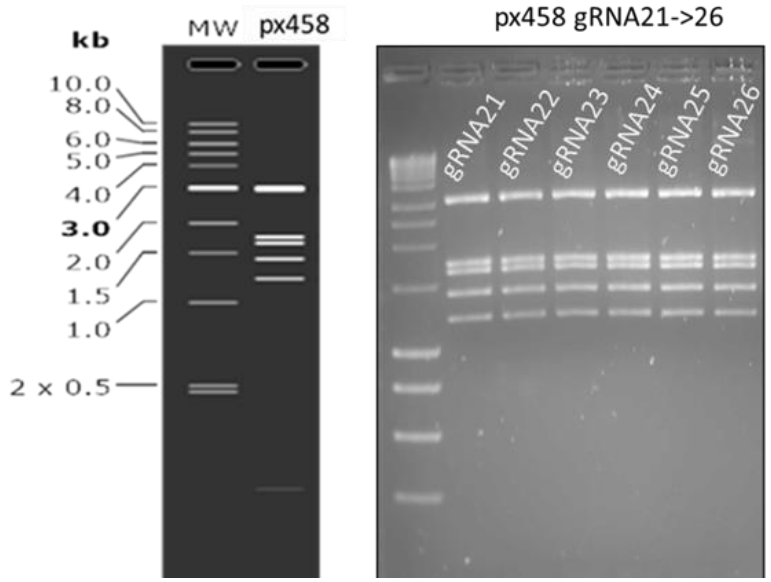

Figure 11. Plasmid integrity testing.

Comparison between virtual simulation of the expected gel band pattern obtained after plasmid digestion using PstI restriction enzymes performed with SnapGene (on the left) with a representative gel after px458 plasmid PstI digestion (on the right). In the simulation, MW column represents the 1kb DNA molecular weight marker and the px458 column the digested plasmid expected fragments (3016pb, 1744pb, 1661pb, 1422pb, 121pb, 204pb, and 30pb).

Cell culture transfection.

Two different transfection protocols were used depending on the cell type used. Validation of sgRNA cleavage efficacy *in vivo* was first carried out in HEK 293 cultures. HEK 293, cells were seeded in 6-well plates at 70-80% confluence and plasmids containing different combinations of sgRNAs were transfected using 1.25 µg of each plasmid and Lipofectamine 2000® (Thermo Scientific™) transfection reagent (1:5 ratio). The guide RNA combination that showed DNA cleavage was selected for myoblast transfection.

Myoblasts were seeded in 6 well plates at 70-80% confluence with 1.5 µg of each selected plasmid using ViaFect™ (Promega) transfection reagent (1:5 ratio).

Fluorescence activated cell sorting (FACS) of the GFP-positive myoblasts.

At 48 hours post-transfection, fluorescence was checked under the microscope and myoblasts were trypsinised and collected for fluorescence-activated cell sorting (FACS) using a BD FACS Jazz (Becton Dickinson) at the Cell Analytics Facility of the Achucarro Basque Center for Neuroscience (Leioa, Spain). GFP-positive cells were seeded individually in microplates containing SMMC medium for clonal selection. Approximately 7 days after sorting, the first colonies were visible and, when confluence was reached, clones were expanded from microplates to larger well plates. Finally, cells were harvested approximately 15-30 days after sorting. Harvested cultures were aliquoted: some aliquots were frozen for archiving; others were pelleted for DNA analysis and others were re-cultured for expansion and further characterisation by immunocytochemistry, western blot, myoblot, and digital droplet PCR (Figure 12).

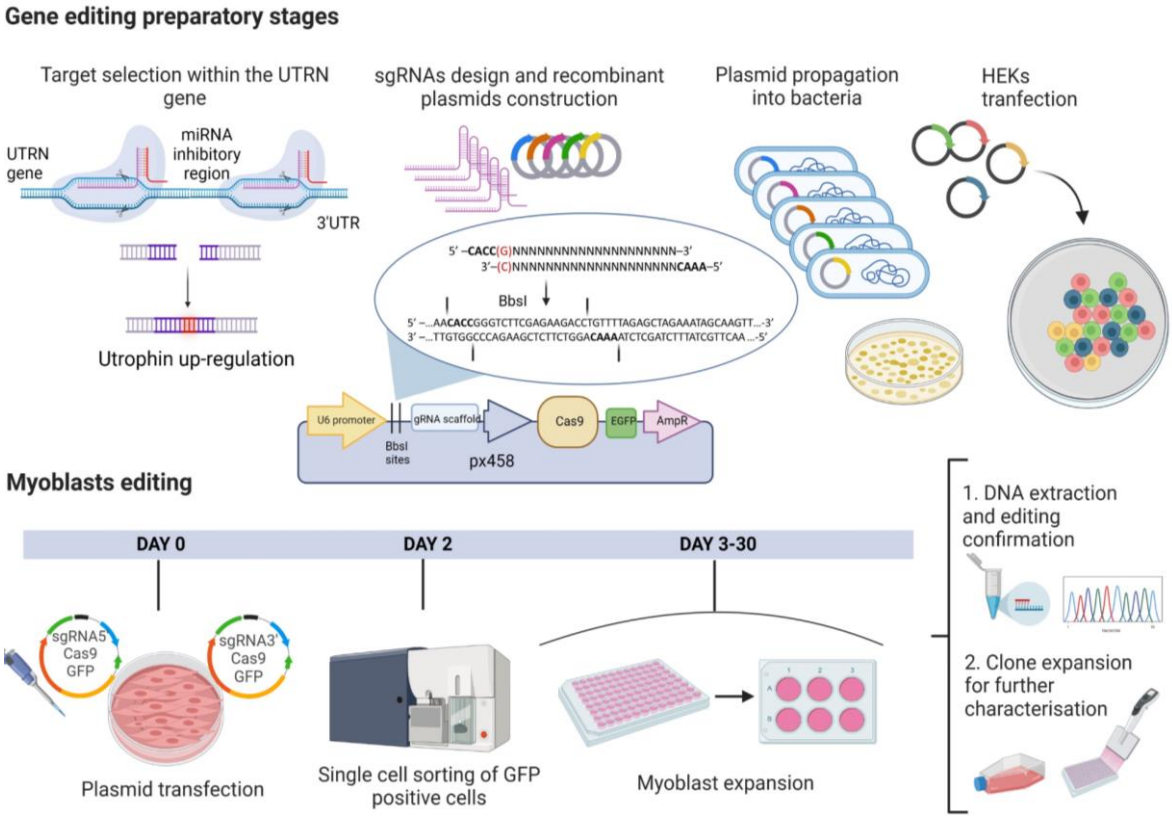

Figure 12. Schematic of CRISPR/Cas9 gene editing workflow.

Preparatory stages included selection of the editing target, sgRNAs design and recombinant plasmid construction, plasmid propagation into bacteria, and plasmids transfection into HEK cells to select the best sgRNA combination. Best plasmid combination was transfected into myoblasts, GFP positive clones were selected by fluorescence single cell sorting, and finally clones were expanded for confirmation of editing and further characterisation of the positive clones. Figure adapted from Soblechero-Martin P, *et al*.

Confirmation of gene edition

DNA was extracted from cell pellets using a QIAamp® DNA Mini Kit (Qiagen). The edited regions were amplified by PCR using Taq DNA Polymerase (Recombinant), (Invitrogen), with primers UTRN F1 and UTRN R1 (Table 3) under the following conditions: preheat for 3 minutes at 94ºC, followed by 25 cycles of 94º for 3 minutes, 94º for 20 seconds, 63º for 20 seconds, 72º for 1 minute and a final extension step of 72º for 5 minutes. PCR products were resolved on 2% TAE-agarose gels and analysed with a Gel Doc™ EZ Imager (Bio-Rad). Bands of interest were then purified for sequencing analysis with the QIAquick® Gel extraction Kit, (Qiagen). PCR amplicons were analysed by Sanger sequencing at the sequencing platform at Biobizkaia Health Research Institute using UTRN F1 and UTRN R1 primers (Table 5).

Table 5. Gene edition primer sets.

Name	**Sequence (5'—3')**	**Amplicon length (bp) (non-edited)**	**Amplicon length (bp) (edited)**
UTRN F1	TGATGGTACCTCCACCTACATCT	692	421
UTRN R1	TTACTTCCCATTGTTACTGCAA	692	421

Off-target analysis of mutations in clonal lines

Potential off-target region loci of each sgRNA used were predicted using the CRISPOR bioinformatics tool http://crispor.tefor.net/ (2019). The six most likely off-target sequences per guide listed by this tool were analysed in the edited clones using genomic PCR and Sanger sequencing. The primer sets flanking the off-target sites and the corresponding internal primers used for genomic PCR and Sanger sequencing are listed in Table 6.

Table 6. Potential off-target sequences predicted for single guide RNA 22 (GGTTCTCTTTAGCTGGGATCTGG) and single guide RNA 26 (GTGCTTTCTTGGGTATGACATGG).

Off Target name	Off target sequence	Mis	Chrom	Locus
sgRNA22_Off1	TGTTCTCTCTAACTGGGATCTGG	3	chr18	intergenic:RP11-411B10.6-RP11-411B10.5
sgRNA22_Off2	TGTTCTCTAGAGCTGGGATCTGG	3	chr21	intron: LCA5L
sgRNA22_Off3	TGTTCTCTCCAACTGGGATCTGG	4	chr22	intron: PPP6R2
sgRNA22_Off4	GAATCCTTTTAGCTGGGATCAGG	4	chr19	intron: ZNF536
sgRNA22_Off5	GGTTCATCTTAGCTGGGATATGG	4	chr13	intron: FLT1
sgRNA22_Off6	TGTTCTCTCTAACTGGGGTCTGG	4	chr21	intergenic: PPP6R2P1-AP001347.6
sgRNA26_Off1	AAGCTTTCCTGGATATGACAAGG	4	chr4	intron: RNF150
sgRNA26_Off2	GTGCTTACTTGGGTAAGACGTGG	3	chr17	intergenic:RP11-212E8.1-RP11-642M2.1
sgRNA26_Off3	GAGTTAACTTGGGTATGACAGGG	4	chr4	intron:RGS12
sgRNA26_Off4	GTGCTCTCATGAGAATGACAGGG	4	chr4	intergenic: GABRG1-RP11-320H14.1
sgRNA26_Off5	GAGCTTTCCTGGGAATGACAGGG	3	chr1	intergenic: FOXO6-RNA5SP45
sgRNA26_Off6	GTGCTTTATAGGATATAACATGG	4	chr6	intron: GSTA3

Table 7. Off-target primer sets.

Name	Primer sequence (5’—3’)
sgRNA22_Off1_F	ATGAGCCTCACAGATGCCTG
sgRNA22_Off1_R	GAAGACAGGGCCTGGATGTC
sgRNA22_Off1_Seq	TTAAAGTCTGTGCCCCTC
sgRNA22_Off2_F	AGGCTCTGCAGTTCAACCTC
sgRNA22_Off2_R	AACAGGCTCCAAACGTGTGA
sgRNA22_Off2_Seq	AATGACTTATACAGGGGACAT
sgRNA22_Off3_F	GGCCTTCTTTCGTGGACAGA

sgRNA22_Off3_R	GAATCATAGGCCTCCCGTGG
sgRNA22_Off3_Seq	TCGTGTTCTCTGTTGTGA
sgRNA22_Off4_F	GCCATAATCACACATCAAACCCT
sgRNA22_Off4_R	TGTTGCCATGCGAATTCGAG
sgRNA22_Off4_Seq	GAGAAGTTGAGGGAACCG
sgRNA22_Off5_F	GAGGTGGCATTCGGTAAAAGTTC
sgRNA22_Off5_R	TTGACAACCACGGGAGGCAG
sgRNA22_Off5_Seq	TGATTCTTTCCAGGCTCAT
sgRNA22_Off6_F	GGAGTGTGAGGGCTTCCTTC
sgRNA22_Off6_R	AGATGCCTGCTTACCTGCTG
sgRNA22_Off6_Seq	CATCTGTGTTCTCTGTTGTG
sgRNA26_Off1_F	GGGCAGGCTTGGGAGACATA
sgRNA26_Off1_R	GTGTCCAGCCCATTCTTTGAAGT
sgRNA26_Off1_Seq	TGCTCCCACTGCTGTTAG
sgRNA26_Off2_F	AGGTGCTCGCTTCTTTCCAA
sgRNA26_Off2_R	CCAGAAGTGAAGCTTTGCACC
sgRNA26_Off2_Seq	AACTTCTTGCACAGCCTT
sgRNA26_Off3_F	GGCATTCCTAGATCAGTGTGTGC
sgRNA26_Off3_R	CCCCAACTCAAACCAAGACGG
sgRNA26_Off3_Seq	CTGGGGGGATGTTACTGT
sgRNA26_Off4_F	TGGCTCTGTTTCTTGCCCAA
sgRNA26_Off4_R	TGGTTACTGGGCAGACATGG
sgRNA26_Off4_Seq	AAGCTAAAAGACATTGACAGT
sgRNA26_Off5_F	CACTGGAAAGAACATGGGCTCTG
sgRNA26_Off5_R	TGGTGTGTCCTGGGAGCATC
sgRNA26_Off5_Seq	CTCGGTTTCTACTGTGTGA
sgRNA26_Off6_F	TTTTATGTCCCCCACCCCTCA
sgRNA26_Off6_R	CCATGCCCAGCCCTAGTTTG
sgRNA26_Off6_Seq	GGGAAGCAGAGAAGTTGT

Immunocytochemistry assays

Chamber slides were pretreated with 1% Matrigel-1% collagen (1:1) for half an hour in the incubator. After removal of excess coating solution, cultures were seeded in SMMC medium. At 80% confluence, the cultures were treated with a MyoD-carrying adenovirus, in differentiation medium (1:20) to facilitate differentiation into myotubes (144). After seven days in differentiation medium, myotubes were fixed with 4% PFA for 10 minutes at room temperature, washed with PBS and stored at 4ºC in PBS until further analysis. Cultures were permeabilised with Triton 1-100X (Thermo Scientific™) 0.5% in PBS during 10 minutes at room temperature and then blocked with 2% bovine serum albumin (BSA) (Thermo Scientific™) in PBS for half an hour. This was followed by incubation with primary antibodies overnight at 4ºC. The primary antibodies used were Mancho 7 (kindly provided by Professor Morris of the MDA Monoclonal Antibody Resource) diluted at 1:50 in blocking solution for utrophin staining, MF20 (Developmental Studies Hybridoma Bank) diluted 1:100 for myosin heavy chain, or anti-sirtuin2 antibody (Abcam 51023) diluted 1:100 for sirtuin2 staining. The following day, samples were washed with PBS-Tween 0.1%, and stained with Alexa Fluor 488 goat anti-mouse antibody (Invitrogen) for 1 hour at room temperature for utrophin and MF20 immunostaining and with Alexa Fluor 594 goat anti-rabbit antibody (Invitrogen) for 1 hour at room temperature for sirtuin 2 immunostaining. Hoechst (Thermo Scientific™ 33342, 20 mM) diluted 1:2000 in PBS was used for nuclear staining and chamber slides were mounted with PermaFluor™ Aqueous Mounting Medium (Thermo Scientific™). Images were captured using a LEICA DMI 6000B microscope at the Microscopy Platform of Biobizkaia Health Research Institute.

Western blot

Cell cultures from confluent 6-well plates (9,5cm2) were trypsinised, washed twice with cold PBS and centrifuged at 2500 x g for 5 minutes. Cell pellets were then solubilised in 50 μL of lysis/loading buffer (75mM Tris/HCl, 25% glycerol, 60% SDS, 5% β-mercaptoethanol, 0.5% bromophenol blue, one Complete™ ULTRA Tablet, Mini, EASYpack Protease Inhibitor Cocktail (Roche) and denatured at 95°C for 5 minutes. All cell culture samples were loaded without quantification.

Electrophoresis was performed by loading samples onto a NuPAGE® Novex® 3–8% Tris-Acetate Gel (Thermo Scientific™) and using Novex Tris-Acetate SDS Running Buffer (Thermo Scientific™) for 60 min at 70 V followed by 120 min at 150 V at 4ºC. Protein wet transfer was performed overnight at 4°C on an Immobilon®-FL PVDF membrane (Merck™). The next day, the membranes were stained with Revert TM 700 Total Protein Stain (Li-Cor) for total protein quantification and measured using an Odyssey Clx imaging system. The membranes were then blocked with Intercept® (PBS) Blocking Buffer (Li-Cor) for 2 hours and incubated overnight at 4°C with the primary antibody (1:50 anti-utrophin antibody Mancho 7). The next day, the membranes were washed three times for 5 minutes with 0.1% PBS-Tween, followed by incubation with the secondary antibody (1:5000 IRDye 800CW goat anti-mouse Li-Cor) for 1 hour at room temperature, protected from light. After incubation, the membranes were washed again three times for 5 minutes with 0.1% PBS-Tween and scanned using an Odyssey Clx imaging system. Quantification of bands was performed using Empiria Studio ^{TM} software (Li-Cor).

Myoblot assay (In-cell western assay)

Myoblots were performed as previously described (63, 145). In short, myoblasts were seeded onto 96-well plates in SMCM and, when confluence was reached (typically 24-48 hours after seeding), the cells were changed to differentiation medium and incubated until myotube formation. Plates were fixed with ice-cold methanol, permeabilised with 0.1% Triton X-100 in PBS, and blocked with Intercept® PBS Blocking Buffer (Li-Cor) for 2

hours before overnight incubation with the required primary antibodies (anti-utrophin Mancho 7, anti-myosin heavy chain MF20, anti α-sarcoglycan (NCL-L-aSARC), anti β-dystroglycan (NCL-b-DG), anti-SIRT1 or anti-SIRT2 (see Table 8). The next day, the plates were washed 4 times for 5 minutes with 0.1% PBS-Tween, and incubated with a mixture of the secondary antibodies, IRDye 800CW goat anti-mouse antibody and CellTag 700 Stain (Li-Cor), diluted in blocking buffer (1:500 and 1:1000 respectively) and incubated for 1 hour at room temperature, protected from light. After incubation, the plates were washed again 4 times for 5 minutes with 0.1% PBS-Tween, filled with 100 µL PBS and scanned using the Odyssey® CLx Imager (Li-Cor).

For cell linearity assays, cells were seeded in increasing numbers from row 2 (500 cells per well) to row 7 (12.000 cells per well) in SMCM. Wells at the edge of the plate were filled with PBS. The next day, the medium was changed to DM. 7 days after differentiation, the cells were fixed for the myoblot assay. Background wells were treated with the blocking buffer only, while the remaining wells were stained with Cell Tag 700 Stain diluted 1:1000 in blocking buffer for 1 hour at room temperature protected from light after the blocking step. The plates were washed four times with PBS-Tween 0.1%, filled with PBS and scanned in the Odyssey Clx scanner using the automatic settings.

Table 8. List of primary antibodies employed in myoblot, western blot (WB) and immunofluorescence assays (IFI).

Antibody	**Use and dilution**	**Manufacture**	**Type**
Mancho7 anti-utrophin	Myoblot: 1:400 WB: 1:50 IFI: 1:50	The MDA Monoclonal Antibody Resource	Primary mouse monoclonal
MF20 anti-myosin heavy chain	Myoblot: 1:100 IFI: 1:100	Developmental Studies Hybridoma Bank	Primary mouse monoclonal
NCL-L-a_SARC Anti α-sarcoglycan	Myoblot: 1:10	Leica Biosystems	Primary mouse monoclonal

NCL-b-DG Anti β-dystroglycan	Myoblot: 1:20	Leica Biosystems	Primary mouse monoclonal
Anti-SIRT2 antibody [EP1668Y]	Myoblot: 1:100 IF: 1:100	Abcam	Primary rabbit monoclonal
Anti-SIRT1 antibody [19A7AB4]	Myoblot: 1:100	Abcam	Primary mouse monoclonal
Anti-Laminin α2 antibody	IFI: 1:1000	Sigma Aldrich	Primary rat monoclonal

Droplet digital PCR (ddPCR)

RNA was extracted from cell pellets using the RNeasy mini kit (Qiagen), followed by reverse transcription of the samples using 1µg RNA and the SuperScrip™ IV Reverse Transcriptase (Invitrogen) according to the manufacturer's protocols. cDNA samples were diluted in nuclease-free water to a concentration of 10 ng/µL.

Gene expression was confirmed and quantified using a QX200™ Droplet Digital™ PCR system (Bio-Rad). The reaction was performed using 2 µl of cDNA in a 20 µl reaction volume containing: 2 µl of Taqman probes (see table 7), 10 µl of ddPCR™ Supermix for Probes (no dUTP) (Bio-Rad) and 6 µl of DNase/RNase-free H_2O. All samples were analysed in triplicate and a no template control (NTC) was included as a negative control in all the experiments performed.

To generate the droplets, 20 µL of the previous ddPCR reaction and 70 µL of Droplet Generation Oil for Probes (Bio-Rad) were added to the 8-channel droplet generation cartridge (Bio-Rad), according to the manufacturer's instructions and this cartridge was placed in the QX200 droplet generator (Bio-Rad). After approximately 2 min, 40 µL of the resulting droplet emulsion was transferred to a semi-skirted 96-well PCR plate (Eppendorf), sealed with foil, and amplified on a thermal cycler using the following amplification conditions: enzyme activation for 10 min, 40 cycles of 94°C for 30 s and 55°C for 1 min. Finally, heat deactivation was performed at 98°C for 10 min.

Plates containing the amplified droplets were loaded into the QX200 droplet reader and results were analysed using QuantaSoft software™ (Bio-Rad). As a quality control, data were only included in the analysis if 10,000 or more droplets were obtained per sample.

Table 9. Taqman probes used digital droplet PCR analysis.

Gene	Id	Label	Manufacter
UTRN	Hs01125975_m1	FAM	ThermoFisher Scientific
MyH3	Hs01074230_m1	VIC	ThermoFisher Scientific
MyH2	dHsaCPE5050991	HEX	Bio-rad
Myf5	dHsaCPE5026295	HEX	Bio-rad
SIRT1	dHsaCPE5033410	FAM	Bio-rad
SIRT2	dHsaCPE5057131	HEX	Bio-rad

***In vivo* treatment**

C57BL/10ScSn-DMDmdx/J mice (*mdx*) and C57BL/10ScSnJ mice (wild-type), were obtained from The Jackson Laboratory (Bar Harbor, ME, USA). All experimental procedures were conducted at Biogipuzkoa Health Research Institute in accordance with protocols approved by the Institutional Animal Care Ethical Board Committee of the Donostia University Hospital. The mice were aged between 11 and 12 months.

Three mice per group were treated with 50 mg/kg AGK dissolved in PEG400 in saline solution and three mice per group were treated with vehicle (146) (saline). Treatment was administered by intraperitoneal injection once daily for 8 days. At the end of the treatment, mice were sacrificed by cervical dislocation and quadriceps muscles were dissected for histological and western blot analyses.

Quadriceps were embedded in OCT medium and snapped frozen in liquid nitrogen cooled isopentane. All muscles were stored at -80ºC until sectioning.

Cross-sections of 8 µm were made in a Leica CM1950 cryostat and samples were sent to our laboratory for further analysis.

Immunohistochemistry assays

Sections were fixed with pre-cooled acetone, air dried for 30 min, and incubated in a blocking buffer (20% FBS, 20% NGS in PBS) for 1 hour. The samples were then double stained with primary antibodies, Mancho 7 mouse monoclonal anti-utrophin (1:50, The MDA Monoclonal Antibody Resource) and rat monoclonal anti-Laminin α2 antibody (1:1000, Sigma Aldrich), both diluted in blocking buffer and incubated for 2 hours at room temperature. After three washes with PBS, samples were incubated for 1 hour at room temperature in the dark with secondary antibodies Alexa Fluor 488 goat anti-mouse IgG (H+L) and Alexa Fluor 594 donkey anti-rat IgG (H+L) both diluted in PBS (1:200). The samples were then washed 3 times with PBS and the nuclei were stained incubating them in Hoechst diluted in PBS (1:2000) for 5 min at room temperature and protected from light. After three washes with PBS, samples were mounted using PermaFluor Aqueous Mounting Medium (Thermo Scientific™) and coverslips. Images were captured using a ZEISS AXIO OBSERVER microscope at the Microscopy Platform of Biobizkaia Health Research Institute.

Analysis was performed according to the Arechavala-Gomeza method (20). Using Image J software, 10 regions of interest (ROIs) were randomly selected. ROIs were placed at the junction between two different muscle fibres. For each ROI, the lower intensity detected (representing the cytoplasm) was considered the background signal and subtracted from the higher intensity value (corresponding to the sarcolemma). Different fields of view of 5 different slides per condition (100 ROIs in total) were selected for the analysis. This procedure was performed for both stains, utrophin and laminin. The utrophin signal was then normalised to the laminin signal of the same ROI to obtain the final data for analysis.

Statistical analysis

Statistical analyses were performed using GraphPad Prism 9.1.2 software. After detection and removal of outlier data (ROUT method, Q = 1%), the distribution was analysed using the Shapiro Wilk test. For data that followed normal distribution, t-Student or one-way analysis of variance (ANOVA) followed by Tukey's post hoc tests was used, while for data that did not follow a normal distribution Kruskal-Wallis or Mann-Whitney U test followed by Dunn's post hoc test was used instead throughout this study to calculate P-values to determine statistical significance (*p-value<0.05, ** p-value<0.01, ****p-value<0.0001). All results are expressed as mean ± standard error of the mean (SEM).

RESULTS

Establishment of the utrophin quantification platform

In this study we have established a platform for *in vitro* utrophin quantification combining:

- accurate measurements of protein by myoblot assays,
- gene expression by droplet digital PCR
- a reliable positive utrophin overexpression control generated by CRISPR/Cas9 gene edition.

Myoblot optimisation for utrophin quantification

The myoblot method, routinely used in our laboratory for dystrophin quantification, was adapted and optimised for utrophin quantification. Three principal modifications were performed: selection of the appropriate 96-well plate, cell linearity assays, and antibody selection and titration.

1. Selection of the appropriate 96 well plate:

Preliminary experiments carried out in our laboratory using transparent tissue culture microplates for myoblot assays, revealed an important variability across the plate when reading at the 700 nm channel. The 700 nm channel is commonly used for cell number normalisation using Cell Tag 700 Stain, an antibody that accumulates in both the nucleus and the cytoplasm of permeabilized cells. As normalisation is a critical step in obtaining reliable and reproducible quantitative results, we investigated how much this variable cell number quantification between wells affected our results. The Cell Tag signal was clearly lower in the central wells of the plate compared to the edge wells (figure 13). This variability has been also reported previously by other groups and is related to the edge effect as well as the autofluorescence caused by the type of plate used (135).

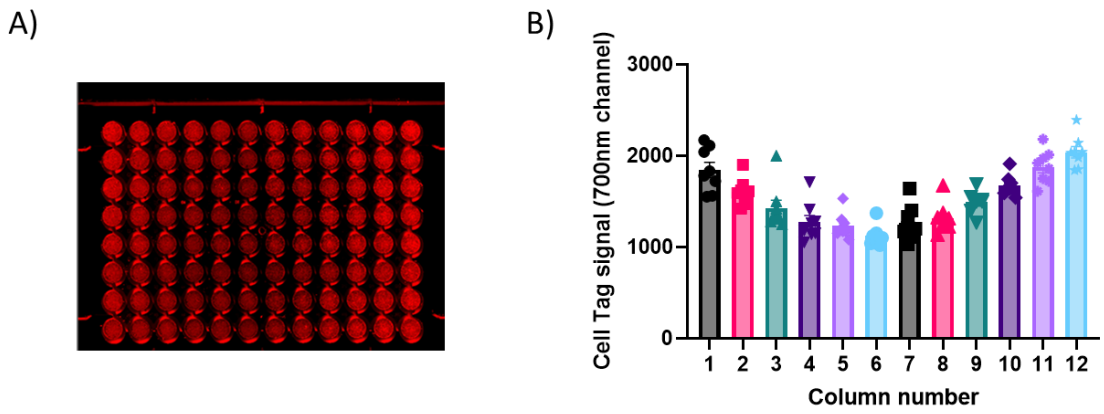

Figure 13. Cell Tag signal variability using transparent microplates.

A) Microplate image after myoblot assay using DMD myoblasts (7500 cells per well). Cell Tag signal detected for 700 nm channel showed lower intensity in the middle wells that was probed after quantification. B) Cell Tag signal, grouped by columns (n=8 wells), showed significant differences especially between columns 1,2,11 and 12 and the rest of the columns in the plate. Data are presented as mean ± SEM.

As a part of the validation process, two different types of 96-well plate, transparent (Costar) and black (Greiner), were scanned completely empty on the Odyssey CLx imaging system using the same settings under which the experiments would be later performed.

We found that the variation in raw signal magnitude between columns was higher for the transparent plates for both 700 and 800 nm channels, but also the raw signals obtained in the 700nm channel with the transparent plate were higher for all the columns compared to the black plate (Figure 14).

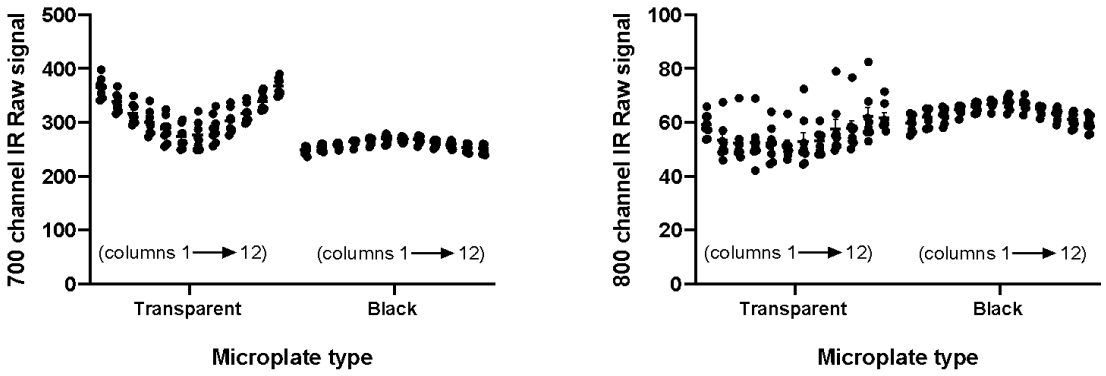

Figure 14. IR raw signal comparison between two types of microplates.

Transparent 96-well plate (Costar) and black 96-well plate (Greiner) were scanned empty on the Odyssey Clx system using the auto acquisition settings. Data from the 12 columns (1-12) are represented on the graph from left to right for each plate type. On the left graph, black microplates exhibited better inter-well column consistency and low auto-fluorescence in the 700 channel. On the right graph, auto-fluorescence signal intensity is similar for both types of plates while inter-well column consistency is better in the black microplate in the 800 channel. Data are presented as mean ± SEM (n=8 wells per column).

As black plates appeared to have better properties, they were selected for further use in the myoblot protocol. In later experiments we could corroborate that the Cell Tag signal was more uniform and intense across the plate using black plates. Additionally, we decided not to use the wells in the outer rows and columns of the plates for analysis, leaving them filled only with PBS to avoid edge effects (figure 15).

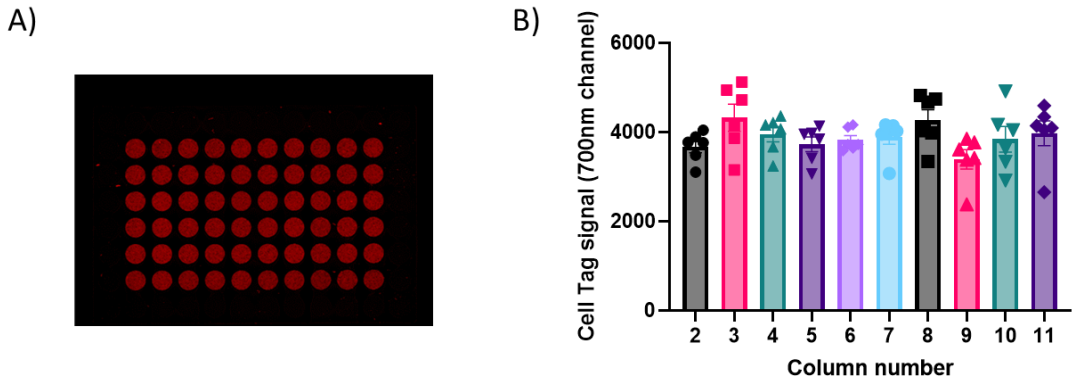

Figure 15. Cell tag signal variability using black microplates.

A) Microplate image after myoblot assay using DMD myoblasts (7500 cells per well). Cell Tag signal detected in the 700 nm channel showed uniform intensity between wells that was probed after

quantification. B) Cell Tag signal, grouped by columns (n=6 wells), showed no significant differences between columns. Data are presented as mean ± SEM.

2. *Cell linearity assays:*

Determining the relationship between cell number and signal intensity is important to ensure that signals are within the linear range of detection, as quantification performed outside this range will be inaccurate. Cell linearity assays were performed following the recommendations of the In-Cell Western™ Assay Development Handbook provided by LI-COR Biosciences and then analysed using Empiria Studio (Figure 16A) software. The appropriate cell seeding range for accurate target detection was found to be between 2500 and 5500 cells/well for control myoblasts and between 2500 and 7500 cells/well for DMD myoblasts (Figure 16B).

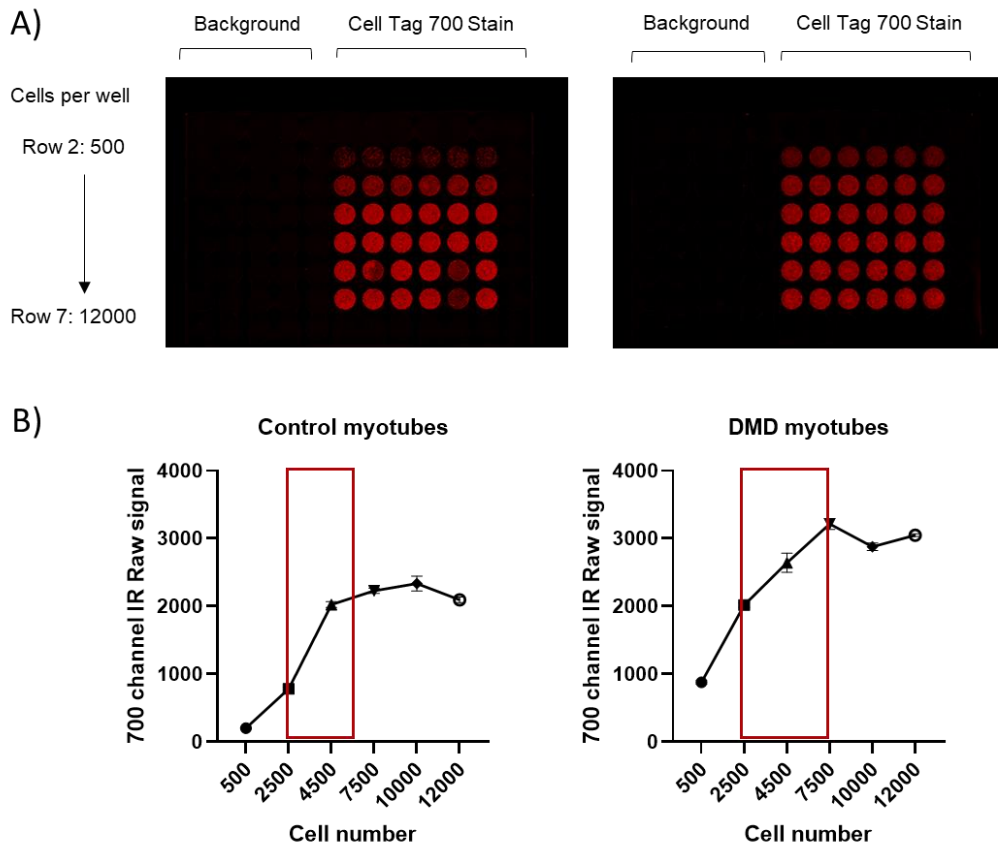

Figure 16. Cell linearity assays.

A) Microplate images after cell linearity assays in control myotubes and DMD myotubes. B) Quantification of Cell Tag 700 Stain signal according to cell density in each cell culture analysed. Linear range of detection

was determined using Empiria Studio software and is highlighted with a red rectangle in the graphs. Data expressed as mean ± SEM (N=6).

3. Antibody selection:

After reviewing the literature, we decided to select the mouse monoclonal anti-utrophin Mancho 7 antibody (from The MDA Monoclonal Antibody Resource), which had been previously validated for western blot and immunofluorescence, as the best option for utrophin myoblot assays. We first performed an antibody titration experiment to select the optimal antibody concentration for our experiments. We compared utrophin expression by myoblot in control and DMD myotubes at 1:200, 1:400, 1:600 and 1:800 dilutions, determining that 1:400 was the optimal dilution according to the linear range of detection and an optimal signal-to noise ratio (figure 17A).

Although Mancho 7 was our first option due to previous western blot and immunohistochemistry characterisation, we performed a comparison with other monoclonal anti-utrophin antibodies (figure 17B) in which Mancho 7 offered a significantly higher signal at lower concentrations that the other antibodies, which corroborated our selection.

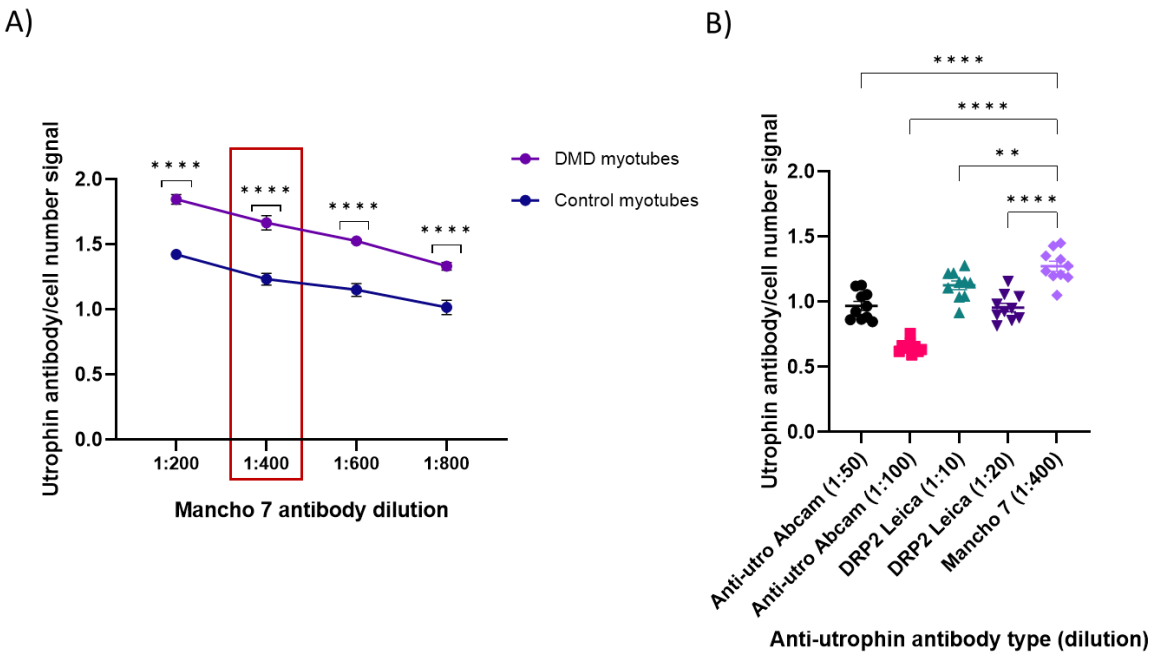

Figure 17. Utrophin antibody selection.

A) Utrophin quantification by myoblot assay in control and DMD myotubes for different Mancho 7 antibody dilutions. Data expressed as mean ± SEM (two-way ANOVA, Bonferroni's multiple comparisons test), n=10 per each dilution tested. Significant differences in utrophin signal between cell lines (****p<0.000,1). The selected dilution was chosen according to the linear range of detection and an optimal signal-to noise ratio and is highlighted in red. B) Utrophin quantification by myoblot assay in DMD myotubes for Abcam and DRP2 Leica anti-utrophin antibodies at different dilutions compared to anti-utrophin Mancho 7 antibody diluted at 1:400. Data expressed as mean ± SEM (one-way ANOVA, Dunnett's multiple comparisons test). N=10 per each condition tested. Significant differences in utrophin signal between Mancho 7 (1:400) and all the other antibodies tested (**p<0.01, ****p<0.000,1).

To summarise, the optimisation made in myoblot assays for utrophin quantification consisted in using black, 96 well plates from a specific vendor instead of transparent ones to avoid interferences, selecting the appropriate cell seeding range depending on the cell type used for each experiment, and the use of Mancho 7 anti-utrophin antibody at 1:400 dilution for an optimal utrophin signal.

Digital droplet PCR optimisation for utrophin quantification

The experimental set-up of ddPCR technology for the absolute quantification of utrophin expression was performed using RNA extracted from myotube cultures of healthy controls and DMD patients. For this analysis, a pre-designed UTRN TaqMan probe, already validated for RT-qPCR use in human DMD myoblasts, was selected (2). Optimisation steps involved the evaluation of different parameters, including selection of the total amount of cDNA template and setting up the appropriate annealing temperature for the probe to maximise the difference between negative and positive droplets, which helped to establish a threshold. To reduce quantification bias due to pipetting errors, samples were analysed in triplicate and non-template controls (NTCs) were included in all the experiments performed. Some of the following results were part of a Masters project carried out in our laboratory.

1. Selection of optimal cDNA template amount.

The amount of cDNA template required for ddPCR gene expression experiments varies depending on the expression level of the target genes. To determine the optimal

amount of cDNA template for our assay, we compared utrophin expression between control and DMD myotubes using the following range of cDNA template concentrations: 40 ng/µl, 20 ng/µl, 10 ng/µl, 6 ng/µl and 3 ng/µl. We observed a well-differentiated cluster of positive droplets in FAM in all the range studied (Figure 18A). As expected, copies per µl were lower at lower template concentrations. Utrophin expression was significantly higher in DMD myotubes compared to control myotubes at cDNA concentrations of 40 ng/µl, 20 ng/µl and 10 ng/µl, however, as the expression of the utrophin gene is not very high, a lower template concentration of 6 ng/µl or less might not be enough to detect a statistically significant difference between patients and controls (Figure 18B). For that reason, a concentration of 10 ng/µl of cDNA template was chosen.

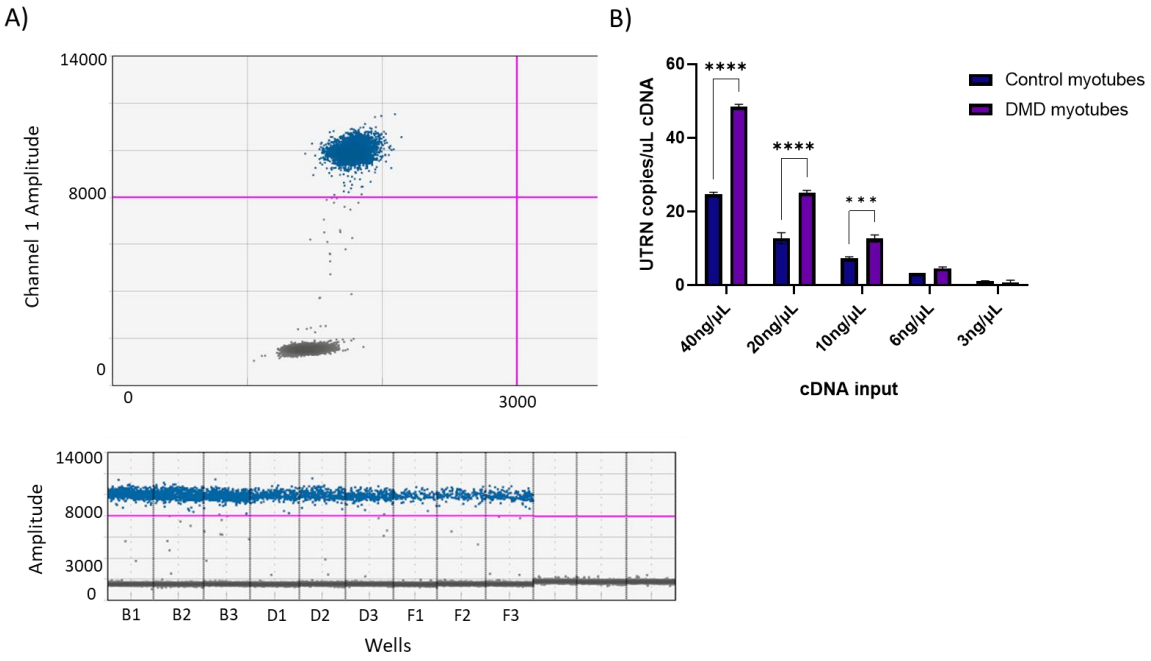

Figure 18. Serial dilutions of cDNA input.

A) Representative 2D and 1D plots showing positive droplet clusters in blue and negative events in grey. The pink lines correspond to the threshold line. B) Utrophin copies per µl at different cDNA input concentrations comparing control and DMD myotubes. Data expressed as mean ± SEM of n=3 technical replicates per concentration tested. Significant differences in utrophin expression between cell lines were determined by two-way ANOVA and Bonferroni's multiple comparisons test (***p<0.001, ****p<0.000,1).

2. Annealing temperature selection and threshold setting.

The annealing temperature was optimised using a gradient PCR range between 60 and 50°C using 10 ng/µl of cDNA generated from DMD myotube RNA samples. For all temperatures tested, the quality of the cluster separation was very good, and the concentration was similar between the different conditions (Figure 19). We selected as optimal the intermediate temperature of 55ºC, which was also used in the previous experiments for cDNA input selection as recommended by the experts of the Genomics Facility of our institute. As the separation between the positive and the negative clusters was very clear, the concentration was not significantly affected by the position of the threshold and the number of false negatives or false positives was minimal.

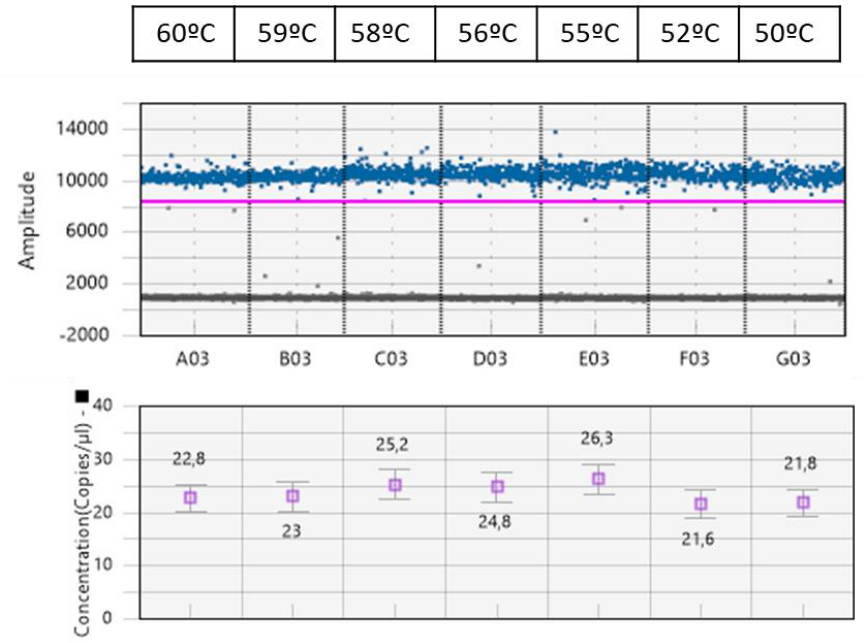

Figure 19. Annealing temperature gradient range.

Above, 1D plot showing positive droplet clusters in blue and negative events in grey at the corresponding temperatures from 60ºC to 50ºC. The pink line corresponds to the threshold line. Below, utrophin concentration at each temperature tested.

Utrophin over-expressing cell culture model generated by CRISPR/Cas9 gene editing.

CRISPR/Cas9 is a very efficient tool that has been successfully employed to correct mutations but also to provide many new cellular and animal models to further understand DMD pathology and conduct preclinical studies. *In vitro* cellular models are particularly useful for assessing the efficacy of novel therapies for DMD due to the wide spectrum of DMD mutations and the difficulty of obtaining muscle biopsies from DMD patients.

The first objective of this work was to generate a cell culture model that overexpresses utrophin that could be applied in *in vitro* drug screening.

1. CRISPR/Cas9 editing strategy and validation in HEK239 cells.

In order to perform a CRISPR/Cas9 mediated deletion in the 3' UTR region of the human UTRN gene we designed a total of ten sgRNAs flanking the inhibitory microRNAs (miR135, miR202 and let7) binding site region, five cutting before (sgRNAs 21-25) and five cutting after (sgRNAs 26-30) the target region, aiming to generate two double-stranded breaks (DDBs) leading to the removal of this region (Figure 20).

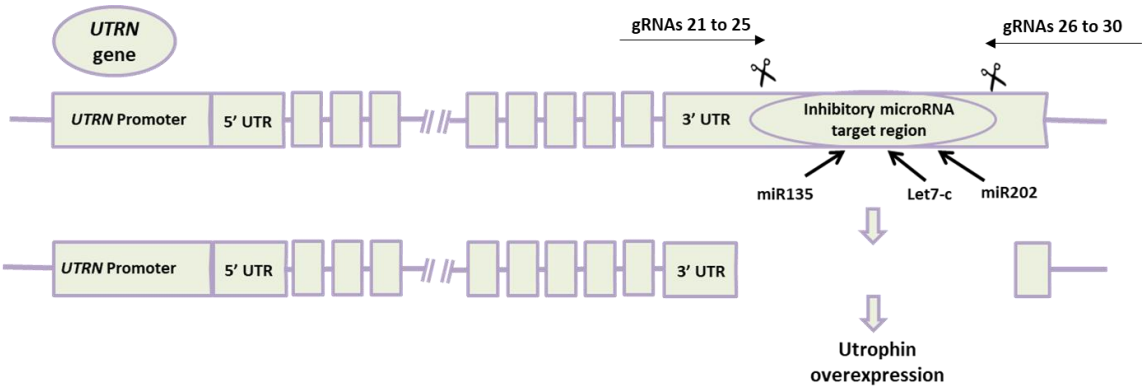

Figure 20. Editing approach.

Schematic representation of our strategy for editing the UTRN loci. A pair of flanking sgRNAs were co-transfected to delete the inhibitory microRNA target region contained in the 3'UTR of UTRN gene.

Each sgRNA was cloned into a px458 plasmid expressing the Cas9 nuclease and a GFP reporter. All the different combinations of sgRNAs pairs (Figure 21A) were first transfected into HEK293 cultures to test their deletion efficiency by genomic PCR (Figure 21B). The combination of sgRNA22 and sgRNA26 was the one that showed DNA cleavage and was therefore selected for transfection of DMD human immortalised myoblasts.

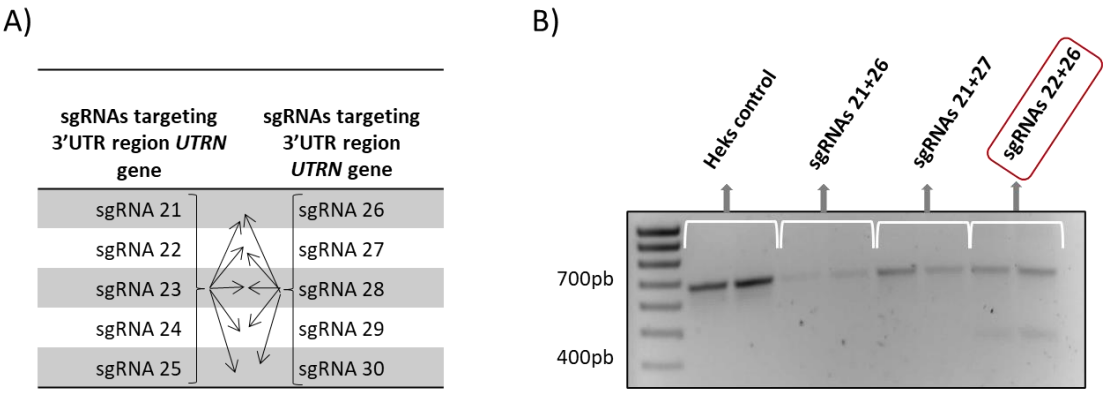

Figure 21. sgRNAs pairs test: sgRNAs' combinations and evaluation of the best combinations in HEK293 cells.

A) Representation of all the different sgRNAs combinations tested for editing the UTRN loci. B) Representative PCR analysis of HEK293 cells transfected with some of the sgRNAs combinations tested. Upper bands correspond to wild type or non-edited cells, while the lower bands correspond to the edited ones. Samples were analysed in duplicates (marked in white). Selected sgRNA combination is highlighted in red: sgRNA22+sgRNA26.

2. Myoblasts transfection and FAC sorting.

Human DMD immortalised myoblasts were transfected with the recombinant plasmids containing sgRNAs 22 and 26. At 48 hours post-transfection, and after confirming under the microscope that fluorescence was present (Figure 22A), the myoblasts were trypsinised and collected for fluorescence activated cell sorting (FACS). This showed that only 1.19% of the total cell population was GFP-positive and these cells were individually seeded into microplates containing SMMC medium for clonal selection (Figure 22B).

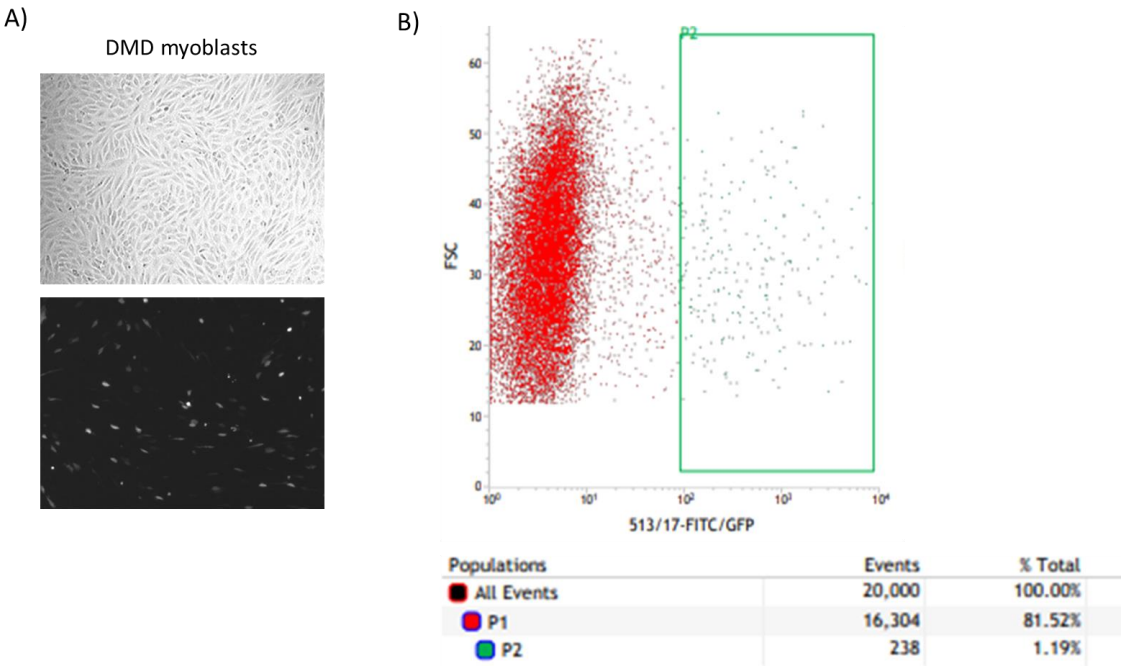

Figure 22. Myoblasts transfection and FAC sorting.

A) Representative bright-field and GFP positive DMD myoblasts images 48 hours after plasmids transfection. Images were taken to check fluorescence just before being trypsinised and collected for fluorescence-activated cell sorting (FACS) sorting. B) Forward scatter (FSC) dot plots obtained after cell sorting. In green, fluorescence population (P2) represents 238 of all the events detected which means 1.19% of total population. GFP-positive cells were individually seeded in microplates containing SMMC medium for clonal selection.

3. Confirmation of the deletion in edited myoblast clones.

After FACS sorting of individual GFP-positive cells, clones were expanded for DNA extraction. Nine clones were analysed to confirm the presence of the desired deletion by genomic PCR (Figure 23A) and the amplicons corresponding in size with the expected deletions were analysed by Sanger sequencing (Figure 23B). Clones number 3 and 4 were edited in one allele only, while clones' number 2 and 8 were completely edited. The expected deletions were confirmed in all the positive clones but only clone number 8 was selected to be used for further analysis and was renamed as "DMD-UTRN-Model".

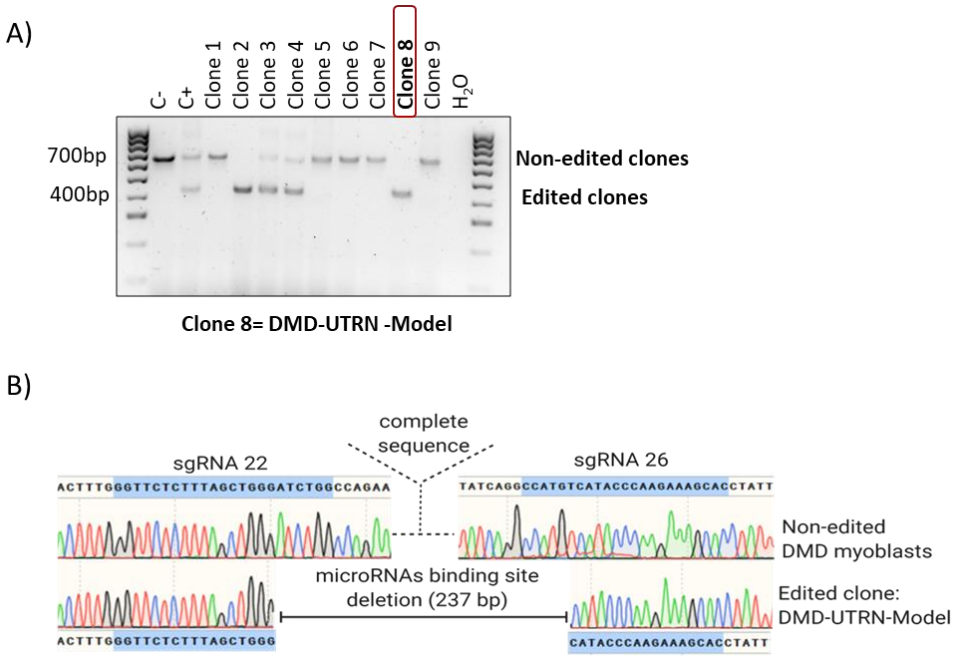

Figure 23. Genotyping UTRN deletion breakpoints in edited myoblast clones.

A) PCR genotyping of the UTRN edited clones. Larger products in agarose gels indicate non-edited clones, and shorter ones correspond with the expected deletion. B) Sanger sequencing of the smaller band corresponding to clone 8 (DMD-UTRN-Model) confirmed the expected gene editing. Sequences were analysed using SnapGene software.

4. Analysis of off targets in the DMD-UTRN-Model.

To evaluate any potential off-target effects, sgRNAs 22 and 26 were analysed *in silico* using the bioinformatics web tool CRISPOR (2019) (147). We selected the six most likely off-target sites for each sgRNA and analysed them in edited clones by PCR followed by Sanger sequencing. We found no off-target effects in any of the 12 sites studied (Figure 24).

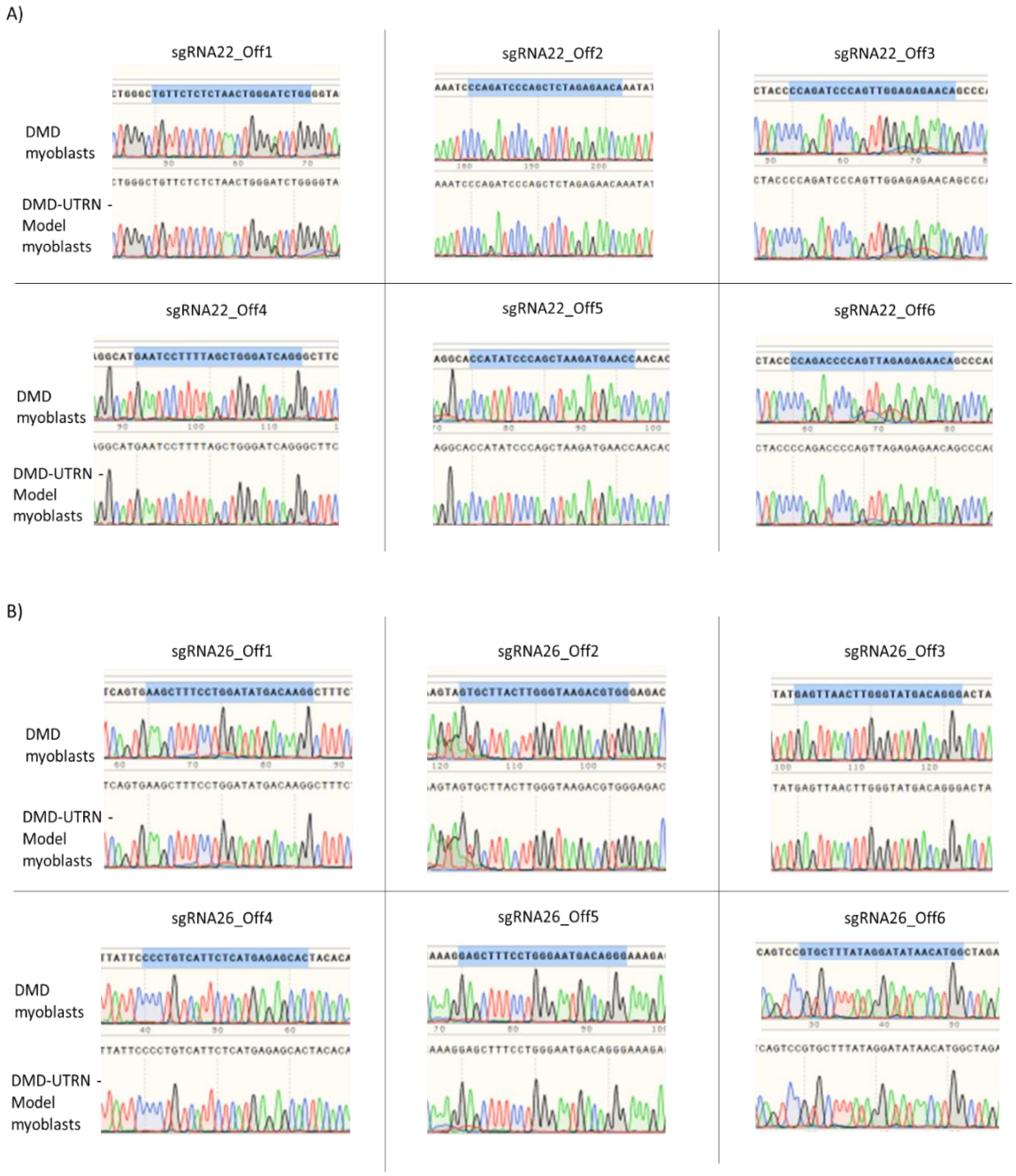

Figure 24. Sequencing results verifying the absence of off target effects.

Sanger sequences comparison between DMD myoblasts and DMD-UTRN-Model myoblasts show the absence of off-target effect of the six predicted off-targets regions for sgRNA22 (A) and the six for

sgRNA26 (B). The predicted sgRNAs binding sites sequences are highlighted in blue Sequences were analysed using SnapGene software.

5. Characterisation of the DMD-UTRN-Model.

Utrophin expression in DMD-UTRN-Model

to characterise the cell cultures, we first used traditional methods, like immunocytochemistry and western blotting, to detect and quantify utrophin expression in DMD-UTRN-Model cultures compared to unedited DMD cultures. Immunocytochemistry showed the increase in utrophin expression between unedited DMD and DMD-UTRN-Model myotubes (Figure 25A) and this increase was corroborated by western blot with a 195% increase between DMD and DMD-UTRN-Model myotubes (Figure 25B).

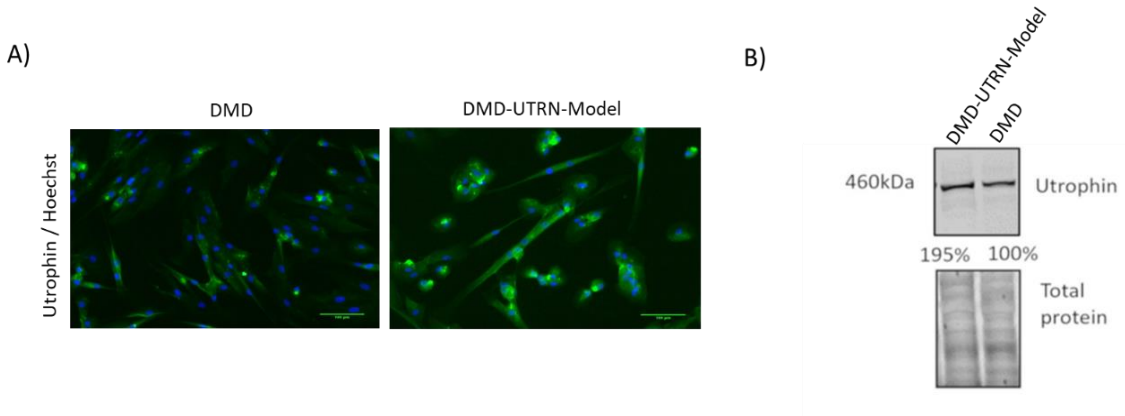

Figure 25. Utrophin expression in DMD-UTRN-Model cultures by traditional methods.

Characterization of DMD-UTRN-Model cultures. Utrophin expression in DMD myotubes compared to DMD-UTRN-Model studied by immunocytochemistry (A) and western blotting (B).

We completed the characterisation of the cell culture using our recently implemented utrophin quantification platform. However, we first performed a cell linearity assay to determine the appropriate number of cells needed for DMD-UTRN-Model myoblot

assays. The optimal seeding range for DMD- UTRN-Model was between 3500 and 7000 cells per well (Figure 26). As the seeding range for DMD myotubes was between 2500 and 7500 cells per well, we selected 6000 cells per well as the optimum number to perform DMD and DMD- UTRN-Model myoblot comparisons.

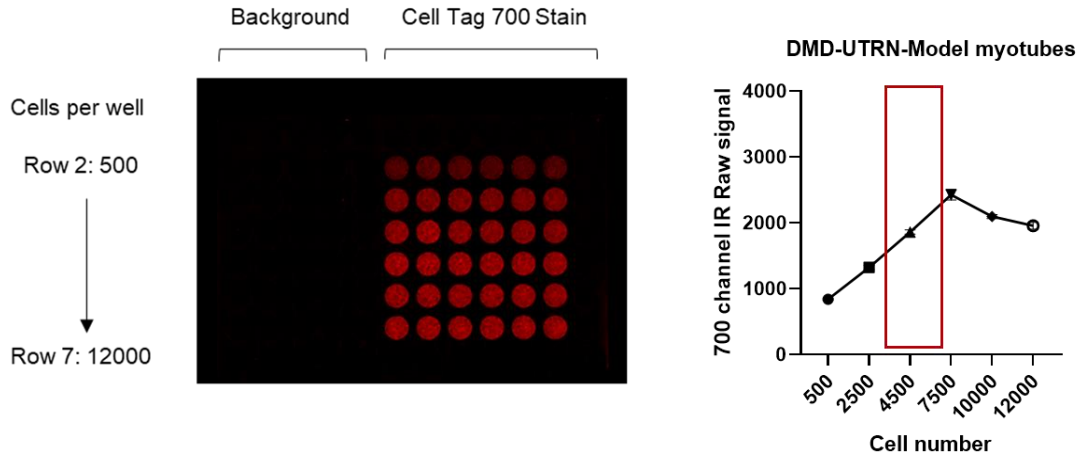

Figure 26. DMD-UTRN-Model cell linearity assay.

On the left, a microplate image of the cell linearity assay in DMD-UTRN-Model. Increasing number of cells was seeded from row 2 (500 cells per well) to row 7 (12.000 cells per well). On the right, Cell Tag 700 Stain signal quantification according to cell density in DMD-UTRN-Model. Linear range of detection was determined using Empiria Studio software and is highlighted with a red rectangle in the graphs. Data expressed as mean ± SEM (N=6).

Myoblot analysis of unedited DMD and DMD-UTRN-Model myotubes showed an increase in utrophin expression of approximately 50% (Figure 27A) and ddPCR analysis showed an increase of 148%, (Figure 27B) corroborating the previous results obtained using traditional methods.

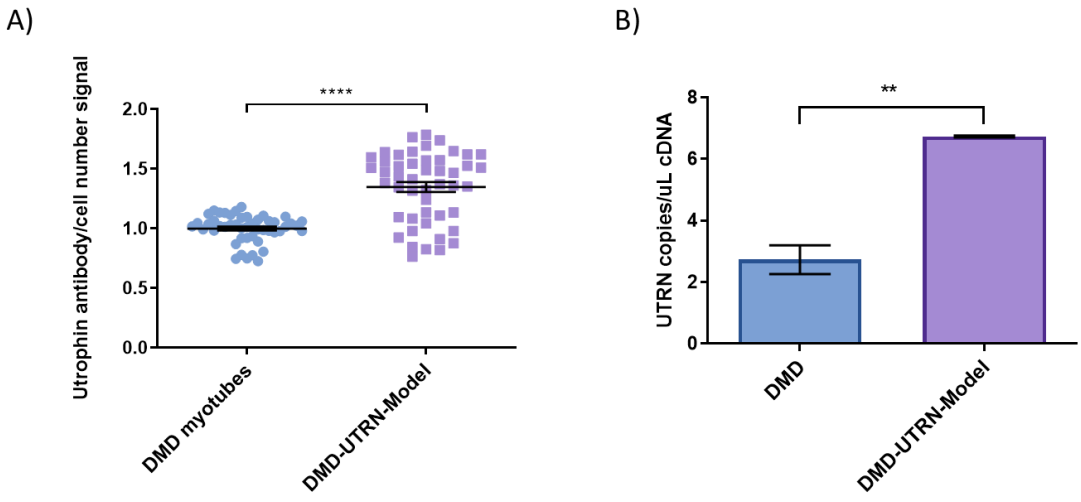

Figure 27. Utrophin expression in DMD-UTRN-Model cultures by utrophin quantification platform.

Utrophin expression in DMD myotubes compared to DMD-UTRN-Model studied by immunocytochemistry myoblots (A) and ddPCR (B). In myoblot n = 48 wells per cell type were compared and experiments were performed twice. For ddPCR experiments three technical replicates per sample and condition were run in parallel and a no template control (NTC) was included as negative control. (*p value < 0.05, **p value < 0.01, ****p value < 0.0001). (p values were determined with Mann–Whitney U test and error bars represent mean ± SEM).

Analysis of differentiation markers expression in the DMD-UTRN-Model

Observing the morphology of DMD-UTRN-Model cultures, we suspected that the editing and cloning process might have affected the differentiation of the edited model. To investigate differentiation, the fusion index (%) of edited and unedited myotubes was calculated after MF20 and Hoechst immunocytochemistry. Although the fusion index was lower in DMD-UTRN-Model compared to DMD myotubes, no significant differences were found between them (Figure 28).

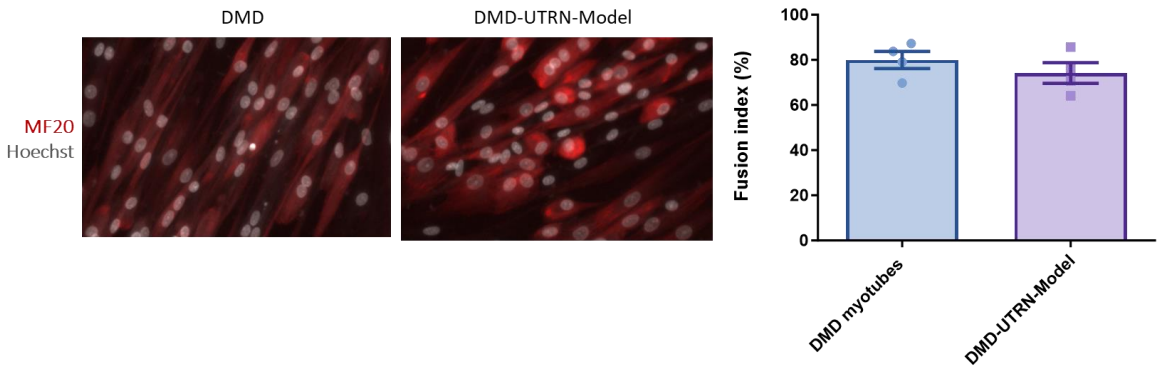

Figure 28. Fusion index in the edited DMD-UTRN Model.

Figure 28. Fusion index in the edited DMD-UTRN Model. Differentiated myotubes of and DMD and DMD-UTRN-Model cultures were immunostained for MF20 and Hoechst. Fusion index was calculated as the ratio between the number of nuclei in differentiated myotubes (defined as >2 nuclei and MF20-positive cells) compared to the total number of nuclei. For quantification, five fields per cell line were randomly chosen and more than 200 nuclei were counted.

To further study the differentiation of the DMD-UTRN-Model, the differentiation marker MF20 was analysed by myoblot. We could observe a significantly reduced expression of MF20 in the edited model compared to DMD myotubes (Figure 29A). Based on these findings, other myogenic regulatory factors like the myogenic factor 5 (Myf5) and the myosin heavy chain isoform 3 (MyH3) were analysed by ddPCR at different time points during myotube formation. As expected, Myf5 expression decreased during the differentiation process, while MyH3 increased in the same pattern in both cell types. However, we observed that the MyH3 marker was significantly lower in the edited model on days 5 and 7 after the onset of the differentiation process (Figure 29B).

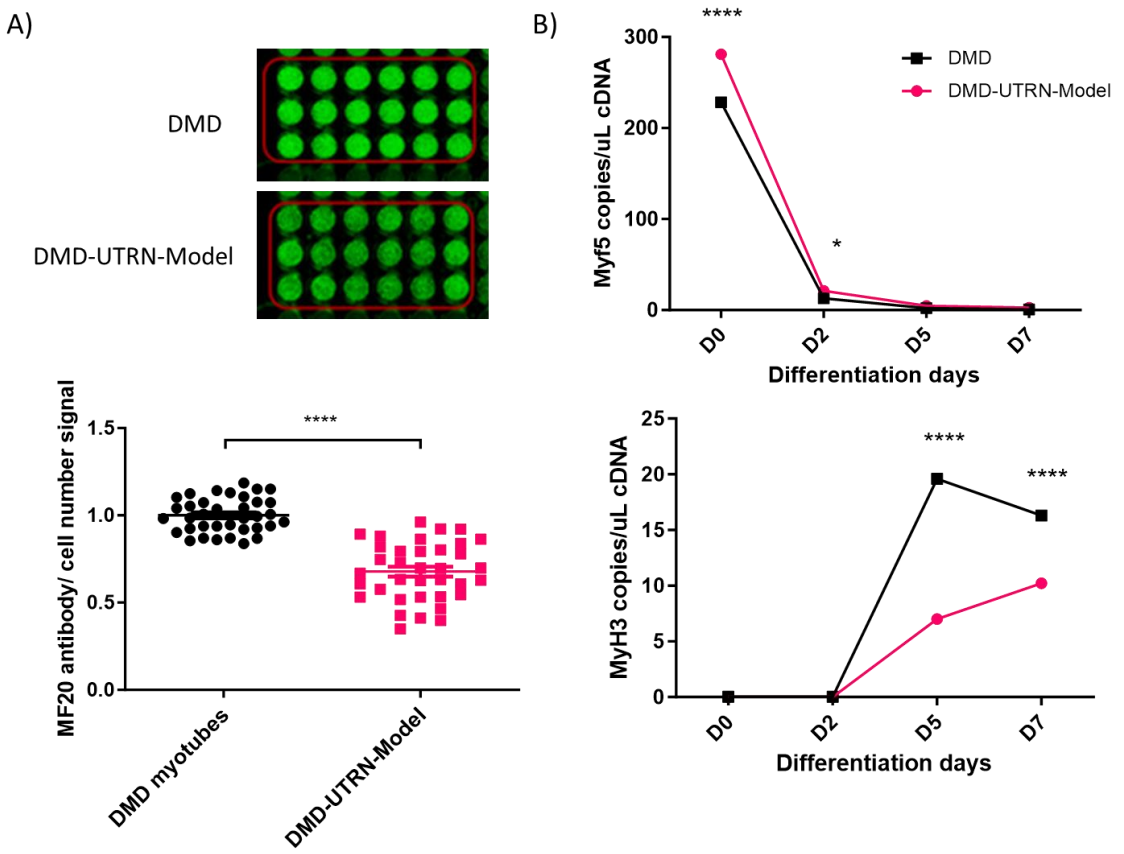

Figure 29. Differentiation markers analysis in the DMD-UTRN-Model.

A) MF20 expression determined by myoblot in DMD-UTRN-Model compared to DMD myoblasts. Myoblot analysis was performed using n=18 replicate wells for MF20 staining. B) Differentiation markers, Myf5 and MyH3, were studied by ddPCR at different fusion times in DMD-UTRN-Model cultures compared to DMD myotubes. For ddPCR experiments three technical replicates per sample and condition were run in parallel and a no template control (NTC) was included as negative control. (*p value < 0.05, **p value < 0.01, ****p value < 0.0001). (p values were determined with Mann–Whitney U test and error bars represent mean ± SEM).

According to these data, the gene editing process affected myotube formation, as differentiation markers were reduced in the DMD-UTRN-Model compared to unedited DMD cultures.

Study of dystrophin/utrophin glycoprotein complex proteins in the edited model

Based on recent studies where utrophin upregulation mediates the restoration of other DGC/UGC protein members, we studied whether the expression of two of the DGC/UGC, α-sarcoglycan and β-dystroglycan, was increased in DMD-UTRN-Model myotubes to further characterise our edited model. Myoblot analysis showed no significant differences between α-sarcoglycan (Figure 30A) and β-dystroglycan (Figure 30B) expression between the DMD-UTRN-Model and DMD myotubes.

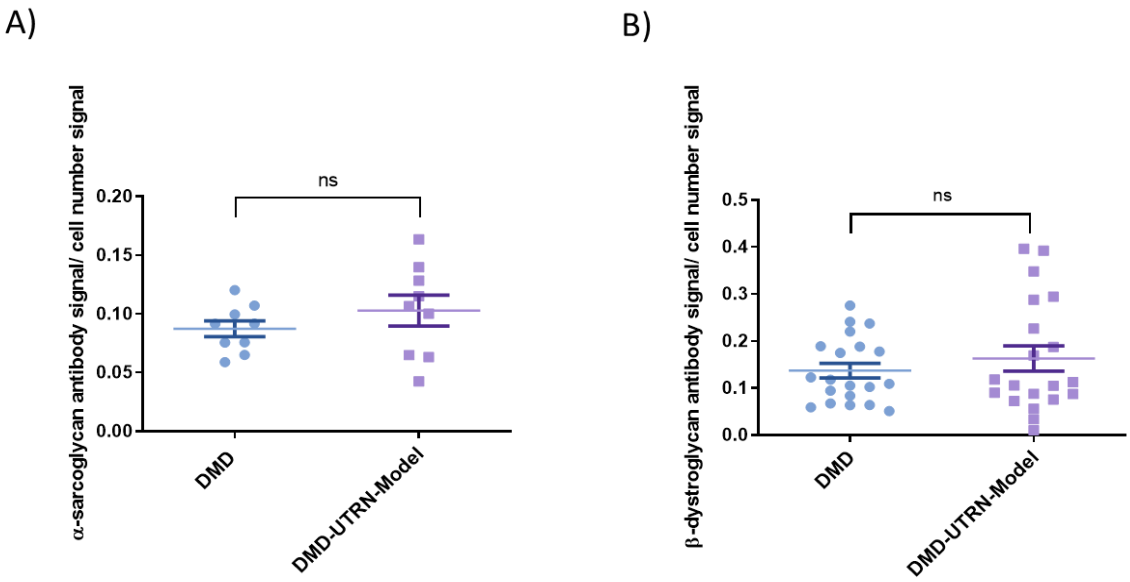

Figure 30. Dystrophin/Utrophin glycoprotein complex protein expression in DMD-UTRN Model.

α-sarcoglycan (A) and β-dystroglycan (B) expression was studied in DMD myotubes compared to DMD-UTRN-Model myotubes by myoblot. No significant differences were found between either α-sarcoglycan expression (n=10) or β-dystroglycan expression (n=20) between both cell types (P values were determined with Mann-Whitney U test and error bars represent mean ±SEM).

The accumulation of α-sarcoglycan and β-dystroglycan proteins and the formation of the DGC complex are closely associated with the myogenic differentiation process, therefore the reduction in matured myotubes in the DMD-UTRN-Model complicates the comparison of these proteins between DMD and edited cultures.

Evaluation of small molecules using the utrophin quantification platform.

Drug repurposing screening assay.

During the implementation of the utrophin quantification platform we collaborated with SOM Biotech, a Spanish biopharmaceutical company focused on accelerating the development of therapies for rare diseases using drug repurposing among other strategies. Initially, we performed a compound screening to identify up-regulators of utrophin expression using the myoblot assay. As the compound evaluation progressed, we optimised the ddPCR assays and generated the DMD-UTRN Model, both of which were included in the final experiments.

First, a battery of 60 small molecules was screened using the myoblot assay to identify small molecules capable of increasing utrophin expression in immortalised DMD myotubes. Ezutromid was used as a positive control at the company's request and all compounds were diluted first in DMSO and then in fresh differentiation medium to reach a common concentration of 5 µM (final DMSO concentration was 0.1% in DM) when added to cell cultures after 6 days of differentiation in fresh differentiation medium. 24 hours after treatment, utrophin protein levels were evaluated. A total of 44 compounds, including ezutromid, showed an increase in utrophin expression in DMD myotubes compared to non-treated cells (Figure 31). According to these results and considering the individual compounds' solubility, four of them (C03, C13, C32 and C42) were selected for further analysis.

To verify these results, DMD myotubes were treated with the selected compounds at increasing concentrations of 0.01, 0.1, 1 and 10 µM for 24 or 48 hours, and compared to the vehicle. Utrophin protein levels were assessed using the recently optimised myoblot. Ezutromid and halofuginone were also evaluated as positive controls. All compounds appeared to be inactive at any of the concentrations tested when being treated for 24 hours (data not shown) or for 48 hours (Figure 32) except for halofuginone at 10µM.

Once the ddPCR assay and the DMD-UTRN model were established in our laboratory and incorporated into the utrophin quantification platform, these candidates were reassessed. DMD myotubes were treated for 24 hours with halofuginone, ezutromid and compounds C03, C13, C32 and C42 at 0.01, 0.1, 1 and 10 µM, and compared to vehicle alone as a negative control and the DMD-UTRN model as a positive control. In this case, the results corroborate the upregulation of utrophin in DMD myotubes after treatment with halofuginone and ezutromid as well as compounds C03 and C13 at some of the concentrations (Figure 33).

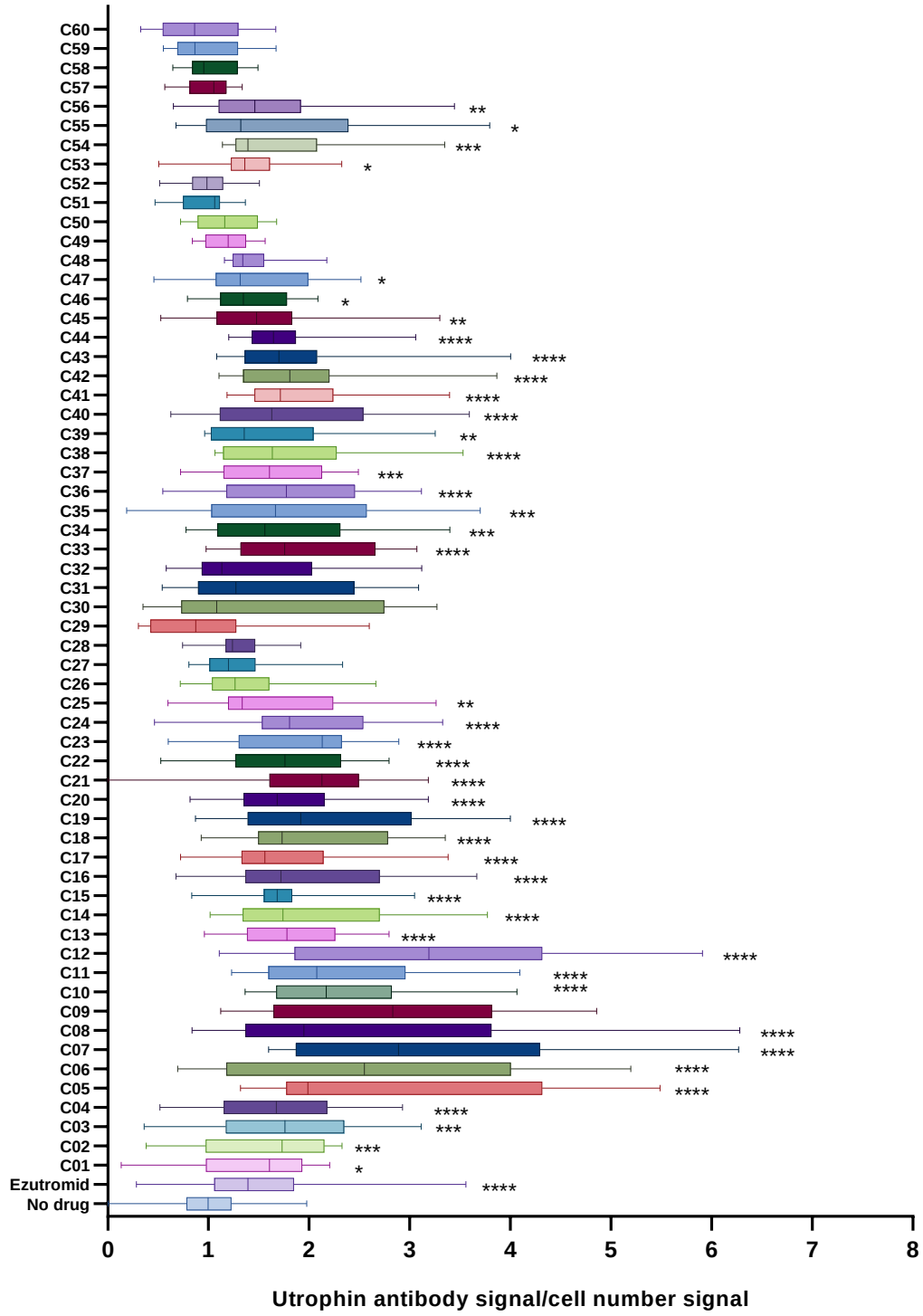

Figure 31. Small molecules' screening. Results of myoblot assays quantifying utrophin expression after treatment of DMD myotubes with 60 different compounds.

DMD myotubes were treated for 24h with each compound (C01 to C60) dissolved in differentiation medium (DM) with DMSO 0.1%. DMSO 0.1% in DM was also added to "no drug" wells. Each myoblot assays included 7 technical replicates per condition. Data are expressed as the mean fold change ± SEM over no drug (Kruskal Wallis test). N=3 independent experiments. (****p< 0.001, ***p<0.01, **p<0.1. *p<0.5).

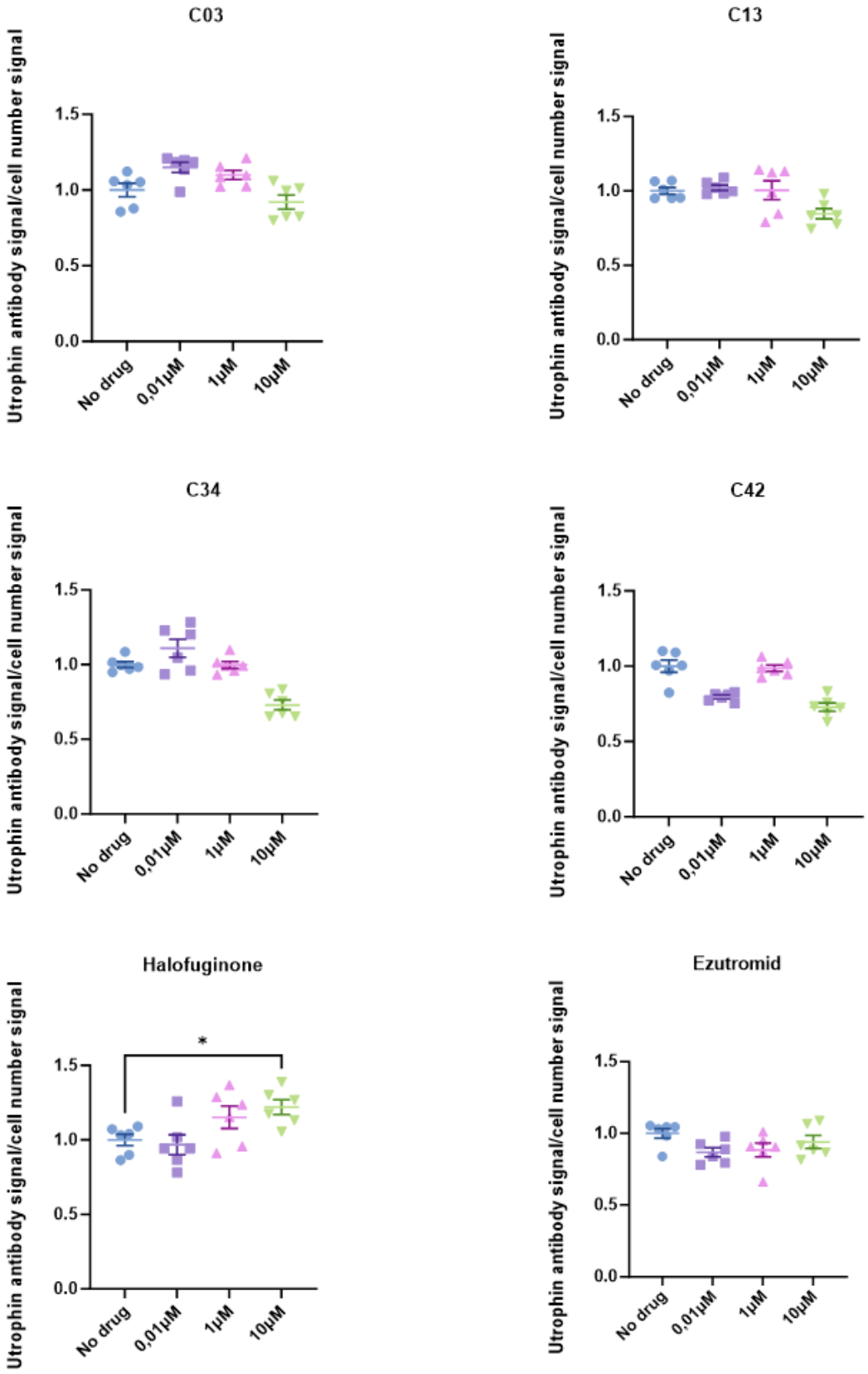

Figure 32. Myoblot utrophin evaluation of several doses of the selected small molecules.

DMD myotubes were treated for 48h with each compound (C03, C13, C34, C42, halofuginone and ezutromid) dissolved in differentiation medium (DM) with DMSO 0.1%. "No drug" wells were only treated with DMSO 0.1% in DM. Each myoblot assay included 5 technical replicates per condition. Data are

expressed as the mean fold change ± SEM over no drug (one-way ANOVA). N=3 independent experiments. (****p< 0.001, ***p<0.01, **p<0.1. *p<0.5).

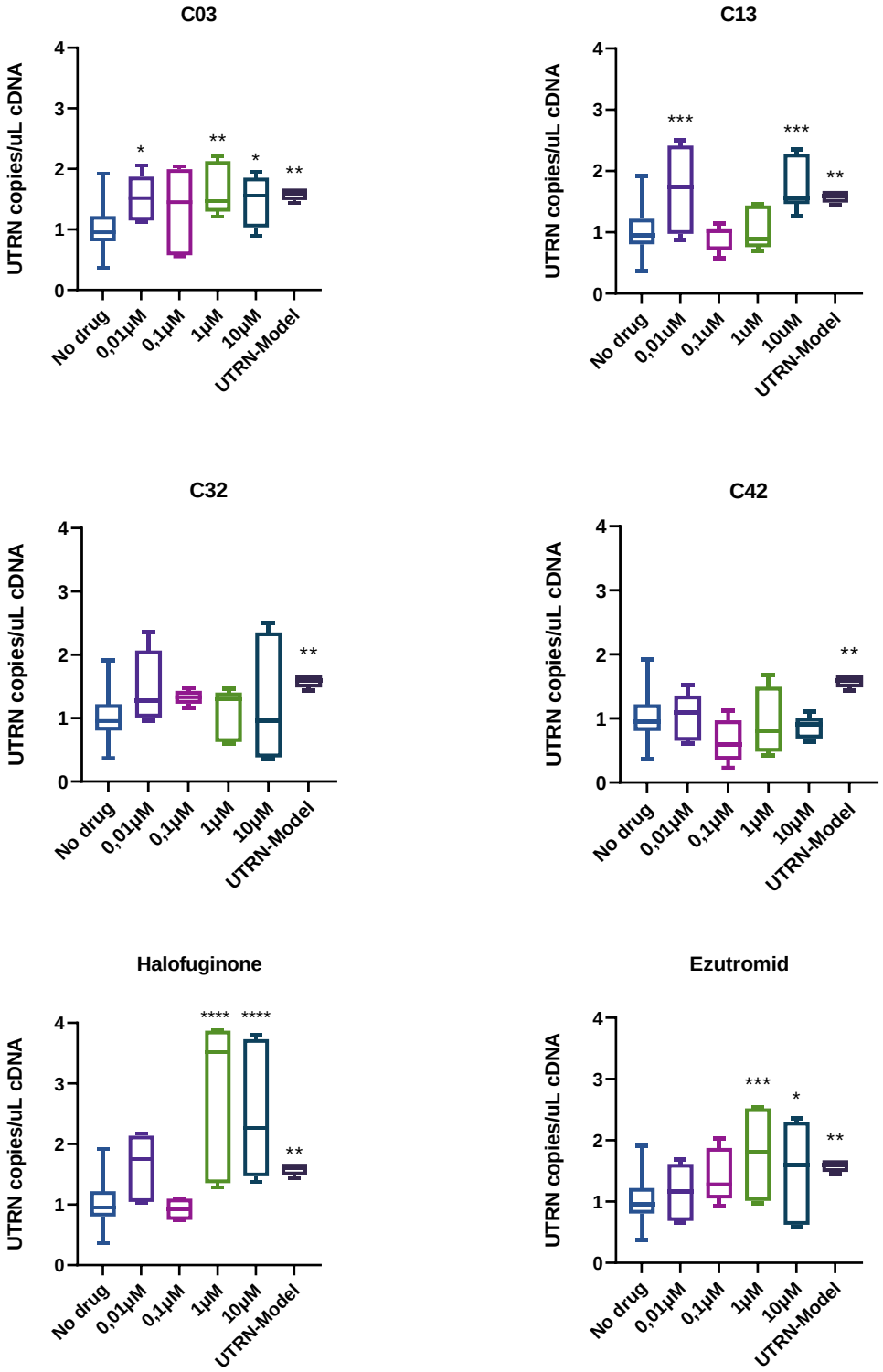

Figure 33. Evaluation of utrophin expression by ddPCR in the selected small molecules.

DMD myotubes were treated for 24h with each compound (C03, C13, C34, C42, halofuginone and ezutromid) dissolved in differentiation medium (DM) with DMSO 0.1%. No drug wells were only treated

with DMSO 0.1% in DM. ddPCR experiments included three technical replicates per sample and conditions were run in parallel with a “no template” control (NTC) included as negative control. Data are expressed as the mean fold change ± SEM over no drug (one-way ANOVA). N=3 independent experiments. (****p< 0.001, ***p<0.01, **p<0.1. *p<0.5).

New targets for utrophin overexpression: inhibition of histone deacetylases.

In the search for new therapeutic targets that could modulate utrophin expression, we decided to focus our studies on the histone deacetylase (HDAC) type III inhibitor AGK2, as other HDAC inhibitors, such as trichostatin A (TSA), had demonstrated utrophin upregulation and functional improvement in the *mdx* mouse model of DMD (148).

AGK2 is a small molecule that binds to the ATP binding site of sirtuin 2 (SIRT2) enzyme, blocking the substrate binding and inhibiting its activity. The benefits of SIRT2 modulation by small molecules have been demonstrated in cancer, metabolic and neurodegenerative disorders (149).

We hypothesised that inhibition of sirtuin 2 by AGK2 might increase utrophin expression, thereby promoting the oxidative phenotype of the cell and perhaps by increasing the expression of other sirtuins such as sirtuin 1, which is widely associated with utrophin upregulation in DMD muscles.

For that reason, we first studied sirtuin 2 expression in control and DMD immortalised cultures, after which we treated the DMD myotubes with AGK2 to measure utrophin levels using our utrophin quantification platform. Finally, we performed a small *in vivo* assay thanks to the collaboration with the Neuromuscular Disorders group at Biogipuzkoa Health Research Institute.

Relationship between utrophin and sirtuin 2 expression in control and DMD human myotubes.

Since sirtuins are regulators of cellular stress responses, we asked whether the expression of SIRT2 is deregulated in dystrophic cell cultures.

First, to verify that utrophin is upregulated in DMD myotubes we analysed utrophin expression in control and DMD cultures using ddPCR and myoblots. As expected, utrophin was overexpressed in DMD myotubes compared to control myotubes (Figure 34).

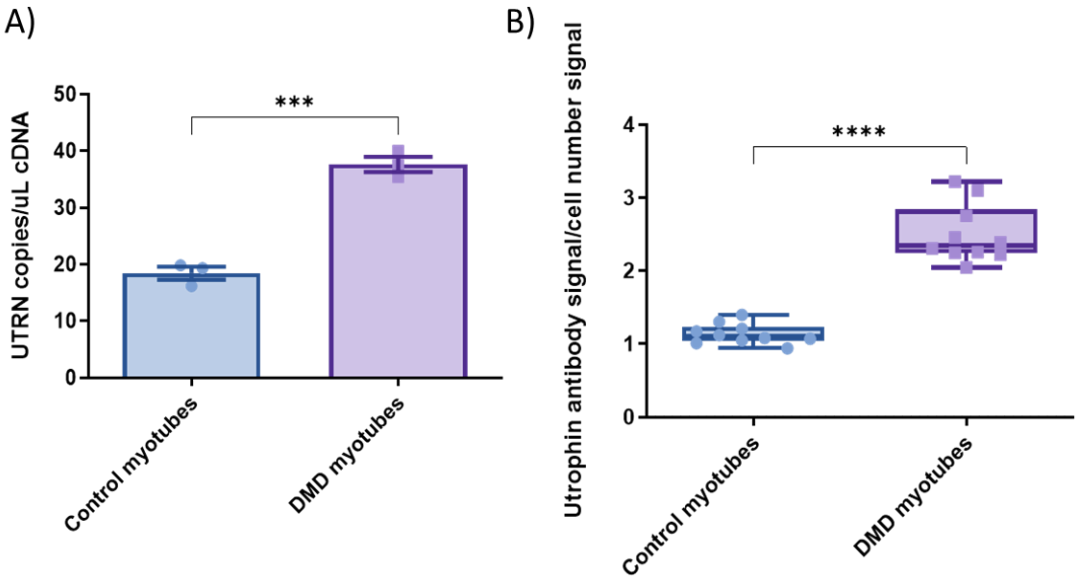

Figure 34. Utrophin expression in control vs DMD myotubes.

Utrophin Utrophin expression in DMD myotubes compared to control myotubes was studied by dddPCR (A) and myoblot (B). In ddPCR experiments 3 technical replicates per sample were run in parallel and a no template control (NTC) was included as negative control. In myoblot assays 10 technical replicates (individual wells) per cell type were compared. (***p value < 0.001, ****p value < 0.0001). (p values were determined with Unpaired t test and error bars represent mean ± SEM).

To study the expression of Sirtuin 2 in our cell cultures, both control and DMD myotubes were then immunostained. Sirtuin 2 was expressed along the cytoplasm in both control

and DMD myotubes, whereas no expression was observed prior to differentiation (Figure 35A). Sirtuin 2 levels were then quantified using the ddPCR and myoblot quantification combination in immortalised myotubes from DMD patients and controls.

The ddPCR assay showed no differences in *SIRT2* expression between DMD and control myotubes at the mRNA level (Figure 35B). However, myoblot quantification showed that sirtuin 2 protein was significantly upregulated in DMD myotubes compared to controls (Figure 35C).

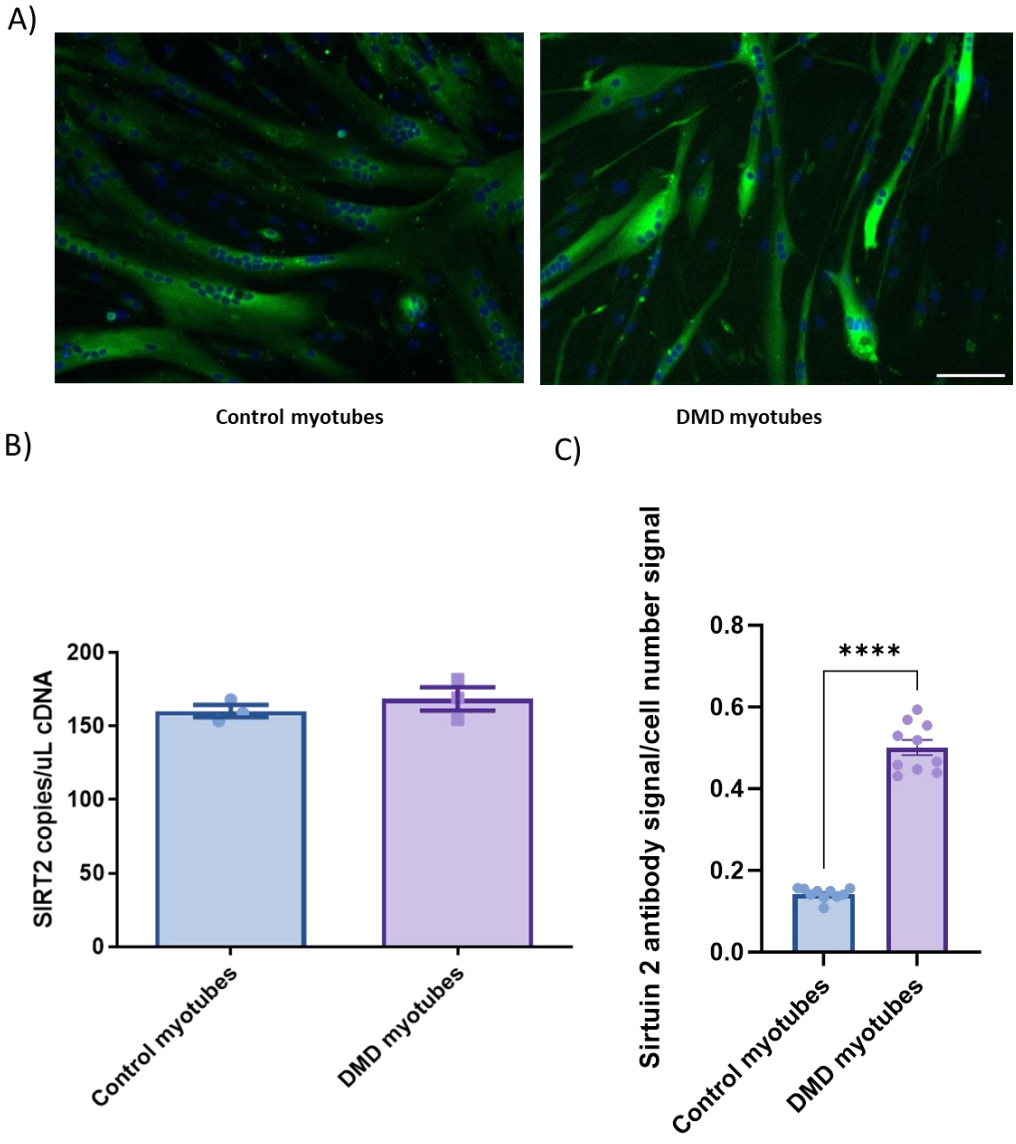

Figure 35. Sirtuin 2 expression in control vs DMD myotubes.

A) Representative images of immunofluorescence sirtuin 2 staining (in green) and nuclei staining with Hoechst (in blue). Scale bar 50 µM. Sirtuin 2 expression in DMD myotubes compared to control myotubes was studied by dddPCR (B) and myoblots (C). For ddPCR experiments 3 technical replicates per sample were run in parallel and a no template control (NTC) was included as negative control. In myoblot assays

n = 10 wells per cell type were compared as technical replicates (***p value < 0.001, ****p value < 0.0001). (p values were determined with Unpaired t test and error bars represent mean ± SEM).

According to these data, sirtuin 2 appears to be deregulated in DMD cultures compared to controls, making it an interesting target for the study of DMD pathogenesis and for DMD therapy research.

Evaluation of the ability of AGK2 to upregulate utrophin in DMD myotubes.

Considering that DMD myotubes showed increased levels of sirtuin2 protein, we hypothesised that inhibition of sirtuin 2 expression might further increase utrophin levels in DMD cell culture.

For this study, we chose the compound AGK2 (MedChemExpress, USA), as it is a cell-permeable, selective inhibitor of SIRT2 with an IC50 of 3.2 µM.

Initially, DMD myotubes were treated with increasing concentrations (0.01µM, 0.1µM, 1µM and 10µM) of AGK2 dissolved in differentiation medium and 0.1% DMSO for 24 hours. Cell pellets were then collected and UTRN expression was analysed by ddPCR.

Although AGK2 appeared to increase UTRN expression, no significant differences were found between untreated and treated DMD cultures (Figure 36A). We decided to repeat the experiments, increasing the exposure time to the drug from 24 to 48 hours and the concentrations of AGK2 used to 3µM, 10µM and 30µM respectively. After changing these conditions, we found that AGK2 significantly increased UTRN expression at all the concentrations tested overcoming the DMD-UTRN-Model UTRN expression used as a positive control (Figure 36B).

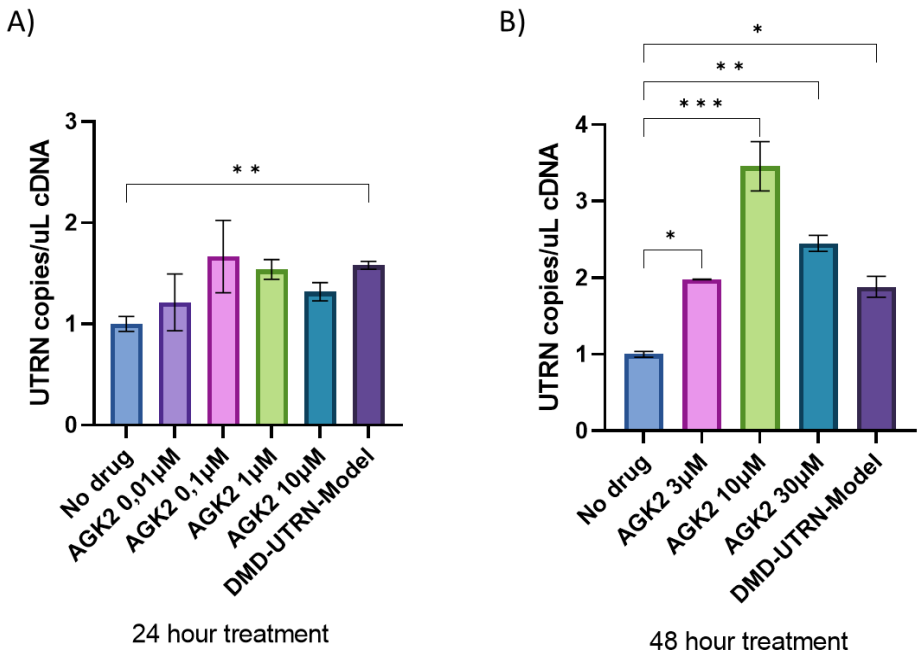

Figure 36. Utrophin evaluation by ddPCR after AGK2 treatment.

DMD myotubes were treated first for 24 hours (A) and then for 48 hours (B) with AGK2 dissolved in differentiation medium (DM) with DMSO 0.1% to reach increasing concentrations. "No drug" wells were only treated with DMSO 0.1% in DM and the DMD-UTRN-Model culture was used as a positive control. In ddPCR experiments, two technical replicates per sample and condition were run in parallel and a no template control (NTC) was included as negative control. Data are expressed as the mean fold change ± SEM over no drug (Kruskal-Wallis test ANOVA). N=3 independent experiments. (****p< 0.001, ***p<0.01, **p<0.1. *p<0.5).

We then used these optimised conditions to study utrophin expression by myoblot. Thereby, DMD myotubes were treated with AGK2 for 48 hours and microplates were fixed for myoblot analysis. Although AGK2 did not appear to affect myotube formation during the experiment (Figure 37A) we included some wells for MF20 evaluation in the myoblot assay (Figure 37B). Our results confirmed that AGK2 increased utrophin protein levels at all the concentrations studied (Figure 37C) while differentiation was not significantly affected (Figure 37D).

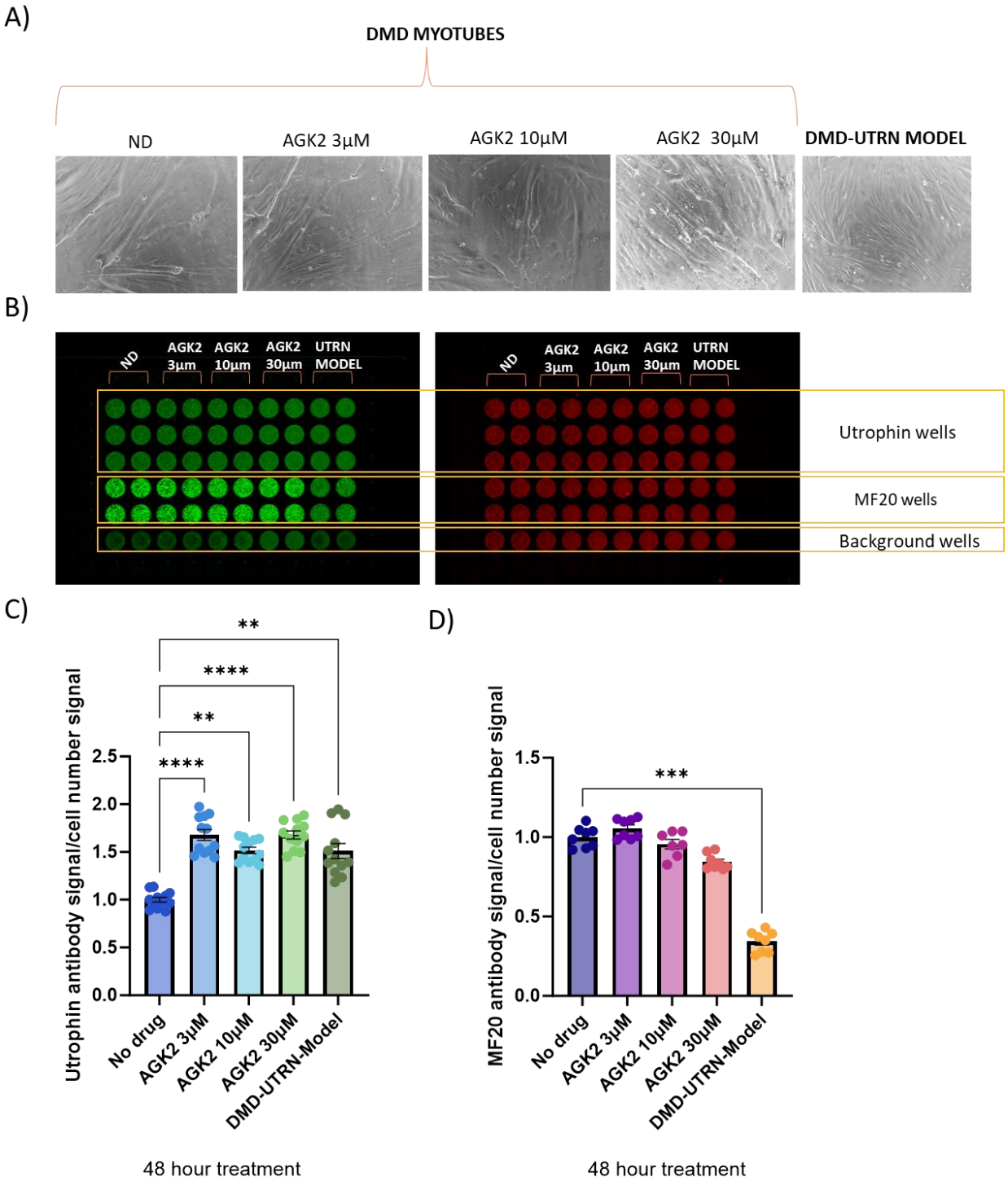

Figure 37. Utrophin and differentiation evaluation by myoblot after AGK2 treatment.

DMD myotubes were treated for 48h with AGK2 at 3µM, 10µM and 30µM dissolved in differentiation medium (DM) with DMSO 0.1%. No drug and DMD-UTRN-Model wells were only treated with DMSO 0.1% in DM. A) Representative bright-field images of DMD and DMD-UTRN Model myotubes after treatments and before being fixed for myoblot assay. B) Representative microplates images showing utrophin and MF20 signals detected at the 800 nm channel and cell tag signal detected at the 700 nm channel. Myoblot assay included between 4 and 6 technical replicates per condition. Data are expressed as the mean fold change ± SEM over no drug (Kruskal-Wallis test ANOVA). N=2 independent experiments. (****p< 0.001, ***p<0.01, **p<0.1. *p<0.5)

Effect of AGK2 in *mdx* model

After confirming AGK2-induced utrophin overexpression in human DMD myotubes, we decided to perform a small *in vivo* assay and study utrophin expression in *mdx* mice treated with this SIRT2 inhibitor. To this end, *mdx* and control males aged 11-12 months, were randomly assigned to either vehicle or treatment groups. 50 mg/kg/day AGK2 dissolved in PEG400+saline treatment was administered intraperitoneally to *mdx* and control mice for 8 days (146). The mice were then sacrificed, and quadriceps sections were analysed by quantitative immunostaining and western blot. During the treatment, the mice did not show any significant changes in body weight (Figure 38). However, one of the mdx mice died on the last day of treatment.

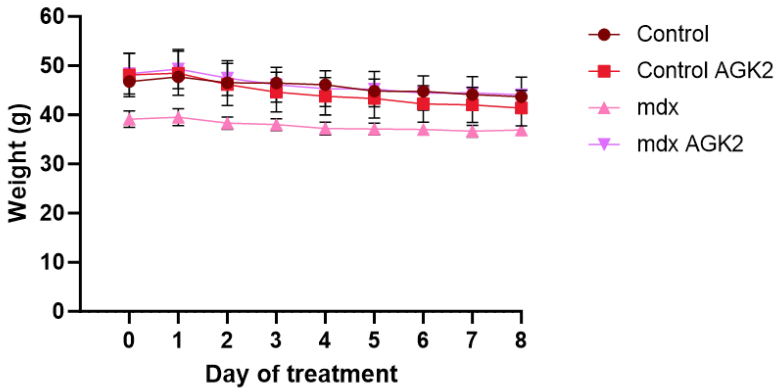

Figure 38. Body weight during AGK2 treatment.

Data are expressed as mean ± SEM of 3 adult mice per condition (N=3 vehicle-treated control mice, N=3 AGK2 (50 mg/kg) treated control, N=3 vehicle-treated *mdx* and N=3 AGK2 (50 mg/kg) treated *mdx* mice). No significant differences in body weight were observed in any group along treatment (two-way ANOVA, Dunnet's multiple comparison test).

Immunostaining confirmed that utrophin was overexpressed in untreated *mdx* mice compared to untreated control mice as described previously. Moreover, AGK2 treatment increased utrophin expression in muscle fibres in both control and *mdx* mice groups (Figure 39).

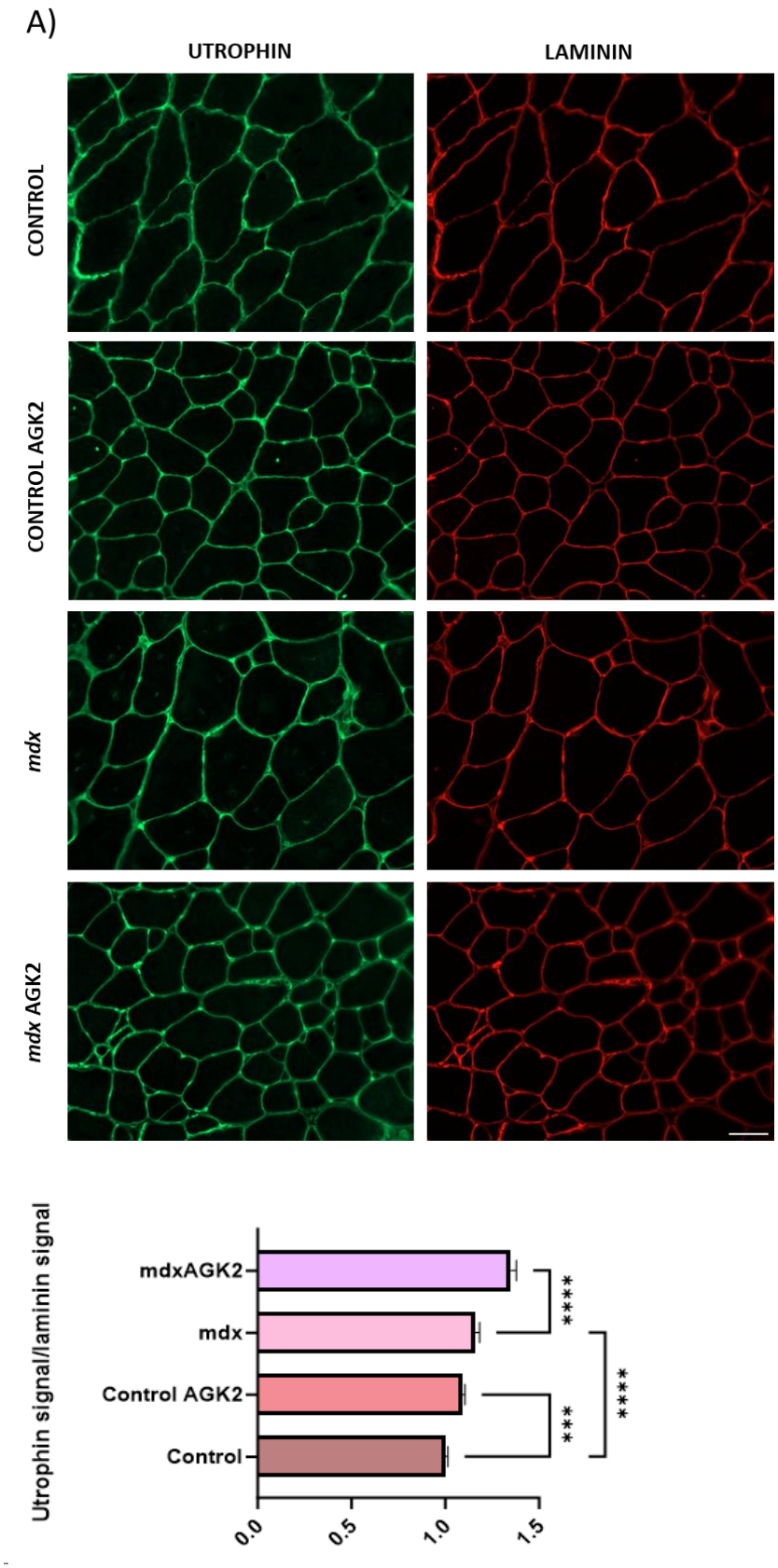

Figure 39. Utrophin expression in adult mice after AGK2 treatment.

A) Representative images of utrophin (in green) and laminin (in red) on quadriceps cryosections. Scale bar 50 µM. B) Quantification of utrophin expression in quadriceps cryosections. Data are expressed as mean

± SEM of 100 ROIs per condition (10 ROIs of 10 FOV per mice being N=3 vehicle-treated control mice, N=3 AGK2 (50 mg/kg) treated control mice, N=3 vehicle-treated *mdx* mice and N=3 AGK2 (50 mg/kg) treated *mdx* mice). Significant differences were observed in both control and *mdx* mice after treatment as well as between non-treated control and non-treated *mdx* mice (****p< 0.001, ***p<0.01 determined by Kruskal Wallis ANOVA test).

Taken together, these data indicate that sirtuin 2 inhibition leads to utrophin overexpression both in DMD cultures and in the *mdx* mouse model, which is an interesting target in the search for new utrophin upregulating drugs for DMD.

DISCUSSION

This project aimed to establish a new cell-based platform for *in vitro* utrophin quantification, including a cell culture model generated by gene editing, to serve as a tool for drug screening in DMD.

Using various experimental approaches, we have demonstrated the suitability of two methods, ddPCR and myoblots, for quantification of utrophin expression at RNA and protein level in cell culture, as well as the use of CRISPR/Cas9 gene editing to generate a cell model that overexpresses utrophin. On the other hand, these methods have allowed us to perform a drug screening with a battery of 60 repurposing compounds and to study new targets for utrophin upregulation like sirtuin 2 inhibition.

Optimised mytoblot and ddPCR methods allow reliable utrophin quantification.

Preclinical research in neuromuscular diseases suffers from a fragmentation of approaches and the quality and robustness of preclinical studies need to be improved. Reliability of preclinical studies is essential to assure clinical translatability, and this includes the reproducibility of the methodology and its validation across different laboratories (150).

During the last years, several luciferase-based assays to screen chemical libraries of thousands of compounds have been developed to identify molecules that could target utrophin at both transcriptional and posttranscriptional level (88, 148, 151). However, after this high-throughput format, traditional semi-quantitative methods, including immunoblotting, immunostaining, and real-time quantitative PCR (RT-qPCR) have been widely used to validate utrophin upregulation in the hit compounds identified and assess the drug efficacy.

Our group has worked for many years in the establishment of novel quantitative methods for accurately quantifying protein, that offer numerous advantages compared to traditional ones and enable harmonisation of protocols between laboratories. In this study, we propose that the combination of myoblot and ddPCR techniques is suitable for semi-high-throughput analysis in drug screening.

In-Cell Western methods have been applied to the identification on siRNAs an small molecule inhibitors from libraries targeting particular signalling pathways (152); the

screening of genotoxic drugs (153); the screening of chemical libraries potentially related with cancer progression (154) and, more recently, it has been used as an efficient technique for clonal selection of cells initially identified using the CRISPR/Cas9 gene editing tools (155).

Previous studies performed in our group validated In-Cell Western (myoblot) for dystrophin quantification in cultured myoblasts and proposed it as an alternative to western blotting as it offers numerous advantages (145). The myoblot technique allows the analysis of protein expression within intact cells, avoiding sample preparation artefacts derived from cell lysis and homogenization that may affect the accuracy of protein quantification. Furthermore, myoblots are less time-consuming as they eliminate the need for protein extraction, gel electrophoresis and membrane transference. In addition, they require smaller sample volumes, allowing the analysis of multiple samples simultaneously, making it useful for drug screening.

In this study, we have optimised some myoblot conditions like plate selection, cell seeding range and which anti-utrophin antibody to use, all of them crucial for reliable utrophin quantification. First, like other groups before us (156), we observed that the use of transparent plates revealed a significant variability across the plate when read at the 700 nm channel, used for cell number normalisation. We concluded that the use of specific black plates improved intensity and uniformity in the cell tag signal across the plate, as well as reduced undesirable auto-fluorescence and edge effects. This improvement in signal intensity, contributed to the selection of a new optimal seeding range after cell linearity assays, which was reduced from previous experiments and established at 6000 cells per well for all the different cell types used in this study. Furthermore, we selected the primary antibody dilution according to the linear range of detection and after testing a range from 1:200 to 1:800 Mancho 7 antibody dilutions, a dilution of 1:400 yielded the best signal-to-noise ratio.

Due to its remarkable analytical sensitivity and specificity, ddPCR has become an increasingly popular tool for the accurate measurement of biomarkers, the quantification of therapeutic efficiencies, prenatal diagnosis, and newborn screening.

Recently, a growing number of studies have proved ddPCR to be a useful method for molecular analysis in many areas, including DMD (157).

The emergence of nucleic acid therapies and molecular biology technologies applied to DMD, including antisense oligonucleotides and CRISPR/Cas9 gene editing, have increased the necessity of precise quantification of nucleic acids. While both RT-qPCR and ddPCR are valuable tools for nucleic acid quantification, ddPCR offers advantages in terms of precision and sensitivity for low-abundance targets and robustness against PCR inhibitors, making it especially suitable for applications requiring accurate quantification of rare targets or samples with limited DNA template (158).

Other reports of application of ddPCR technology in DMD take advantage of its high precision for absolute quantification and focus on drug efficiency validation (159), gene editing analysis and biomarker discovery (160, 161). Our laboratory previously collaborated in a multicentre comparison of quantification methods of ASOs-induced exon skipping in DMD cultures. In this study, ddPCR showed to be the most precise method for assessing exon skipping levels (162). Other groups have used ddPCR to evaluate the turnover dynamics of dystrophin and other dystrophin-glycoprotein complex proteins in *mdx* mice after exon skipping therapy (163).

As utrophin could be considered a low abundance target gene, in this work we established the experimental set up of ddPCR method for absolute utrophin quantification in cell cultures. The optimisation steps involved selecting the appropriate cDNA template amount and the annealing temperature. We compared utrophin expression between control and DMD myotubes through a range of cDNA template concentrations. As expected, utrophin expression was significantly higher in DMD myotubes compared to control myotubes however, a lower template concentration of 6 ng/µl or less was not enough to establish a statistically significant difference between patients and controls and, for that reason, a higher concentration of 10 ng/µl of cDNA template was finally chosen.

In addition to standard techniques such as immunohistochemistry and western blotting, we have used myoblots and ddPCR to validate two cell culture models generated by CRISPR/Cas technology that we developed to be used in the preclinical evaluation of

new DMD therapies (63). One cell culture model replicates a patient's exon 52 deletion (DMDΔ52-Model) and the other one, which we describe in detail in this thesis, overexpresses utrophin (DMD-UTRN-Model). The validation of these cell culture models included the study of the expression of dystrophin, utrophin, myogenic factors (Myf5 and MyH3), and other DGC/UGC proteins (α-sarcoglycan and β-dystroglycan) both in DMDΔ52-Model cell cultures compared to control myotubes, and in DMD-UTRN-Model cultures compared to DMD myotubes concluding that myoblot and ddPCR methods are valuable tools for the neuromuscular research community.

DMD-UTRN-Model generated by CRISPR-Cas9 gene editing overexpresses utrophin and serves as a positive control for drug screening in cell culture.

In vitro disease modelling presents a valuable and accessible method for investigating the pathophysiology of DMD and assessing potential therapeutic interventions. Research focusing on DMD has traditionally employed animal models, patient-derived muscle biopsies, and *in vitro* myogenic cell cultures. Over time, *in vitro* culture techniques have advanced to better reflect the characteristics of the original tissue and increase their reproducibility and the length of time in which they may be used for. To this end, DMD myoblasts have been immortalised to broaden their applicability (164), seeded in extracellular three-dimensional matrices enabling highly mature and enduring cultures (165), and gene edited to better replicate disease conditions but also to correct different gene mutations (59, 63). In this context, CRISPR/cas9, has demonstrated to be a powerful tool for generating cell and animal models but also modulating expression of genes that are known to play a critical role in disease pathogenesis (65).

Since one of the possible approaches for DMD therapy is based on increasing utrophin levels, we proposed employing CRISPR/Cas9 technology to achieve permanent up-regulation of endogenous utrophin. In the work presented here, our group has generated a cell culture model, DMD-UTRN-Model, using a CRISPR/Cas9-mediated strategy to increase utrophin expression by disrupting inhibitory microRNA binding sites. Subsequently, this UTRN-DMD-Model culture was evaluated using a battery of characterization tests including evaluating utrophin expression by both traditional and

novel methods, examining myotube differentiation and studying potential changes in other UGC proteins.

The first step for performing targeted genome editing was the induction of two DNA double-stranded breaks at the 3'UTR region of the human *UTRN* gene, flanking an inhibitory microRNAs binding site region. It has been previously described that several microRNAs such as miR-133b, miR-150, miR-196b, miR-296-5p and Let-7c, are able to post-transcriptionally repress utrophin expression binding to a 500bp sequence within the utrophin 3'UTR (97).

For this purpose, we engineered ten CRISPR/Cas9+sgRNA expression plasmids and tested their ability of cleaving the human UTRN in HEK 293 cultures. We analysed the targeted region by Sanger sequencing and selected the guide combination sgRNA22+sgRNA26 to be transfected in immortalised DMD human myoblasts. After transfection, myoblasts were collected for fluorescence activated cell sorting (FACS) and only 1.19% of cells sorted resulted GFP positive. These cells were individually seeded in microplates for clonal selection and 9 grew enough to be expanded and analysed. PCR screening of sorted cells identified 2 positive clones out of these 9. The desired deletion was confirmed in both clones, and one clone was selected for further analysis and called DMD-UTRN-Model. Finally, to identify potential mutations induced at off-target sites, we performed an *in silico* analysis using the CRISPR design tools, which predict and score off-targets for the CRISPR/Cas9 system. PCR amplification of the predicted off-target sites followed by Sanger sequencing has shown no indel mutations on the potential off-target sites identified.

Utrophin was significantly increased in DMD-UTRN-Model cultures compared to DMD cultures, however, the amount of overexpression varies significantly when evaluated by western blot (close to 2 times) or our preferred method, myoblots (close to 1.5 times). We like to consider that myoblot evaluation reflects more closely the actual protein expression, as it is not subjected to many of the inherent problems of western blotting when evaluating very large proteins and we are able to include many more replicates that contribute to the robustness of our quantification (145).

Some myogenic regulatory factors in muscle cultures were affected after gene editing, for instance, MyH3 expression was significantly decreased in the DMD-UTRN-Model. These findings could be related with changes in the secretory phenotype after single cell sorting in edited models, as it has been shown that myoblasts microenvironment *in vitro* can affect cell proliferation and differentiation. Concretely, some studies reported autocrine factors like transforming growth factor β (TGF-β) that can inhibit myogenic differentiation (166, 167). Other groups have reported before that primary myoblasts lose their differentiation potential following single cell cloning or do not survive the stress of sorting, being no table to produce clonal edited populations (168).

Although other studies have reported a restoration of other DGC/UGC proteins after utrophin upregulation, pointing to a functional restoration (64, 169), we only observed after myoblot analysis a slight increase in α-sarcoglycan and β-dystroglycan expression between our DMD-UTRN-Model and unedited DMD myotubes that was not significant. This could be attributed to the reduced differentiation in the DMD-UTRN-Model compared to DMD cultures and the fact that DGC proteins increase their expression during the myogenic differentiation process (170).

On the other hand, Cas9 transfection into cultures have been traditionally carried out by delivery of DNA plasmids, however, efficient delivery of the components into myoblasts remains a major challenge and lipofection efficiency is regularly less than 10%. In this context, many studies have attempted to improve myoblast transfection efficiency improving transfection protocols and cell selection processes. Interestingly, some have showed how different combinations of cell confluency and extracellular matrix membrane (Matrigel) impacted transfection and editing efficiency in primary human myoblasts (168). On the other hand, in 2014 *Kim et al.* described a novel method for Cas9 delivery into cells using purified Cas9/gRNA ribonucleoprotein (RNP) complexes that has become popular in many contexts due to its higher editing efficiency and reduced off-target effects compared to plasmid-based transfection (171).

Although we acknowledge the efficiency limitations of the gene editing protocol followed, especially due to transfection difficulties in myoblasts and single cell selection, the outcome is a useful example for researchers looking for cell culture models.

The DMD-UTRN-Model is both a proof of principle of a possible therapeutic option to overexpress utrophin as a substitute for dystrophin, and a valuable research tool, serving as a reliable positive control in the screening of utrophin overexpression drugs.

Other research groups have followed similar approaches to ours: Sengupta *et al.* have used CRISPR/Cas9-mediated genome editing to overexpresses utrophin in DMD patient-derived human induced pluripotent stem cells (DMD-hiPSCs) also targeting an inhibitory miRNA target region within the UTRN 3' UTR. In their hands, the UTRN edition resulted in 2-fold higher levels of utrophin protein and dystrophin glycoprotein complex (DGC) restoration (64). Guiraud *et al,* have used a CRISPR/Cas9 gRNA ribonucleoprotein to disrupt several miRNA binding sites in three-dimensional human DMD cultures. Editing resulted in significant utrophin upregulation and functional improvements of calcium dysregulation and muscle contraction. Interestingly, Let-7c binding site was identified as crucial for UTRN repression. Finally, Let-7c binding site disruption in *mdx* mice by systemic rAAVs mediated delivery of Cas9 and gRNA resulted in utrophin upregulation and amelioration of the muscle histopathological phenotype (172). Furthermore, Wojtal *et al,* have successfully engineered a CRISPR/Cas9 system targeting both utrophin A or B promoters with single sgRNAs and a combination of three sgRNAs aiming to upregulate the amount of utrophin 1.7- to 6.9-fold over the basal amount and restored β-dystroglycan expression in muscle cells from DMD patients (169).

<u>Utrophin cell assay allows semi-high-throughput testing of repurposing drugs.</u>

Drug repurposing is a strategy for identifying new uses for approved or investigational drugs that are outside the scope of the original medical indication. This strategy significantly saves time and costs over traditional drug development and is particularly attractive for rare diseases. First, because often there is a lack of information on pathophysiology and biological pathways of the disease are poorly characterised and drug repurposing offers a method to hypothesise new therapeutic targets. Also, there are specific regulatory and commercial measures that are meant to encourage research into rare diseases (173) but, above all, drug repurposing considerably reduces the development timeline, as compounds have already demonstrated to be safe in humans

and Phase 1 trials are not required. The original, and so far, the most successful example of drug repurposing for DMD is prednisone, the first corticosteroid used to treat DMD in the early 1970s. Since then, several repurposed drugs are under investigation and some of them have even reached clinical trials (174).

The process of drug discovery for utrophin upregulation, has been often achieved from high-throughput screening of already approved drugs or new small-compounds. In this sense, several laboratories have developed cell-based assays for compound screening aiming to find up-regulators of utrophin.

Ezutromid (SMT C1100), was the first drug specifically designed to target the utrophin-A promoter which progressed into clinical development. It was developed using a high throughput cell-based phenotypic screening assay. Immortalised *mdx* myoblasts were transfected with 8.4 kb of the human utrophin A promoter (the region contained all the motifs known to control utrophin expression) upstream of firefly luciferase (H2K-*mdx* utrnA-luc) (85, 175). The assay consists of measuring the induced bioluminescent readout which depends on the quantity of luciferase, and hence activation of the utrophin promoter. Using this assay, a collection of 7000 drug-like small molecules was screened and a series of novel 2-arylbenzoxazoles that upregulate the production of utrophin were identified, including ezutromid/SMT C1100 and SMT022357, a second-generation compound structurally related to SMT C1100 with improved physicochemical properties able to upregulate utrophin in all muscle groups resulting in a significant improvement in the muscle pathophysiology of the *mdx* mouse (31).

Later, other groups have focused on designing cell-based high-throughput assays for transcriptional or post-transcriptional utrophin activation:

Moorwood *et al* developed a cell-based assay for utrophin A promoter activation, and used it to screen the Prestwick Chemical Library, which comprises more than 1000 approved drugs and natural compounds. Initial screening generated 20 hits and further testing in independent validation experiments using the C2C12 muscle cell line, showed that one, nabumetone, was able to upregulate endogenous utrophin A mRNA and protein, representing a potential therapeutic candidate for DMD (88).

Post-transcriptional repression mechanisms targeting the 5' and 3' untranslated regions (UTRs) of utrophin mRNA significantly limit the magnitude of utrophin upregulation achievable by promoter activation, for that reason, Moorwood *et al* developed other cell-based luciferase reporter assay, this time for the identification of small molecule drugs that upregulate utrophin via its 5'- and 3'-UTRs. They used the cytomegalovirus promoter to produce a reporter mRNA that consists of the coding sequence of luciferase flanked by the utrophin UTRs. With this approach, any tested substance that alters mRNA stability, rate of translation, or targeted by miRNAs would result in a change in luciferase activity. They validated the assay using a 2-O-methyl phosphorothioate (2OMePS) oligomer that upregulates utrophin by blocking certain miRNAs from binding and finally concluded that was a valuable tool that could be used for high-throughput screening of chemical libraries for utrophin-activating compounds (148). Loro *et al* developed a utrophin 5'3'UTR reporter assay and performed a high-throughput screen for small molecules capable of relieving utrophin post-transcriptional repression. They identified 27 hits and the top one, Trichostatin A (TSA), demonstrated utrophin upregulation and functional improvement in the *mdx* mouse model of DMD (103).

More recently, Gleneadie *et al* developed a preclinical mouse model in which expression of endogenous *Dmd* and *Utrn* can be simultaneously visualised *in vivo*. Afterwards they performed a bioluminescence screen for compounds that enhance Utrn expression in adult primary and immortalised myoblasts isolated from the adult mice reporters. Amongst 40 candidates tested, 7 compounds produced statistically significant increases of *Utrn* expression confirmed independently by quantitative analyses of Utrn-mRNA transcripts: EZH2 inhibitors (GSK343, GSK503), bromodomain inhibitors (GSK602, GSK959) or ERK pathway inhibitors (LY3009, Ravox, LY32) (176).

In the present work, we have established the viability of myoblot and ddPCR assays combined with DMD-UTRN Model to identify up-regulators of utrophin expression in immortalised DMD myotubes. A battery of 60 small molecules together with ezutromid and halofuginone was screened using the myoblot assay, and 44 showed an increase in utrophin expression in DMD myotubes compared to non-treated cells using a generic concentration of 5 µM for 24 hours. Afterwards, 6 of those compounds (C03, C13, C32, C42, ezutromid and halofuginone) were further analysed and myoblasts were treated

with 0.01, 0.1, 1 and 10 µM for 24 or 48 hours with the selected drugs. Although ddPCR analyses showed utrophin upregulation in DMD myotubes after treatment with halofuginone and ezutromid as well as compounds C03 and C13, all compounds except halofuginone seemed to be inactive at any of the new concentrations studied when re-analysed by larger myoblot assays.

Transcript to protein quantitative relationship may be strongly influenced by several biological processes. When comparing protein and mRNA levels during dynamic adaptation processes, such as cellular differentiation, post-transcriptional processes may lead to stronger deviations from an ideal correlation. On the other hand, the delay between transcription and translation needs to be considered. Protein synthesis takes time, and transcript changes will therefore affect protein levels only with a certain temporal delay (177). Considering this, we conclude that transcript levels by themselves are not sufficient to predict protein levels but also that further experiments considering the possible utrophin translation delay would be required.

Sirtuin 2 inhibition increases utrophin expression in DMD cultures.

Histone acetylation is one of the epigenetic mechanisms controlling gene expression. In humans, there are currently 18 known histone deacetylases (HDACs) grouped into four classes. Class III HDACs are known as sirtuins. In humans, the sirtuin family consists of seven members (Sirt1 – Sirt7), whose activity depends on NAD+. Sirtuins modulate the activity of different nuclear and cytoplasmatic proteins, being involved in several cellular processes like metabolism regulation, proliferation, differentiation, and responses to stress signals (178). Deregulation of HDACs expression or activity is often associated with several pathologies. For example, expression of some HDACs is higher in dystrophic skeletal muscles, suggesting HDAC inhibitors (HDACi) as potential therapies (178).

Sirtuins have been shown to be deregulated in several diseases including DMD, arousing considerable interest as potential targets in the last years. Some of them, like sirtuin 1 and sirtuin 6, have been linked to utrophin expression in DMD. Sirtuin 1 is found in the cell nucleus and expressed in different tissues including skeletal muscle. In skeletal muscle, sirtuin 1 protects muscle from atrophy while promoting growth and is a sensor

of energy metabolism, being triggered by AMPK and deacetylates, thus activating PGC-1α. Different studies have shown some exogenous agents can enhance the expression/activity of sirtuin 1, increase utrophin expression, and improve DMD pathology (139). More recently, Georgieva *et al* found that sirtuin 6 was significantly upregulated whereas sirtuin 1 was downregulated in both *mdx* cell cultures and muscle fibres. Interestingly, they found that sirtuin 6 suppresses Utrn expression in dystrophic muscles via deacetylation of H3K56ac at the downstream utrophin enhancer. Inactivation of sirtuin 6 increases Utrn expression and eliminates several pathological hallmarks characteristic for *mdx* mice (143).

Interestingly, an HDACi identified after a high-throughput screening assay of thousand compounds, Trichostatin A (TSA), when administered to *mdx* mice increased utrophin expression and improved the structure and function of skeletal muscles (103).

Furthermore, Farr and colleagues, identified a novel combination of HDACis, oxamflatin (class I and II HDACi and chemically like TSA) and salermide (SIRT1 and SIRT2 inhibitor), that together improve skeletal muscle structural defects in *dmd* mutant zebrafish (179).

Despite all these preclinical results, the only HDACi drug that has reached clinical trials is givinostat. The phase 3 of EPIDYS trial (NCT02851797) proved/demonstrated that givinostat reduced muscle fat infiltration and ameliorated muscle deterioration in patients with DMD (180) and the FDA granted approval to DUVYZAT™ (givinostat) this year.

In this thesis, we first studied the relationship between a less studied sirtuin, sirtuin 2, and utrophin expression in human control and DMD myotubes. As expected, utrophin was increased in DMD myotubes but interestingly, myoblot quantification of sirtuin 2 protein showed that it was significantly upregulated in DMD myotubes compared to controls. We then confirmed this observation by immunochemistry.

Having confirmed that it was increased in patients' cultures, we hypothesised that inhibiting sirtuin 2 expressions could increase utrophin levels in DMD cell cultures and, for that purpose, we selected the compound AGK2, a sirtuin 2 inhibitor. DMD myotubes were treated with increasing concentrations of AGK2 for 24 hours and no significance

difference in utrophin expression was found. However, after increasing the time of exposure to the drug from 24 to 48 hours and the concentrations of AGK2 used (3µM, 10µM and 30µM), we found that AGK2 significantly increased utrophin expression at all the concentrations tested, even overcoming the DMD-UTRN-Model utrophin expression used as positive control. Then, we decided to perform a small *in vivo* assay and study utrophin expression in *mdx* mice treated with AGK2.

During the treatment no significant changes in body weight were experienced by the treated mice. The immunostaining assay verified that AGK2 treatment increased utrophin expression in muscle fibres in both groups, wild type and *mdx* mice. To our knowledge, the relationship between sirtuin 2 and utrophin in human muscle cultures has never been reported before. In this study, we reported that sirtuin 2 inhibition increases utrophin expression in human DMD cultures as well as in *mdx* muscle samples. Despite these data, further experiments are required to elucidate whether sirtuin2 are directly implicated in the pathophysiology of DMD and, if so, a compound with good ADME properties might be selected as a putative candidate, once AGK2 has provided us with a good proof of concept of this approach.

CONCLUSIONS

1. The combination of droplet digital PCR and in-cell western assays/myoblots, is suitable for semi-high-throughput analysis and we propose it as a **platform for utrophin quantification** in drug screening using DMD cultures.

2. **The DMD-UTRN-Model** is a cell culture model generated by CRISPR/Cas9-mediated genome editing in DMD immortalised patient-derived cultures that overexpresses utrophin. The editing target region was an inhibitory miRNA binding site located within the UTRN gene 3'UTR. Cleavage of this region was confirmed, and no off-target effects were found after the edition.

   The DMD-UTRN-Model overexpresses utrophin compared to unedited DMD cultures, however the expression of some myogenic factors, like MyH3, are significantly decreased in this model. These changes could be attributed to the cell editing process and the single cell sorting. Although α-sarcoglycan and β-dystroglycan expression is slightly increased in the DMD-UTRN-Model cultures, which could inform on DGC/UGC restoration, no significant differences were found compared to DMD myotubes, likely due to the lower differentiation rate of this cultures.

   We conclude that DMD-UTRN-Model serves as a reliable positive control in the screening of utrophin overexpression drugs and as a proof of principle of a possible therapeutic option to upregulate utrophin.

3. After **screening a battery of potential utrophin upregulating compounds**, ddPCR analyses showed utrophin increase in DMD myotubes treated with two compounds from our panel, as well as with the positive controls used (ezutromid and halofuginone). However, no compounds except halofuginone showed an increase in utrophin protein expression when reanalysed by myoblot assays, suggesting the possibility of an utrophin translation delay that needs to be considered in future experiments.

4. The histone deacetylase **sirtuin 2,** is significantly upregulated in DMD myotubes compared to controls when analysed both by myoblot and ddPCR assays, being identified as a potential target to explore in DMD. Sirtuin 2 inhibition by treatment with AGK2 significantly increases utrophin expression in DMD cultures exceeding the utrophin expression in the DMD-UTRN-Model cultures. AGK2 treatment in mice showed increased utrophin expression in muscle fibres in both groups, control and *mdx* mice by immunostaining assay. These results provide a proof of concept describing sirtuin 2 inhibition as a potential target for utrophin upregulation.

In the present study, we describe a cell-based platform applicable for semi-high-throughput drug screening of potential utrophin modulators. We have also used an *in vitro* innovative gene editing strategy to upregulate the expression of endogenous utrophin in human DMD cultures generating new cell model. Finally, we have used both, the optimised platform, and the cell culture model, to test a battery of small molecules but also to find new targets for utrophin upregulation. Although further studies are needed, we propose sirtuin 2 as a potential target in DMD and sirtuin 2 inhibition as a novel approach for utrophin upregulation.

REFERENCES

1. Hoffman EP, Brown RH, Jr., Kunkel LM. Dystrophin: the protein product of the Duchenne muscular dystrophy locus. Cell. 1987;51(6):919-28.
2. Lee SH, Lee JH, Lee KA, Choi YC. Clinical and Genetic Characterization of Female Dystrophinopathy. J Clin Neurol. 2015;11(3):248-51.
3. Crisafulli S, Sultana J, Fontana A, Salvo F, Messina S, Trifirò G. Global epidemiology of Duchenne muscular dystrophy: an updated systematic review and meta-analysis. Orphanet J Rare Dis. 2020;15(1):141.
4. Doorenweerd N, Mahfouz A, van Putten M, Kaliyaperumal R, PAC TH, Hendriksen JGM, et al. Timing and localization of human dystrophin isoform expression provide insights into the cognitive phenotype of Duchenne muscular dystrophy. Sci Rep. 2017;7(1):12575.
5. Ervasti JM. Dystrophin, its interactions with other proteins, and implications for muscular dystrophy. Biochim Biophys Acta. 2007;1772(2):108-17.
6. Ohlendieck K, Swandulla D. Complexity of skeletal muscle degeneration: multi-systems pathophysiology and organ crosstalk in dystrophinopathy. Pflugers Arch. 2021;473(12):1813-39.
7. Koenig M, Beggs AH, Moyer M, Scherpf S, Heindrich K, Bettecken T, et al. The molecular basis for Duchenne versus Becker muscular dystrophy: correlation of severity with type of deletion. Am J Hum Genet. 1989;45(4):498-506.
8. Love DR, Hill DF, Dickson G, Spurr NK, Byth BC, Marsden RF, et al. An autosomal transcript in skeletal muscle with homology to dystrophin. Nature. 1989;339(6219):55-8.
9. Weir AP, Burton EA, Harrod G, Davies KE. A- and B-utrophin have different expression patterns and are differentially up-regulated in mdx muscle. J Biol Chem. 2002;277(47):45285-90.
10. Burton EA, Tinsley JM, Holzfeind PJ, Rodrigues NR, Davies KE. A second promoter provides an alternative target for therapeutic up-regulation of utrophin in Duchenne muscular dystrophy. Proc Natl Acad Sci U S A. 1999;96(24):14025-30.
11. Malik D, Basu U. Repression-free utrophin-A 5'UTR variants. Mol Biol Res Commun. 2019;8(3):129-33.
12. Wilson J, Putt W, Jimenez C, Edwards YH. Up71 and up140, two novel transcripts of utrophin that are homologues of short forms of dystrophin. Hum Mol Genet. 1999;8(7):1271-8.
13. Soblechero-Martín P, López-Martínez A, de la Puente-Ovejero L, Vallejo-Illarramendi A, Arechavala-Gomeza V. Utrophin modulator drugs as potential therapies for Duchenne and Becker muscular dystrophies. Neuropathol Appl Neurobiol. 2021.
14. Rajaganapathy S, McCourt JL, Ghosal S, Lindsay A, McCourt PM, Lowe DA, et al. Distinct mechanical properties in homologous spectrin-like repeats of utrophin. Sci Rep. 2019;9(1):5210.
15. Li D, Bareja A, Judge L, Yue Y, Lai Y, Fairclough R, et al. Sarcolemmal nNOS anchoring reveals a qualitative difference between dystrophin and utrophin. J Cell Sci. 2010;123(Pt 12):2008-13.
16. Love DR, Morris GE, Ellis JM, Fairbrother U, Marsden RF, Bloomfield JF, et al. Tissue distribution of the dystrophin-related gene product and expression in the mdx and dy mouse. Proc Natl Acad Sci U S A. 1991;88(8):3243-7.
17. Clerk A, Morris GE, Dubowitz V, Davies KE, Sewry CA. Dystrophin-related protein, utrophin, in normal and dystrophic human fetal skeletal muscle. Histochem J. 1993;25(8):554-61.
18. Lin S, Burgunder JM. Utrophin may be a precursor of dystrophin during skeletal muscle development. Brain Res Dev Brain Res. 2000;119(2):289-95.
19. Galvagni F, Cantini M, Oliviero S. The utrophin gene is transcriptionally up-regulated in regenerating muscle. J Biol Chem. 2002;277(21):19106-13.
20. Arechavala-Gomeza V, Kinali M, Feng L, Brown SC, Sewry C, Morgan JE, et al. Immunohistological intensity measurements as a tool to assess sarcolemma-associated protein expression. Neuropathol Appl Neurobiol. 2010;36(4):265-74.

21. Anthony K, Arechavala-Gomeza V, Ricotti V, Torelli S, Feng L, Janghra N, et al. Biochemical characterization of patients with in-frame or out-of-frame DMD deletions pertinent to exon 44 or 45 skipping. JAMA Neurol. 2014;71(1):32-40.
22. Ruiz-Del-Yerro E, Garcia-Jimenez I, Mamchaoui K, Arechavala-Gomeza V. Myoblots: dystrophin quantification by in-cell western assay for a streamlined development of Duchenne muscular dystrophy (DMD) treatments. Neuropathol Appl Neurobiol. 2017.
23. Kleopa KA, Drousiotou A, Mavrikiou E, Ormiston A, Kyriakides T. Naturally occurring utrophin correlates with disease severity in Duchenne muscular dystrophy. Hum Mol Genet. 2006;15(10):1623-8.
24. Vainzof M, Passos-Bueno MR, Man N, Zatz M. Absence of correlation between utrophin localization and quantity and the clinical severity in Duchenne/Becker dystrophies. Am J Med Genet. 1995;58(4):305-9.
25. Bulfield G, Siller WG, Wight PA, Moore KJ. X chromosome-linked muscular dystrophy (mdx) in the mouse. Proc Natl Acad Sci U S A. 1984;81(4):1189-92.
26. Tinsley JM, Potter AC, Phelps SR, Fisher R, Trickett JI, Davies KE. Amelioration of the dystrophic phenotype of mdx mice using a truncated utrophin transgene. Nature. 1996;384(6607):349-53.
27. Tinsley J, Deconinck N, Fisher R, Kahn D, Phelps S, Gillis JM, et al. Expression of full-length utrophin prevents muscular dystrophy in mdx mice. Nat Med. 1998;4(12):1441-4.
28. Weir AP, Morgan JE, Davies KE. A-utrophin up-regulation in mdx skeletal muscle is independent of regeneration. Neuromuscul Disord. 2004;14(1):19-23.
29. Deconinck AE, Rafael JA, Skinner JA, Brown SC, Potter AC, Metzinger L, et al. Utrophin-dystrophin-deficient mice as a model for Duchenne muscular dystrophy. Cell. 1997;90(4):717-27.
30. Guiraud S, Edwards B, Babbs A, Squire SE, Berg A, Moir L, et al. The potential of utrophin and dystrophin combination therapies for Duchenne muscular dystrophy. Hum Mol Genet. 2019;28(13):2189-200.
31. Guiraud S, Squire SE, Edwards B, Chen H, Burns DT, Shah N, et al. Second-generation compound for the modulation of utrophin in the therapy of DMD. Hum Mol Genet. 2015;24(15):4212-24.
32. Gilbert R, Nalbantoglu J, Petrof BJ, Ebihara S, Guibinga GH, Tinsley JM, et al. Adenovirus-mediated utrophin gene transfer mitigates the dystrophic phenotype of mdx mouse muscles. Hum Gene Ther. 1999;10(8):1299-310.
33. Kennedy TL, Moir L, Hemming S, Edwards B, Squire S, Davies K, et al. Utrophin influences mitochondrial pathology and oxidative stress in dystrophic muscle. Skelet Muscle. 2017;7(1):22.
34. Chen HC, Chin YF, Lundy DJ, Liang CT, Chi YH, Kuo P, et al. Utrophin Compensates dystrophin Loss during Mouse Spermatogenesis. Sci Rep. 2017;7(1):7372.
35. McDonald CM, Henricson EK, Abresch RT, Duong T, Joyce NC, Hu F, et al. Long-term effects of glucocorticoids on function, quality of life, and survival in patients with Duchenne muscular dystrophy: a prospective cohort study. Lancet. 2018;391(10119):451-61.
36. Marden JR, Freimark J, Yao Z, Signorovitch J, Tian C, Wong BL. Real-world outcomes of long-term prednisone and deflazacort use in patients with Duchenne muscular dystrophy: experience at a single, large care center. J Comp Eff Res. 2020;9(3):177-89.
37. Keam SJ. Vamorolone: First Approval. Drugs. 2024;84(1):111-7.
38. Birnkrant DJ, Bushby K, Bann CM, Apkon SD, Blackwell A, Brumbaugh D, et al. Diagnosis and management of Duchenne muscular dystrophy, part 1: diagnosis, and neuromuscular, rehabilitation, endocrine, and gastrointestinal and nutritional management. Lancet Neurol. 2018;17(3):251-67.
39. Birnkrant DJ, Bushby K, Bann CM, Alman BA, Apkon SD, Blackwell A, et al. Diagnosis and management of Duchenne muscular dystrophy, part 2: respiratory, cardiac, bone health, and orthopaedic management. Lancet Neurol. 2018;17(4):347-61.

40. Birnkrant DJ, Bushby K, Bann CM, Apkon SD, Blackwell A, Colvin MK, et al. Diagnosis and management of Duchenne muscular dystrophy, part 3: primary care, emergency management, psychosocial care, and transitions of care across the lifespan. Lancet Neurol. 2018;17(5):445-55.
41. Bladen CL, Salgado D, Monges S, Foncuberta ME, Kekou K, Kosma K, et al. The TREAT-NMD DMD Global Database: analysis of more than 7,000 Duchenne muscular dystrophy mutations. Hum Mutat. 2015;36(4):395-402.
42. Malik V, Rodino-Klapac LR, Viollet L, Wall C, King W, Al-Dahhak R, et al. Gentamicin-induced readthrough of stop codons in Duchenne muscular dystrophy. Ann Neurol. 2010;67(6):771-80.
43. Welch EM, Barton ER, Zhuo J, Tomizawa Y, Friesen WJ, Trifillis P, et al. PTC124 targets genetic disorders caused by nonsense mutations. Nature. 2007;447(7140):87-91.
44. McDonald CM, Campbell C, Torricelli RE, Finkel RS, Flanigan KM, Goemans N, et al. Ataluren in patients with nonsense mutation Duchenne muscular dystrophy (ACT DMD): a multicentre, randomised, double-blind, placebo-controlled, phase 3 trial. Lancet. 2017;390(10101):1489-98.
45. Charleston JS, Schnell FJ, Dworzak J, Donoghue C, Lewis S, Chen L, et al. Eteplirsen treatment for Duchenne muscular dystrophy: Exon skipping and dystrophin production. Neurology. 2018;90(24):e2146-e54.
46. Frank DE, Schnell FJ, Akana C, El-Husayni SH, Desjardins CA, Morgan J, et al. Increased dystrophin production with golodirsen in patients with Duchenne muscular dystrophy. Neurology. 2020.
47. Dhillon S. Viltolarsen: First Approval. Drugs. 2020;80(10):1027-31.
48. Shirley M. Casimersen: First Approval. Drugs. 2021;81(7):875-9.
49. Wilton-Clark H, Yokota T. Recent Trends in Antisense Therapies for Duchenne Muscular Dystrophy. Pharmaceutics. 2023;15(3).
50. Aartsma-Rus A, Arechavala-Gomeza V. Why dystrophin quantification is key in the eteplirsen saga. Nat Rev Neurol. 14. England2018. p. 454-6.
51. Godfrey C, Desviat LR, Smedsrod B, Pietri-Rouxel F, Denti MA, Disterer P, et al. Delivery is key: lessons learnt from developing splice-switching antisense therapies. EMBO Mol Med. 2017;9(5):545-57.
52. Gregorevic P, Blankinship MJ, Allen JM, Crawford RW, Meuse L, Miller DG, et al. Systemic delivery of genes to striated muscles using adeno-associated viral vectors. Nat Med. 2004;10(8):828-34.
53. Zaidman CM, Proud CM, McDonald CM, Lehman KJ, Goedeker NL, Mason S, et al. Delandistrogene Moxeparvovec Gene Therapy in Ambulatory Patients (Aged ≥4 to <8 Years) with Duchenne Muscular Dystrophy: 1-Year Interim Results from Study SRP-9001-103 (ENDEAVOR). Ann Neurol. 2023;94(5):955-68.
54. Mojica FJ, Díez-Villaseñor C, García-Martínez J, Soria E. Intervening sequences of regularly spaced prokaryotic repeats derive from foreign genetic elements. J Mol Evol. 2005;60(2):174-82.
55. Jinek M, Chylinski K, Fonfara I, Hauer M, Doudna JA, Charpentier E. A programmable dual-RNA-guided DNA endonuclease in adaptive bacterial immunity. Science. 2012;337(6096):816-21.
56. Cong L, Ran FA, Cox D, Lin S, Barretto R, Habib N, et al. Multiplex genome engineering using CRISPR/Cas systems. Science. 2013;339(6121):819-23.
57. Hsu PD, Scott DA, Weinstein JA, Ran FA, Konermann S, Agarwala V, et al. DNA targeting specificity of RNA-guided Cas9 nucleases. Nat Biotechnol. 2013;31(9):827-32.
58. Miyaoka Y, Mayerl SJ, Chan AH, Conklin BR. Detection and Quantification of HDR and NHEJ Induced by Genome Editing at Endogenous Gene Loci Using Droplet Digital PCR. Methods Mol Biol. 2018;1768:349-62.

59. Alizadeh F, Abraghan YJ, Farrokhi S, Yousefi Y, Mirahmadi Y, Eslahi A, et al. Production of Duchenne muscular dystrophy cellular model using CRISPR-Cas9 exon deletion strategy. Mol Cell Biochem. 2023.
60. Soblechero-Martín P, Albiasu-Arteta E, Anton-Martinez A, de la Puente-Ovejero L, Garcia-Jimenez I, González-Iglesias G, et al. Duchenne Muscular Dystrophy Cell Culture Models Created By CRISPR/Cas 9 Gene Editing And Their Application To Drug Screening. bioRxiv. 2021:2020.02.24.962316.
61. Chey YCJ, Arudkumar J, Aartsma-Rus A, Adikusuma F, Thomas PQ. CRISPR applications for Duchenne muscular dystrophy: From animal models to potential therapies. WIREs Mech Dis. 2023;15(1):e1580.
62. Qi LS, Larson MH, Gilbert LA, Doudna JA, Weissman JS, Arkin AP, et al. Repurposing CRISPR as an RNA-guided platform for sequence-specific control of gene expression. Cell. 2013;152(5):1173-83.
63. Soblechero-Martín P, Albiasu-Arteta E, Anton-Martinez A, de la Puente-Ovejero L, Garcia-Jimenez I, González-Iglesias G, et al. Duchenne muscular dystrophy cell culture models created by CRISPR/Cas9 gene editing and their application in drug screening. Sci Rep. 2021;11(1):18188.
64. Sengupta K, Mishra MK, Loro E, Spencer MJ, Pyle AD, Khurana TS. Genome Editing-Mediated Utrophin Upregulation in Duchenne Muscular Dystrophy Stem Cells. Mol Ther Nucleic Acids. 2020;22:500-9.
65. Chen G, Wei T, Yang H, Li G, Li H. CRISPR-Based Therapeutic Gene Editing for Duchenne Muscular Dystrophy: Advances, Challenges and Perspectives. Cells. 2022;11(19).
66. Muntoni F, Tejura B, Spinty S, Roper H, Hughes I, Layton G, et al. A Phase 1b Trial to Assess the Pharmacokinetics of Ezutromid in Pediatric Duchenne Muscular Dystrophy Patients on a Balanced Diet. Clin Pharmacol Drug Dev. 2019;8(7):922-33.
67. Hafner P, Bonati U, Klein A, Rubino D, Gocheva V, Schmidt S, et al. Effect of Combination l-Citrulline and Metformin Treatment on Motor Function in Patients With Duchenne Muscular Dystrophy: A Randomized Clinical Trial. JAMA Netw Open. 2019;2(10):e1914171.
68. Levi O, Genin O, Angelini C, Halevy O, Pines M. Inhibition of muscle fibrosis results in increases in both utrophin levels and the number of revertant myofibers in Duchenne muscular dystrophy. Oncotarget. 2015;6(27):23249-60.
69. Call JA, Ervasti JM, Lowe DA. TAT-muUtrophin mitigates the pathophysiology of dystrophin and utrophin double-knockout mice. J Appl Physiol (1985). 2011;111(1):200-5.
70. Sonnemann KJ, Heun-Johnson H, Turner AJ, Baltgalvis KA, Lowe DA, Ervasti JM. Functional substitution by TAT-utrophin in dystrophin-deficient mice. PLoS Med. 2009;6(5):e1000083.
71. Duan D. Micro-utrophin Therapy for Duchenne Muscular Dystrophy. Mol Ther. 2019;27(11):1872-4.
72. Young MF, Fallon JR. Biglycan: a promising new therapeutic for neuromuscular and musculoskeletal diseases. Curr Opin Genet Dev. 2012;22(4):398-400.
73. Amenta AR, Yilmaz A, Bogdanovich S, McKechnie BA, Abedi M, Khurana TS, et al. Biglycan recruits utrophin to the sarcolemma and counters dystrophic pathology in mdx mice. Proc Natl Acad Sci U S A. 2011;108(2):762-7.
74. Durko M, Allen C, Nalbantoglu J, Karpati G. CT-GalNAc transferase overexpression in adult mice is associated with extrasynaptic utrophin in skeletal muscle fibres. J Muscle Res Cell Motil. 2010;31(3):181-93.
75. Zygmunt DA, Xu R, Jia Y, Ashbrook A, Menke C, Shao G, et al. rAAVrh74.MCK.GALGT2 Demonstrates Safety and Widespread Muscle Glycosylation after Intravenous Delivery in C57BL/6J Mice. Mol Ther Methods Clin Dev. 2019;15:305-19.

76. Barraza-Flores P, Fontelonga TM, Wuebbles RD, Hermann HJ, Nunes AM, Kornegay JN, et al. Laminin-111 protein therapy enhances muscle regeneration and repair in the GRMD dog model of Duchenne muscular dystrophy. Hum Mol Genet. 2019;28(16):2686-95.
77. Goudenege S, Lamarre Y, Dumont N, Rousseau J, Frenette J, Skuk D, et al. Laminin-111: a potential therapeutic agent for Duchenne muscular dystrophy. Mol Ther. 2010;18(12):2155-63.
78. Marshall JL, Oh J, Chou E, Lee JA, Holmberg J, Burkin DJ, et al. Sarcospan integration into laminin-binding adhesion complexes that ameliorate muscular dystrophy requires utrophin and alpha7 integrin. Hum Mol Genet. 2015;24(7):2011-22.
79. Peter AK, Marshall JL, Crosbie RH. Sarcospan reduces dystrophic pathology: stabilization of the utrophin-glycoprotein complex. J Cell Biol. 2008;183(3):419-27.
80. Corbi N, Libri V, Fanciulli M, Tinsley JM, Davies KE, Passananti C. The artificial zinc finger coding gene 'Jazz' binds the utrophin promoter and activates transcription. Gene Ther. 2000;7(12):1076-83.
81. Onori A, Desantis A, Buontempo S, Di Certo MG, Fanciulli M, Salvatori L, et al. The artificial 4-zinc-finger protein Bagly binds human utrophin promoter A at the endogenous chromosomal site and activates transcription. Biochem Cell Biol. 2007;85(3):358-65.
82. Onori A, Pisani C, Strimpakos G, Monaco L, Mattei E, Passananti C, et al. UtroUp is a novel six zinc finger artificial transcription factor that recognises 18 base pairs of the utrophin promoter and efficiently drives utrophin upregulation. BMC Mol Biol. 2013;14:3.
83. Pisani C, Strimpakos G, Gabanella F, Di Certo MG, Onori A, Severini C, et al. Utrophin up-regulation by artificial transcription factors induces muscle rescue and impacts the neuromuscular junction in mdx mice. Biochim Biophys Acta Mol Basis Dis. 2018;1864(4 Pt A):1172-82.
84. Wilkinson IVL, Perkins KJ, Dugdale H, Moir L, Vuorinen A, Chatzopoulou M, et al. Chemical Proteomics and Phenotypic Profiling Identifies the Aryl Hydrocarbon Receptor as a Molecular Target of the Utrophin Modulator Ezutromid. Angew Chem Int Ed Engl. 2020;59(6):2420-8.
85. Tinsley JM, Fairclough RJ, Storer R, Wilkes FJ, Potter AC, Squire SE, et al. Daily treatment with SMTC1100, a novel small molecule utrophin upregulator, dramatically reduces the dystrophic symptoms in the mdx mouse. PLoS One. 2011;6(5):e19189.
86. Chatzopoulou M, Claridge TDW, Davies KE, Davies SG, Elsey DJ, Emer E, et al. Isolation, Structural Identification, Synthesis, and Pharmacological Profiling of 1,2-trans-Dihydro-1,2-diol Metabolites of the Utrophin Modulator Ezutromid. J Med Chem. 2019.
87. Babbs A, Berg A, Chatzopoulou M, Davies KE, Davies SG, Edwards B, et al. Synthesis of SMT022357 enantiomers and in vivo evaluation in a Duchenne muscular dystrophy mouse model. Tetrahedron. 2020;76(2):130819.
88. Moorwood C, Lozynska O, Suri N, Napper AD, Diamond SL, Khurana TS. Drug discovery for Duchenne muscular dystrophy via utrophin promoter activation screening. PLoS One. 2011;6(10):e26169.
89. Basu U, Gyrd-Hansen M, Baby SM, Lozynska O, Krag TO, Jensen CJ, et al. Heregulin-induced epigenetic regulation of the utrophin-A promoter. FEBS Lett. 2007;581(22):4153-8.
90. Juretic N, Diaz J, Romero F, Gonzalez G, Jaimovich E, Riveros N. Interleukin-6 and neuregulin-1 as regulators of utrophin expression via the activation of NRG-1/ErbB signaling pathway in mdx cells. Biochim Biophys Acta Mol Basis Dis. 2017;1863(3):770-80.
91. Rodova M, Brownback K, Werle MJ. Okadaic acid augments utrophin in myogenic cells. Neurosci Lett. 2004;363(2):163-7.
92. Lecompte S, Abou-Samra M, Boursereau R, Noel L, Brichard SM. Skeletal muscle secretome in Duchenne muscular dystrophy: a pivotal anti-inflammatory role of adiponectin. Cell Mol Life Sci. 2017;74(13):2487-501.

93. Abou-Samra M, Selvais CM, Boursereau R, Lecompte S, Noel L, Brichard SM. AdipoRon, a new therapeutic prospect for Duchenne muscular dystrophy. J Cachexia Sarcopenia Muscle. 2020.
94. Abou-Samra M, Lecompte S, Schakman O, Noel L, Many MC, Gailly P, et al. Involvement of adiponectin in the pathogenesis of dystrophinopathy. Skelet Muscle. 2015;5:25.
95. Peladeau C, Adam N, Bronicki LM, Coriati A, Thabet M, Al-Rewashdy H, et al. Identification of therapeutics that target eEF1A2 and upregulate utrophin A translation in dystrophic muscles. Nat Commun. 2020;11(1):1990.
96. Bulaklak K, Xiao B, Qiao C, Li J, Patel T, Jin Q, et al. MicroRNA-206 Downregulation Improves Therapeutic Gene Expression and Motor Function in mdx Mice. Mol Ther Nucleic Acids. 2018;12:283-93.
97. Basu U, Lozynska O, Moorwood C, Patel G, Wilton SD, Khurana TS. Translational regulation of utrophin by miRNAs. PLoS One. 2011;6(12):e29376.
98. Amirouche A, Tadesse H, Lunde JA, Bélanger G, Côté J, Jasmin BJ. Activation of p38 signaling increases utrophin A expression in skeletal muscle via the RNA-binding protein KSRP and inhibition of AU-rich element-mediated mRNA decay: implications for novel DMD therapeutics. Hum Mol Genet. 2013;22(15):3093-111.
99. Peladeau C, Ahmed A, Amirouche A, Crawford Parks TE, Bronicki LM, Ljubicic V, et al. Combinatorial therapeutic activation with heparin and AICAR stimulates additive effects on utrophin A expression in dystrophic muscles. Hum Mol Genet. 2016;25(1):24-43.
100. Cramer ML, Xu R, Martin PT. Soluble Heparin Binding Epidermal Growth Factor-Like Growth Factor Is a Regulator of GALGT2 Expression and GALGT2-Dependent Muscle and Neuromuscular Phenotypes. Mol Cell Biol. 2019;39(14).
101. Peladeau C, Adam NJ, Jasmin BJ. Celecoxib treatment improves muscle function in mdx mice and increases utrophin A expression. Faseb j. 2018;32(9):5090-103.
102. Hadwen J, Farooq F, Witherspoon L, Schock S, Mongeon K, MacKenzie A. Anisomycin Activates Utrophin Upregulation Through a p38 Signaling Pathway. Clin Transl Sci. 2018;11(5):506-12.
103. Loro E, Sengupta K, Bogdanovich S, Whig K, Schultz DC, Huryn DM, et al. High-throughput identification of post-transcriptional utrophin up-regulators for Duchenne muscle dystrophy (DMD) therapy. Sci Rep. 2020;10(1):2132.
104. Miura P, Chakkalakal JV, Boudreault L, Belanger G, Hebert RL, Renaud JM, et al. Pharmacological activation of PPARbeta/delta stimulates utrophin A expression in skeletal muscle fibers and restores sarcolemmal integrity in mature mdx mice. Hum Mol Genet. 2009;18(23):4640-9.
105. Ljubicic V, Miura P, Burt M, Boudreault L, Khogali S, Lunde JA, et al. Chronic AMPK activation evokes the slow, oxidative myogenic program and triggers beneficial adaptations in mdx mouse skeletal muscle. Hum Mol Genet. 2011;20(17):3478-93.
106. Ljubicic V, Burt M, Lunde JA, Jasmin BJ. Resveratrol induces expression of the slow, oxidative phenotype in mdx mouse muscle together with enhanced activity of the SIRT1-PGC-1α axis. Am J Physiol Cell Physiol. 2014;307(1):C66-82.
107. Ljubicic V, Jasmin BJ. Metformin increases peroxisome proliferator-activated receptor gamma Co-activator-1alpha and utrophin a expression in dystrophic skeletal muscle. Muscle Nerve. 2015;52(1):139-42.
108. Gonzalez-Sanchez J, Sanchez-Temprano A, Cid-Diaz T, Pabst-Fernandez R, Mosteiro CS, Gallego R, et al. Improvement of Duchenne muscular dystrophy phenotype following obestatin treatment. J Cachexia Sarcopenia Muscle. 2018;9(6):1063-78.
109. Ballmann C, Denney TS, Beyers RJ, Quindry T, Romero M, Amin R, et al. Lifelong quercetin enrichment and cardioprotection in Mdx/Utrn+/- mice. Am J Physiol Heart Circ Physiol. 2017;312(1):H128-h40.

110. Ebihara S, Guibinga GH, Gilbert R, Nalbantoglu J, Massie B, Karpati G, et al. Differential effects of dystrophin and utrophin gene transfer in immunocompetent muscular dystrophy (mdx) mice. Physiol Genomics. 2000;3(3):133-44.
111. Cerletti M, Negri T, Cozzi F, Colpo R, Andreetta F, Croci D, et al. Dystrophic phenotype of canine X-linked muscular dystrophy is mitigated by adenovirus-mediated utrophin gene transfer. Gene Ther. 2003;10(9):750-7.
112. Kennedy TL, Guiraud S, Edwards B, Squire S, Moir L, Babbs A, et al. Micro-utrophin Improves Cardiac and Skeletal Muscle Function of Severely Affected D2/mdx Mice. Mol Ther Methods Clin Dev. 2018;11:92-105.
113. Filareto A, Parker S, Darabi R, Borges L, Iacovino M, Schaaf T, et al. An ex vivo gene therapy approach to treat muscular dystrophy using inducible pluripotent stem cells. Nat Commun. 2013;4:1549.
114. Song Y, Morales L, Malik AS, Mead AF, Greer CD, Mitchell MA, et al. Non-immunogenic utrophin gene therapy for the treatment of muscular dystrophy animal models. Nat Med. 2019;25(10):1505-11.
115. Bowe MA, Mendis DB, Fallon JR. The small leucine-rich repeat proteoglycan biglycan binds to alpha-dystroglycan and is upregulated in dystrophic muscle. J Cell Biol. 2000;148(4):801-10.
116. Rooney JE, Gurpur PB, Burkin DJ. Laminin-111 protein therapy prevents muscle disease in the mdx mouse model for Duchenne muscular dystrophy. Proc Natl Acad Sci U S A. 2009;106(19):7991-6.
117. Yoon JH, Chandrasekharan K, Xu R, Glass M, Singhal N, Martin PT. The synaptic CT carbohydrate modulates binding and expression of extracellular matrix proteins in skeletal muscle: Partial dependence on utrophin. Mol Cell Neurosci. 2009;41(4):448-63.
118. Martin PT, Xu R, Rodino-Klapac LR, Oglesbay E, Camboni M, Montgomery CL, et al. Overexpression of Galgt2 in skeletal muscle prevents injury resulting from eccentric contractions in both mdx and wild-type mice. Am J Physiol Cell Physiol. 2009;296(3):C476-88.
119. Flanigan KM, Vetter TA, Simmons TR, Iammarino M, Frair EC, Rinaldi F, et al. A first-in-human phase I/IIa gene transfer clinical trial for Duchenne muscular dystrophy using rAAVrh74.MCK.GALGT2. Mol Ther Methods Clin Dev. 2022;27:47-60.
120. Dennis CL, Tinsley JM, Deconinck AE, Davies KE. Molecular and functional analysis of the utrophin promoter. Nucleic Acids Res. 1996;24(9):1646-52.
121. Gyrd-Hansen M, Krag TO, Rosmarin AG, Khurana TS. Sp1 and the ets-related transcription factor complex GABP alpha/beta functionally cooperate to activate the utrophin promoter. J Neurol Sci. 2002;197(1-2):27-35.
122. Chakkalakal JV, Stocksley MA, Harrison MA, Angus LM, Deschenes-Furry J, St-Pierre S, et al. Expression of utrophin A mRNA correlates with the oxidative capacity of skeletal muscle fiber types and is regulated by calcineurin/NFAT signaling. Proc Natl Acad Sci U S A. 2003;100(13):7791-6.
123. Strimpakos G, Corbi N, Pisani C, Di Certo MG, Onori A, Luvisetto S, et al. Novel adeno-associated viral vector delivering the utrophin gene regulator jazz counteracts dystrophic pathology in mdx mice. J Cell Physiol. 2014;229(9):1283-91.
124. Tinsley J, Robinson N, Davies KE. Safety, tolerability, and pharmacokinetics of SMT C1100, a 2-arylbenzoxazole utrophin modulator, following single- and multiple-dose administration to healthy male adult volunteers. J Clin Pharmacol. 2015;55(6):698-707.
125. Casper RF, Quesne M, Rogers IM, Shirota T, Jolivet A, Milgrom E, et al. Resveratrol has antagonist activity on the aryl hydrocarbon receptor: implications for prevention of dioxin toxicity. Mol Pharmacol. 1999;56(4):784-90.
126. Babbs A, Chatzopoulou M, Edwards B, Squire SE, Wilkinson IVL, Wynne GM, et al. From diagnosis to therapy in Duchenne muscular dystrophy. Biochem Soc Trans. 2020;48(3):813-21.

127. Handschin C, Kobayashi YM, Chin S, Seale P, Campbell KP, Spiegelman BM. PGC-1alpha regulates the neuromuscular junction program and ameliorates Duchenne muscular dystrophy. Genes Dev. 2007;21(7):770-83.
128. Gramolini AO, Angus LM, Schaeffer L, Burton EA, Tinsley JM, Davies KE, et al. Induction of utrophin gene expression by heregulin in skeletal muscle cells: role of the N-box motif and GA binding protein. Proc Natl Acad Sci U S A. 1999;96(6):3223-7.
129. Krag TO, Bogdanovich S, Jensen CJ, Fischer MD, Hansen-Schwartz J, Javazon EH, et al. Heregulin ameliorates the dystrophic phenotype in mdx mice. Proc Natl Acad Sci U S A. 2004;101(38):13856-60.
130. Miura P, Thompson J, Chakkalakal JV, Holcik M, Jasmin BJ. The utrophin A 5'-untranslated region confers internal ribosome entry site-mediated translational control during regeneration of skeletal muscle fibers. J Biol Chem. 2005;280(38):32997-3005.
131. Miura P, Andrews M, Holcik M, Jasmin BJ. IRES-mediated translation of utrophin A is enhanced by glucocorticoid treatment in skeletal muscle cells. PLoS One. 2008;3(6):e2309.
132. Morgoulis D, Berenstein P, Cazacu S, Kazimirsky G, Dori A, Barnea ER, et al. sPIF promotes myoblast differentiation and utrophin expression while inhibiting fibrosis in Duchenne muscular dystrophy via the H19/miR-675/let-7 and miR-21 pathways. Cell Death Dis. 2019;10(2):82.
133. Mishra MK, Loro E, Sengupta K, Wilton SD, Khurana TS. Functional improvement of dystrophic muscle by repression of utrophin: let-7c interaction. PLoS One. 2017;12(10):e0182676.
134. Sengupta K, Loro E, Khurana TS. PMO-based let-7c site blocking oligonucleotide (SBO) mediated utrophin upregulation in mdx mice, a therapeutic approach for Duchenne muscular dystrophy (DMD). Sci Rep. 2020;10(1):21492.
135. Garbincius JF, Michele DE. Dystrophin-glycoprotein complex regulates muscle nitric oxide production through mechanoregulation of AMPK signaling. Proc Natl Acad Sci U S A. 2015;112(44):13663-8.
136. Mantuano P, Sanarica F, Conte E, Morgese MG, Capogrosso RF, Cozzoli A, et al. Effect of a long-term treatment with metformin in dystrophic mdx mice: A reconsideration of its potential clinical interest in Duchenne muscular dystrophy. Biochem Pharmacol. 2018;154:89-103.
137. Hafner P, Bonati U, Erne B, Schmid M, Rubino D, Pohlman U, et al. Improved Muscle Function in Duchenne Muscular Dystrophy through L-Arginine and Metformin: An Investigator-Initiated, Open-Label, Single-Center, Proof-Of-Concept-Study. PLoS One. 2016;11(1):e0147634.
138. Vianello S, Yu H, Voisin V, Haddad H, He X, Foutz AS, et al. Arginine butyrate: a therapeutic candidate for Duchenne muscular dystrophy. Faseb j. 2013;27(6):2256-69.
139. Domi E, Hoxha M, Prendi E, Zappacosta B. A Systematic Review on the Role of SIRT1 in Duchenne Muscular Dystrophy. Cells. 2021;10(6).
140. Hollinger K, Shanely RA, Quindry JC, Selsby JT. Long-term quercetin dietary enrichment decreases muscle injury in mdx mice. Clin Nutr. 2015;34(3):515-22.
141. Ballmann C, Hollinger K, Selsby JT, Amin R, Quindry JC. Histological and biochemical outcomes of cardiac pathology in mdx mice with dietary quercetin enrichment. Exp Physiol. 2015;100(1):12-22.
142. Gordon BS, Delgado Diaz DC, Kostek MC. Resveratrol decreases inflammation and increases utrophin gene expression in the mdx mouse model of Duchenne muscular dystrophy. Clin Nutr. 2013;32(1):104-11.
143. Georgieva AM, Guo X, Bartkuhn M, Günther S, Künne C, Smolka C, et al. Inactivation of Sirt6 ameliorates muscular dystrophy in mdx mice by releasing suppression of utrophin expression. Nat Commun. 2022;13(1):4184.
144. Roest PA, van der Tuijn AC, Ginjaar HB, Hoeben RC, Hoger-Vorst FB, Bakker E, et al. Application of in vitro Myo-differentiation of non-muscle cells to enhance gene expression and facilitate analysis of muscle proteins. Neuromuscul Disord. 1996;6(3):195-202.

145. Ruiz-Del-Yerro E, Garcia-Jimenez I, Mamchaoui K, Arechavala-Gomeza V. Myoblots: dystrophin quantification by in-cell western assay for a streamlined development of Duchenne muscular dystrophy (DMD) treatments. Neuropathol Appl Neurobiol. 2018;44:463-73.
146. Gong H, Zheng C, Lyu X, Dong L, Tan S, Zhang X. Inhibition of Sirt2 Alleviates Fibroblasts Activation and Pulmonary Fibrosis via Smad2/3 Pathway. Front Pharmacol. 2021;12:756131.
147. Haeussler M, Schonig K, Eckert H, Eschstruth A, Mianne J, Renaud JB, et al. Evaluation of off-target and on-target scoring algorithms and integration into the guide RNA selection tool CRISPOR. Genome Biol. 2016;17(1):148.
148. Moorwood C, Soni N, Patel G, Wilton SD, Khurana TS. A cell-based high-throughput screening assay for posttranscriptional utrophin upregulation. J Biomol Screen. 2013;18(4):400-6.
149. Fan Z, Bin L. Will Sirtuin 2 Be a Promising Target for Neuroinflammatory Disorders? Front Cell Neurosci. 2022;16:915587.
150. Willmann R, Lee J, Turner C, Nagaraju K, Aartsma-Rus A, Wells DJ, et al. Improving translatability of preclinical studies for neuromuscular disorders: lessons from the TREAT-NMD Advisory Committee for Therapeutics (TACT). Dis Model Mech. 2020;13(2).
151. Loro E, Sengupta K, Bogdanovich S, Whig K, Schultz DC, Huryn DM, et al. Author Correction: High-throughput identification of post-transcriptional utrophin up-regulators for Duchenne muscle dystrophy (DMD) therapy. Sci Rep. 10. England2020. p. 4039.
152. Hoffman GR, Moerke NJ, Hsia M, Shamu CE, Blenis J. A high-throughput, cell-based screening method for siRNA and small molecule inhibitors of mTORC1 signaling using the In Cell Western technique. Assay Drug Dev Technol. 2010;8(2):186-99.
153. Khoury L, Zalko D, Audebert M. Validation of high-throughput genotoxicity assay screening using γH2AX in-cell western assay on HepG2 cells. Environ Mol Mutagen. 2013;54(9):737-46.
154. Schnaiter S, Fürst B, Neu J, Wáczek F, Orfi L, Kéri G, et al. Screening for MAPK modulators using an in-cell western assay. Methods Mol Biol. 2014;1120:121-9.
155. Pal AS, Agredo AM, Kasinski AL. In-Cell Western Protocol for Semi-High-Throughput Screening of Single Clones. Bio Protoc. 2022;12(16).
156. McInerney MP, Pan Y, Short JL, Nicolazzo JA. Development and Validation of an In-Cell Western for Quantifying P-Glycoprotein Expression in Human Brain Microvascular Endothelial (hCMEC/D3) Cells. J Pharm Sci. 2017;106(9):2614-24.
157. Lambrescu I, Popa A, Manole E, Ceafalan LC, Gaina G. Application of Droplet Digital PCR Technology in Muscular Dystrophies Research. Int J Mol Sci. 2022;23(9).
158. Taylor SC, Laperriere G, Germain H. Droplet Digital PCR versus qPCR for gene expression analysis with low abundant targets: from variable nonsense to publication quality data. Sci Rep. 2017;7(1):2409.
159. Berger J, Li M, Berger S, Meilak M, Rientjes J, Currie PD. Effect of Ataluren on dystrophin mutations. J Cell Mol Med. 2020;24(12):6680-9.
160. Antoury L, Hu N, Balaj L, Das S, Georghiou S, Darras B, et al. Analysis of extracellular mRNA in human urine reveals splice variant biomarkers of muscular dystrophies. Nat Commun. 2018;9(1):3906.
161. Koutsoulidou A, Phylactou LA. Circulating Biomarkers in Muscular Dystrophies: Disease and Therapy Monitoring. Mol Ther Methods Clin Dev. 2020;18:230-9.
162. Hiller M, Falzarano MS, Garcia-Jimenez I, Sardone V, Verheul RC, Popplewell L, et al. A multicenter comparison of quantification methods for antisense oligonucleotide-induced DMD exon 51 skipping in Duchenne muscular dystrophy cell cultures. PLoS One. 2018;13(10):e0204485.
163. Novak JS, Spathis R, Dang UJ, Fiorillo AA, Hindupur R, Tully CB, et al. Interrogation of Dystrophin and Dystroglycan Complex Protein Turnover After Exon Skipping Therapy. J Neuromuscul Dis. 2021;8(s2):S383-s402.

164. Massenet J, Gitiaux C, Magnan M, Cuvellier S, Hubas A, Nusbaum P, et al. Derivation and Characterization of Immortalized Human Muscle Satellite Cell Clones from Muscular Dystrophy Patients and Healthy Individuals. Cells. 2020;9(8).
165. Tejedera-Villafranca A, Montolio M, Ramón-Azcón J, Fernández-Costa JM. Mimicking sarcolemmal damagein vitro: a contractile 3D model of skeletal muscle for drug testing in Duchenne muscular dystrophy. Biofabrication. 2023;15(4).
166. Jiwlawat N, Lynch E, Jeffrey J, Van Dyke JM, Suzuki M. Current Progress and Challenges for Skeletal Muscle Differentiation from Human Pluripotent Stem Cells Using Transgene-Free Approaches. Stem Cells Int. 2018;2018:6241681.
167. Melone MA, Peluso G, Petillo O, Galderisi U, Cotrufo R. Defective growth in vitro of Duchenne Muscular Dystrophy myoblasts: the molecular and biochemical basis. J Cell Biochem. 1999;76(1):118-32.
168. Goullée H, Taylor RL, Forrest ARR, Laing NG, Ravenscroft G, Clayton JS. Improved CRISPR/Cas9 gene editing in primary human myoblasts using low confluency cultures on Matrigel. Skelet Muscle. 2021;11(1):23.
169. Wojtal D, Kemaladewi DU, Malam Z, Abdullah S, Wong TW, Hyatt E, et al. Spell Checking Nature: Versatility of CRISPR/Cas9 for Developing Treatments for Inherited Disorders. Am J Hum Genet. 2016;98(1):90-101.
170. Hamed M, Chen J, Li Q. Regulation of Dystroglycan Gene Expression in Early Myoblast Differentiation. Front Cell Dev Biol. 2022;10:818701.
171. Kim S, Kim D, Cho SW, Kim J, Kim JS. Highly efficient RNA-guided genome editing in human cells via delivery of purified Cas9 ribonucleoproteins. Genome Res. 2014;24(6):1012-9.
172. Simon G, Sumitava D, Fetta M, Fatima A, Maelle R, Anne de C, et al. CRISPR-Cas9 mediated endogenous utrophin upregulation improves Duchenne Muscular Dystrophy. bioRxiv. 2023:2023.04.18.536394.
173. Pushpakom S, Iorio F, Eyers PA, Escott KJ, Hopper S, Wells A, et al. Drug repurposing: progress, challenges and recommendations. Nature Reviews Drug Discovery. 2019;18(1):41-58.
174. Vitiello L, Tibaudo L, Pegoraro E, Bello L, Canton M. Teaching an Old Molecule New Tricks: Drug Repositioning for Duchenne Muscular Dystrophy. Int J Mol Sci. 2019;20(23).
175. Chancellor DR, Davies KE, De Moor O, Dorgan CR, Johnson PD, Lambert AG, et al. Discovery of 2-arylbenzoxazoles as upregulators of utrophin production for the treatment of Duchenne muscular dystrophy. J Med Chem. 2011;54(9):3241-50.
176. Gleneadie HJ, Fernandez-Ruiz B, Sardini A, Van de Pette M, Dimond A, Prinjha RK, et al. Endogenous bioluminescent reporters reveal a sustained increase in utrophin gene expression upon EZH2 and ERK1/2 inhibition. Commun Biol. 2023;6(1):318.
177. Liu Y, Beyer A, Aebersold R. On the Dependency of Cellular Protein Levels on mRNA Abundance. Cell. 2016;165(3):535-50.
178. Sandonà M, Cavioli G, Renzini A, Cedola A, Gigli G, Coletti D, et al. Histone Deacetylases: Molecular Mechanisms and Therapeutic Implications for Muscular Dystrophies. Int J Mol Sci. 2023;24(5).
179. Farr GH, 3rd, Morris M, Gomez A, Pham T, Kilroy E, Parker EU, et al. A novel chemical-combination screen in zebrafish identifies epigenetic small molecule candidates for the treatment of Duchenne muscular dystrophy. Skelet Muscle. 2020;10(1):29.
180. Vandenborne K, Willcocks R, Walter G, Forbes S, Cazzaniga S, Bettica P, et al. P129 Givinostat in DMD: results of the Epidys study with particular attention to MR measures of muscle fat fraction. Neuromuscular Disorders. 2023;33:S79-S80.

AGRADECIMIENTOS

En primer lugar, me gustaría mostrar mi más sincero agradecimiento a Virginia, mi directora, por confiar en mí y por darme la oportunidad de incorporarme a su grupo. Gracias por guiarme durante todos estos años en cada paso de mi investigación. Gracias por apoyarme siempre, por tu comprensión y empatía y por todos tus consejos tanto profesionales como personales. Cuando llegué a Bilbao hace ya siete años, muy ilusionada, pero añorando a mi familia y amigos, Esti, Iker y tú fuisteis un gran apoyo para mí, gracias por todo.

A ellos, Esti e Iker, les doy las gracias por ser mis primeros maestros en el laboratorio, porque en unos meses se esforzaron por explicarme todos sus conocimientos y porque este trabajo no hubiera sido posible sin ellos.

A mi codirectora de tesis, Ainara, gracias por todos tus consejos, por los "lab meeting" por zoom que tanto nos han ayudado a poner en común nuevas ideas y darles siempre una vuelta a los experimentos. Gracias a tu grupo por acogerme cuando he ido a Donosti y en especial a Laura por su contribución con los experimentos *in vivo* de este proyecto.

A Edurne, mi otra mitad en el laboratorio. Gracias por todo, porque este trabajo también es tuyo. Por las horas en cultivos, por nuestros In Cell en cadena, por todos tus consejos y tu apoyo. Tu alegría contagiosa nos hacía disfrutar de cada uno de esos momentos y sin ti este proyecto no hubiera sido posible. Conocerte fue una gran suerte, espero que sigamos compartiendo momentos juntas muchos años.

A Andrea, por ser la mejor compañera que podría tener. Qué suerte haber podido trabajar juntas. Gracias por tus conversaciones inspiradoras y tu eterna sonrisa, sin tu ayuda y tu apoyo durante estos años no lo habría conseguido, este logro también es tuyo. Eres una gran investigadora y conseguirás todo aquello que te propongas. Me llevo de esta etapa una amiga para siempre.

Gracias de corazón a todos los colegas y amigos que han formado parte del grupo de enfermedades neuromusculares. Gracias a Irene, Gabi, Aina, Karmele, Laura y Javi por vuestras valiosas contribuciones a mi investigación, pero también por los buenos ratos que hemos compartido juntos.

A mi familia, por su amor y apoyo incondicional durante todo mi camino académico. Sin su ayuda, este logro no habría sido posible. En especial quiero expresar mi agradecimiento a mis padres por haberme brindado la oportunidad de estudiar con la tranquilidad de saber que cuento con su respaldo. Vosotros me enseñasteis la importancia del trabajo duro, la responsabilidad, la perseverancia y la determinación, gracias, sois mi ejemplo a seguir siempre.

A mi abuela, cuyo amor y sabiduría me han guiado a lo largo de mi vida. Este trabajo está también dedicado a ella.

Esta tesis no hubiera sido posible sin el apoyo de Luis, mi pareja. Gracias por creer en mí incluso cuando yo misma no lo hacía, por tu comprensión en los momentos más estresantes y por hacerme reír siempre en los días difíciles. Soy muy afortunada de tenerte a mi lado.

En conclusión, quiero expresar mi profunda gratitud y reconocimiento a las personas dedicadas en este trabajo. Su apoyo, motivación y guía han sido esenciales para la realización de esta investigación. Me siento afortunado de tenerlos en mi vida. Este logro es también suyo y espero que se sientan orgullosos de él.